DOCTORAATSPROEFSCHRIFT

Molecularly Imprinted Polymers: synthetic receptors for diagnostic medical devices

Proefschrift voorgelegd tot het behalen van de graad van doctor in de wetenschappen, chemie, te verdedigen door:

Marloes Peeters

Promotor: prof. dr. Patrick Wagner
Copromotor: prof. dr. Thomas Cleij
Copromotor: dr. Freddy Troost

universiteit
▶▶hasselt
KNOWLEDGE IN ACTION

Jury

Chair: Prof. dr. M. Van Bael

Hasselt University, IMO

Promotor: Prof. Dr. P. Wagner

Hasselt University, IMO-IMOMEC

Co-promotors: Prof. dr. T. J. Cleij

Hasselt University, IMO

Dr. F.J. Troost

Internal Medicine, Maastricht University Medical Center

Members of the jury: Prof. Dr.-Ing M.J. Schöning

Aachen University of Applied Sciences, INB

Prof. Dr. W. De Ceuninck

Hasselt University, IMO-IMOMEC

Prof. Dr. Jeroen Lammertyn

K.U. Leuven

Prof. Dr. Sven Ingebrandt

University of Applied Sciences Kaiserslautern

Prof. dr. Wanda Guedens

Hasselt University

Acknowledgements

Na een aantal maanden roeren in potjes met verf op basis van xyleen, stegen de chemische dampen me naar het hoofd. Het was tijd voor iets anders, daarom ging ik op mijn balkonnetje in de Braziliaanse zon op zoek naar vacatures op Internet. Ik schreef een aantal sollicitatiebrieven met het idee dat, tegen de tijd dat ik terug zou zijn in Nederland, ik misschien wat universiteiten kon bezoeken. Hoe anders zou het gaan; een aantal weken later vroeg een (toen nog onbekende) professor of ik niet een interview via Skype wilde doen. Dat leek me ideaal, als je de mensen namelijk niet ziet hoef je ook geen zenuwen te hebben. De Braziliaanse internetconnectie besliste anders, na een aantal minuten hoorde ik niet anders dan gepiep en gekraak. Gelukkig werd ik vrijwel direct op mijn mobiele telefoon gebeld en dat gesprek ging een stuk vlotter. Een paar dagen later mailde ik de (onbekende) professor enthousiast terug en in gedachten begon ik met de voorbereidingen voor mijn 'emigratie' naar België. Terug in Nederland kreeg ik een urgente mail of ik nog wilde komen naar Hasselt. Mijn toezeggingsmail van zeker een maand geleden was namelijk op mysterieuze wijze in een junkmail box beland. Eventjes schrok ik, maar na het ontmoeten van de 'onbekende' prof, Patrick (Paddy) Wagner, was alles snel in orde.

Prof. Dr. Patrick Wagner: Patrick, allereerst bedankt voor me een kans te bieden mijn onderzoek hier te doen. Je had tenslotte al één Hollander in de groep, dan kon een tweede er óók wel bij! In 4 jaar tijd heb ik veel van je geleerd, zo ben ik een stuk handiger met een aantal ontwerpprogramma's (en niet alleen Paint, Bart!) door je vele potloodtekeningen. En ook met schrijven heb ik de stille hoop dat het beter gaat. De tekst van mijn eerste artikel zat vol met zorgvuldige strepen van jouw vulpen, door middel van deze verbeteringen ging het de volgende keer beter en herkende ik zowaar mijn eigen tekst terug. En ondanks dat je me een aantal metingen liet uitvoeren met 'vieze' samples, vind ik het een eer om langer te mogen blijven. Vielen Dank!

Dan waren er nog mijn 2 copromoteren, het olijke Hollandse duo.

Professor Thomas Cleij: Om niet alleen mijn Nederlandse roots niet te vergeten, maar ook zeker niet mijn chemische roots. Op de organische afdeling heb ik altijd veel steun gehad, zeker met de hulp van Ans en Fré. Ik kon er terecht voor stinkende goedjes, feedback en het volbombarderen van jullie zuurkasten met Soxhlet-opstellingen, hiervoor bedankt!

Dr. Freddy Troost: Niet alleen ik, maar zelfs mijn studenten hebben jouw enthousiasme opgemerkt. Na een bezoekje aan Maastricht kwam ik altijd gemotiveerd terug, misschien had dat ook iets te maken met de heerlijke cappucino uit je eigen autoomaatje (zeker vergeleken met de machinale koffie op het IMO). Langzamerhand begin ik een klein beetje van het complexe systeem de darmen te begrijpen. Hoewel de experimenten niet altijd even smakelijk zijn, wordt het vreemd genoeg steeds interessanter.

Daarnaast nog een woord van dank aan de andere juryleden, prof. Marlies Van Bael, prof. Ward De Ceuninck, prof. Wanda Guedens, prof. Michael Schöning, prof. Jeroen Lammertyn en prof. Sven Ingebrandt. Speciale dank aan dr. Ludo Tolhuizen, voor de broodnodige hulp met het wiskundig model.

Hoewel ik als 'Hollandse' in België terecht kwam, voelde ik me hier direct thuis. Een woord van dank is er voor de mensen van het secretariaat, de technische hulp en ook zeker voor de computerafdeling, maar vooral voor de mensen op 'het BIOS-kantoor'. De elastiekjesoorlog was net voorbij toen ik arriveerde, maar jullie lieten zelfs mij meedoen aan het vrijdagmiddagentertainment hoewel bewezen was dat schietspelletjes niet mijn ding zijn! Speciaalbier evenmin, hoewel ik het in de loop van jaren meer ben gaan waarderen (en hopelijk ook beter tegen kan, maar daar beslissen jullie over). Bedankt voor het entertainment tijdens de vele congressen en buitenlandse tripjes, het ruilen van chocoladekoekjes, het koffie halen voor meer dan 5 man, meegenieten van de vernedering na de wedstrijd Nederland – Duitsland maar bovenal, voor het feit dat ik elke dag met een glimlach achter mijn computer zit. En ja, zelfs nu ik deze thesis aan het schrijven ben. Voorlopig zijn jullie nog niet van me af, maar

ik zou het zeker niet anders willen. Dank je wel: Lars, Jan, Bert, Rob, Bart, Mo, Kasper, Thijs en recentelijk Evelien, Andreas, Karolien en Patricia. Speciaal moet ik Matthie en Kathia bedanken, voor het meegaan naar alle 'foute' feestjes, het skiverlof, zalig eten, het met tegenzin gaan naar de Body Pump op dinsdag en horror movie nights. Ik heb me door jullie nooit hoeven vervelen doordeweeks! De Mannêh van de Xios wil ik daarnaast niet vergeten, Ronald, Michael, Tim, Stijn, Jeroen en Koen: het was een genoegen om met jullie Kerst te vieren maar zeker om op jullie te kunnen schieten met BANG!

Tijdens mijn doctoraat ben ik bijgestaan door een bonte groep studenten die ik zou moeten bedanken in vele talen. Dan maar eerst in het 'Vlaams': Brecht, Mandy, Tesneem, Hannelore, Martijn, Maud en Nazim, bedankt! Tina, the first student I guided, you showed me that German work 'Gründlichkeit and Pünktlichkeit' is always efficient but can also come with a smile on the face. I am looking forward to the next Christmas market in Zweibrücken! Roel, ook jij als 'Hollander' werd moeiteloos door de BIOS groep opgenomen. Het was een plezier om met je samen te werken, zelfs terwijl ik in Mexico zat voor de Biosensors conferentie had ik er volledig vertrouwen in dat jij de experimenten wel in je eentje kon klaren. Je zat altijd bomvol ideeën en ik hoop dat je deze nu in Edingburgh kan uitvoeren! Pedro, you told me they would 'save the best student for last'. It was great to talk to you in Portuguese, it brought back a lot of memories of my time in Brazil. I promise you I will continue to work on my Portuguese skills, especially on improving my 'country side' accent. Obrigada!

Dan is er nog een speciaal woord van dank voor al mijn vrienden en familie. Door naar België te verhuizen werd de afstand tussen ons een stuk groter, maar het leek alsof dit niets heeft veranderd. Rulke en Jolanda, ik weet dat jullie graag mijn 'paranimfen' geweest zouden zijn. Helaas bestaan deze in België niet, dus moeten jullie mij maar op de voorste rij steunen. En ja, dat is ook reden genoeg om een leuk jurkje te kopen! Papa, mama, Bart en oma, ik heb hier nu een week achter mijn laptop gezeten en ben niet echt gezellig geweest, maar heb wel het grootste stuk van mijn thesis hier kunnen schrijven door de goede verzorging. Avondeten op verzoek, eierkoekjes gebakt en een aantal detectives op de harde schijf, de succesformule voor een weekje doorbikkelen.

Bedankt voor alle steun de afgelopen jaren, door jullie vertrouwen heb ik altijd geweten dat ik er wel zou komen.

De jaren zijn voorbij gevlogen en hiermee komt er nu een einde aan mijn doctoraat, maar nog niet aan mijn tijd in België. Ik gok op een weekje relaxen, daarna zie ik jullie weer terug op kantoor! Uiteraard zal ik iedereen eerst op een kopje koffie trakteren, misschien wel met wat dropjes erbij.

The chemist is like someone who is watching people playing chess and, after watching a few games, he may have worked out what the moves in the game are. But understanding the rules is just a trivial preliminary on the long route from being a novice to being a grand master.

-Sir Martin Rees

Table of Contents

Abstract

Irritable Bowel Syndrome (IBS) is a functional bowel disorder which is characterized by abdominal pain and changes in bowel habit. It has a profound negative impact on the quality of a patient's life and is associated with more than €20 billion of indirect and direct medial costs per year. Most IBS therapies are based on relief of the symptoms, since the organic cause of the disease remains largely unknown. Recently, the involvement of biogenic amines such as serotonin and histamine has been postulated. The established technologies to determine the concentration of these target molecules have several disadvantages. The methods are costly, lack in speed, and require a lab-environment and sophisticated equipment. Therefore, the aim of this thesis is to develop a polymer-type sensor for the detection of serotonin and histamine for intestinal –and blood applications. The sensor platform should meet the following criteria: specific recognition in biological samples, low-cost (~10 euro per materials of the chip), fast response time (30 – 60 min), and offering the possibility of measuring *in vivo*. The relevant biological concentrations for the templates serotonin, histamine and L-nicotine are shown in Table 1. L-nicotine was included because it was used for proof-of-principle tests.

Table 1: Physiologically relevant concentrations of serotonin, histamine and L-nicotine.

Target	Biological samples		
	Saliva	**Urine**	**Blood**
serotonin	-	-	10 – 1500 nM
histamine	-	200 -750 nM	10 – 1000 nM
L-nicotine	0.2 – 1000 µM	0.3 – 10 µM	-

Molecularly Imprinted Polymers (MIPs) were used as polymer-type receptors since they are robust, can be produced at low-cost, and have a high affinity for their template molecules. They were synthesized by bulk polymerization and subsequently ground to obtain a powder. Next, aluminum electrodes were functionalized with MIPs by thermal treatment. The particles were then integrated into a sensor platform which can specifically detect small molecules by two read-out technologies. The first technique is based on electrochemical impedance spectroscopy, the second on heat-transfer resistance.

First, a MIP for the specific detection of serotonin was developed. Various MIPs were synthesized and the MIP with the highest affinity for serotonin was selected by optical batch-rebinding experiments. The particles were then integrated in an open impedimetric sensor setup and a dose-response curve was determined in buffer solutions. For biological samples, a refined sensor cell was developed. This flow through cell was closed, ensuring safe administration of patient's samples, and featured an integrated temperature unit which improves stabilization and control over the system. With this setup, native serotonin concentrations in human blood plasma were determined. The obtained results were in agreement with High Performance Liquid Chromatography (HPLC) reference tests. Furthermore, it was demonstrated that the impedimetric response upon binding of serotonin can be attributed to a capacitive effect at the interface between the MIP particles and fluid layer.

Histamine is the other biogenic amine of interest in this thesis. In previous work, histamine concentrations in buffer solutions ranging from pH 7-9 were determined with impedimetric read-out. For diagnostic applications, this target molecule should be detectable in a wider pH range as is it mostly occurs in mildly acidic environments. To understand the pH-dependent response of the MIP sensor, we proposed a statistical binding analysis model. With this model, the theoretical performance of a MIP based on the monomer acrylic acid in the required pH regime was predicted. The results were verified experimentally by UV-vis spectroscopy, microgravimetry and impedance spectroscopy. Histamine could be detected with impedimetric read-out in the physiologically relevant nanomolar concentration range in neutral and in mildly acidic buffer solutions. As last validation step, this platform was used to analyze histamine concentration of mildly acidic bowel fluid samples of several test persons. It was shown that this sensor provides reliable data in the relevant concentration regime, which was validated independently by Enzyme-Linked Immunosorbent Assay (ELISA) tests.

The electronic method requires minimal instrumentation, can perform fast measurements and is specific enough to determine concentrations in the physiologically relevant environment. An alternative read-out technique is also

presented, the heat-transfer method (HTM), which is even more straightforward as it requires only two thermometers, an adjustable heat source and a Proportional-Integral-Derivative (PID) controller. The principle works as follows; upon rebinding of a target molecule, the heat flux through the nanocavity in the MIP is strongly reduced due to the presence of the template. As a result, the total heat transfer resistance (R_{th}) will be increased with the effect size being dependent on the amount of target molecule that is bound. For proof-of-principle purposes, aluminum electrodes were functionalized with MIP particles and L-nicotine measurements were performed in buffer solutions. The main focus of this thesis lies on serotonin and histamine; therefore dose-response curves in buffer solutions were also constructed for these target molecules. The achieved detection limits in buffer solutions are comparable as with impedance spectroscopy. This technique was applied simultaneously with the R_{th} and provided a direct validation of the results. As a proof-of-application, measurements were performed on saliva samples spiked with L-nicotine. A dose-response curve could be constructed, showing the applicability even in complex matrices.

Next, it is evaluated to what degree the developed techniques fulfill the proposed criteria in terms of specificity, costs, speed, and possibility of *in vivo* measurements.

The detection limits for the impedimetric read-out technique and the HTM are summarized in Table 2 for both buffer solutions and biological samples.

Table 2: LOD in 1x PBS and biological samples with HTM and impedimetric read-out.

Target	HTM		Impedance spectroscopy		
	LOD Buffer	LOD Saliva	LOD Buffer	LOD Blood	LOD Bowel fluid
serotonin	20 nM	-	3 nM	5 nM	-
histamine	30 nM	-	15 nM	-	0.2 µM
L-nicotine	100 nM	~0.5 mM	100 nM	-	-

The LOD of both techniques, compared to the physiologically relevant concentrations shown in Table 1, is low enough to specifically detect histamine and serotonin in buffer solutions. However, only the impedimetric read-out has been studied extensively with biological samples. Therefore, further clinical trials

will be performed with this method. It has to be considered that HTM is not an established technology yet and there is still room for improvement, especially on reducing the noise on the signal.

In terms of expenses, the main advantage of MIPs is that they are low cost due to their straightforward synthesis. From this we can conclude that the chemicals do not play an important role for the material costs of the chip. The impedance analyzer and sensor cell are all home made, with a total of around 1000 euro for the equipment. For HTM only two thermometers and an adjustable heat source are required, ensuring this is even less expensive. The material value of 10 euro per chip seems therefore reasonable.

The other criterium is the measurement time, which should be within 60 minutes. For our experiments, the average value is taken of six points with an interval of three minutes. This means that at least the signal should be monitored for 18 minutes, with aditionally a stabilization time between 15 to 30 minutes. Therefore, it should be possible to perform a measurement in the required time frame.

Both techniques are specific, low cost and fast, thereby fulfilling the specified criteria to a great extent. The last criterium, the *in vivo* measuring for intestinal applications, imposes some challenges.

To overcome these problems, the sample preparation needs to be altered possibly by directly polymerizing the MIPs onto the surface of the electrodes. Furthermore, the biocompatibility of the MIPs and the sensor platform should be evaluated. The final step is to enter the industrial market of diagnostics. For this purpose, some future MIP platform designs were suggested. There are two more aspects we will have to consider, before thinking of commercialization of the product:

   i)   A clinical trial should be performed to study a larger amount of
           biological samples and, from a diversity of individuals (healthy

controls and patients). The latter is indispensable to determine if the technique is sensitive enough to detect occurring aberrations.

ii)   The sensor platform should be transformed to an array format which enables the simultaneous detection of a variety of targets.

Due to the speed, low-cost, and high specificity of the developed techniques, they can be considered as methods with a high clinical and commercial potential. These methods could also mean a first step into the direction of incorporating MIPs into sensing devices for *in vivo* purposes. Measurements performed directly in the gastro-intestinal tract would provide an important insight into the pathogenesis of several gastrointestinal system-related disorders. This may lead to the development of novel, effective treatments for these disorders.

Nederlandse samenvatting

Het Prikkelbare Darm Syndroom (PDS) is een darmstoornis die gekarakteriseerd wordt door de aanwezigheid van buikpijn en een afwijkend ontlastingspatroon. Het heeft een sterk negatieve impact op de kwaliteit van leven van patiënten en is verantwoordelijk voor meer dan €20 miljard aan directe en indirecte medische kosten per jaar. De onderliggende oorzaak van PDS is tot op heden grotendeels onbekend en zeer heterogeen. Traditionele therapieën zijn niet gericht op genezing maar op verlichting van de symptomen. Het is aangetoond dat verschillende biogene aminen zoals serotonine en histamine een rol spelen. De conventionele technieken om deze doelmoleculen te detecteren hebben een aantal nadelen. Al deze methodieken zijn kostelijk, vergen een lange meettijd, hebben een laboratorium omgeving nodig en gebruiken uiterst geavanceerde apparatuur. Daarom is het doel van deze thesis om een sensor, gebaseerd op polymeer-technologie, te ontwikkelen voor de detectie van histamine en serotonine in het maagdarmkanaal. Deze sensor zou aan de volgende criteria moeten voldoen; specifieke herkenning van de doelmoleculen in biologische stalen, goedkoop (~10 euro per chip), snelle meettijd (30 – 60 min) en de mogelijkheid tot het doen van *in vivo* metingen. De relevante concentraties van de doelmoleculen serotonine, histamine en L-nicotine in verschillende biologische omgevingen zijn weergegeven in Tabel 1. L-nicotine is toegevoegd omdat het gebruikt werd voor het testen van het sensor principe.

Table 1: Biologisch relevant concentraties van serotonine, histamine and L-nicotine.

Molecuul	Biological samples		
	Speeksel	Urine	Bloed
serotonine	-	-	10 – 1500 nM
histamine	-	200 -750 nM	10 – 1000 nM
L-nicotine	0.2 – 1000 μM	0.3 – 10 μM	-

Moleculair geïmprinte polymeren (MIPs) worden gebruikt als receptoren omdat ze robuust zijn, goedkoop geproduceerd kunnen worden en een hoge affiniteit bezitten voor hun doelmoleculen. Ze worden gesynthetiseerd door middel van bulkpolymerisatie waarna de polymeren gemalen worden om een poeder te verkrijgen. Vervolgens worden aluminium elektroden gefunctionalizeerd met

MIPs door middel van thermische behandeling. Deze worden geïntegreerd in een sensor platform dat kleine moleculen selectief kan herkennen aan de hand van twee methoden. De eerste technologie is gebaseerd op elektrochemische impedantie spectroscopie, de tweede op thermische weerstand.

Als eerste werd een MIP voor de specifieke herkenning van serotonine ontwikkeld. Verschillende MIPs werden gesynthetiseerd en diegene met de hoogste affiniteit voor serotonine is geselecteerd door middel van bindingsexperimenten met optische uitlezing. Deze MIP werd geïntegreerd in een open impedimetrische opstelling en een dosis-respons-curve is opgemeten in bufferoplossingen. Voor metingen in biologische stalen werd een verfijnde sensor ontwikkeld. Deze opstelling is volledig afgesloten, wat een groot voordeel is om oxidatie van het doelmolecule te voorkomen en patiëntveiligheid te garanderen. Een ander sterk punt is de geïntegreerde temperatuur regeling die het systeem tot op 0.02°C nauwkeurig kan controleren. Met deze opstelling werden de oorspronkelijke serotonine concentraties in bloedplasma onderzocht. De behaalde resultaten waren in overeenstemming met wat gemeten is in referentietesten met hogedruk vloeistofchromatografie. Verder werd aangetoond dat de stijging van de impedantie door de binding van serotonine verklaard kan worden door een capacitief effect dat optreedt tussen het grensvlak van de MIP partikels en de vloeistoflaag.

In deze thesis is naast serotonine ook histamine onderzocht. In vorig onderzoek werd aangetoond dat met impedimetrische uitlezing histamine concentraties bepaald kunnen worden in bufferoplossingen van pH 7 tot 9. Voor diagnostische toepassingen zou dit target molecule in een groter pH regime gedetecteerd moeten worden omdat de omgeving in de darm, waar histamine in toekomstig onderzoek in gemeten zal worden, enigszins zuur is. Om deze pH afhankelijke responsie van de MIP sensor te verklaren, hebben we een statistisch model opgesteld. Met dit model is de theoretische bindingscapaciteit van een MIP met het monomeer acrylaatzuur uitgerekend in het vereiste pH gebied. Deze resultaten zijn geverifieerd met UV-vis absorptiespectroscopie, microgravimetrie en impedantiespectroscopie. De specifieke detectie van histamine in het fysiologisch relevante nanomolair gebied in neutrale en lichtelijke zure buffer

oplossingen is aangetoond door middel van impedantiespectroscopie. Als laatste stap in het proces is het platform gebruikt om histamine concentraties te analyseren in lichtelijke zure darmsap monsters van een aantal testpersonen. Hiermee werd bewezen dat de sensor betrouwbare data verstrekt in het relevante concentratiegebied, zoals validatie met onafhankelijke ELISA-testen bevestigt.

De elektronische methodiek vereist geen dure apparatuur, heeft een korte meettijd en is specifiek genoeg om concentraties in het fysiologisch relevante zuurgraadgebied te bepalen. Naast deze techniek presenteerden we ook een alternatief die gebaseerd is op thermische weerstand. Deze methode heeft alleen twee thermometers, een aanpasbare warmtebron en een Proportioneel-Integrerend-Differentieel (PID)-regeling nodig. Het principe werkt als volgt; door binding van de doelmoleculen wordt het warmtetransport door de nanocaviteiten van de MIPs sterk gereduceerd. Als resultaat hiervan wordt de thermische weerstand hoger, de stijging is afhankelijk van de hoeveelheid die gebonden is. De eerste testen om het werkingsprincipe aan te tonen zijn gedaan met L-nicotine oplossingen in buffer. Dit werd verder uitgebreid naar de relevante target moleculen serotonine en histamine, waarvan eveneens dosis-response curves in buffer oplossingen konden worden geconstrueerd. Het was mogelijk om vergelijkbare detectielimieten te behalen als met de referentietechniek impedantiespectroscopie, die simultaan werd gemeten met de thermische weerstand. De detectielimiet is in het fysiologische relevante nanomolair regime, maar de toepasbaarheid in biologische monsters is nog niet uitgebreid getest. Als eerste demonstratie experiment werden metingen uitgevoerd met speekselmonsters waar extra L-nicotine aan was toegevoegd. Het was mogelijk om een dosis-respons curve te construeren, wat een eerste aanwijzing is dat het ook toegepast kan worden in complexe media.

De detectielimieten die behaald zijn met impedantiespectroscopie en thermische weerstand zijn opgesomd in Tabel 2.

Table 2: De behaalde detectielimieten (LOD) in 1x PBS en biologische stalen gemeten met thermische weerstand en impedantie spectroscopie.

Molecuul	Thermische weerstand		Impedantie spectroscopie		
	LOD Buffer	LOD Speeksel	LOD Buffer	LOD Bloed	LOD Darmsap
serotonine	20 nM	-	3 nM	5 nM	-
histamine	30 nM	-	15 nM	-	0.2 µM
L-nicotine	100° nM	~0.5 mM	100 nM	-	-

De detectielimiet van beide technieken, vergeleken met de fysiologisch relevante concentraties in Tabel 1, is goed genoeg om histamine en serotonine specifiek in bufferoplossingen te meten. Maar, biologische stalen zijn alleen met impedantie spectroscopie uitgebreid onderzocht. Er moet wel meegenomen worden dat de methode gebaseerd op thermische weerstand nog in zijn kinderschoenen staat en er nog steeds ruimte voor verbetering is. Een belangrijk aspect hierin is de ruis op het signaal, die sterk verminderd kan worden door parameters van de PID-regeling te optiamliseren.

Als we het kostenaspect in overweging nemen, is het grote voordeel van de MIPs dat ze goedkoop zijn door hun eenvoudige synthese. Aan de chemicaliën zijn dan ook geen grote onkosten aan verbonden. De impedantie analysator en de sensor cel zijn binnen het instituut ontwikkeld, de totale kosten voor de apparatuur zullen de 1000 euro niet overstijgen. Voor de methode die gebruikt maakt van thermische weerstand zijn alleen maar twee thermometers en een regelbare warmtebron nodig, wat zelfs nog goedkoper is. De materiaalwaarde van 10 euro per chip is om deze reden zeker realistisch.

Het andere criterium is de meettijd, die tussen de 30 en 60 min zou moeten bedragen. In onze experimenten is de gemiddelde waarde genomen van zes punten met een interval van drie minuten. Dit betekent dat het signaal tenminste 18 minuten gemoniteerd zou moeten worden, waaraan nog een stabilisatietijd van tussen de 15 en 30 minuten toegevoegd moet worden. Daarom is het zeker mogelijk om metingen uit te voeren in het gewenste tijdsbestek.

Beide technieken meten specifiek, goedkoop en snel en voldoen zo voor een groot gedeelte aan de vooraf geformuleerde criteria. Het laatste criterium, het uitvoeren van mogelijke *in vivo* metingen, is een stuk gecompliceerder. Hiervoor zou de synthese van de MIPs veranderd moeten worden; in plaats van het stempelen van de partikels op de oppervlakte zou het beter zijn de MIPs direct op de electrode te polymeriseren. Daarnaast moet gekeken worden of de MIPs en het sensor platform wel biocompatibel zijn. De laatste stap is in de richting van de industriële markt voor medische apparatuur. In hoofdstuk 5 zijn er een aantal alternatieve MIP platforms voorgesteld die beter geschikt zijn voor commerciële doeleinden. Daarnaast zijn er nog twee andere aspecten waarmee rekening gehouden moet worden voordat deze stap genomen wordt:

i)   Het uitvoeren van een klinische studie op een groter aantal biologische monsters, maar ook op stalen van zowel gezonde testpersonen als patiënten. Dit laatste is onvermijdelijk als we vast willen stellen of onze techniek sensitief genoeg is om voorkomende afwijkingen te detecteren.

ii)   Het transformeren van het sensor platform naar een array format, zodat we meerdere doelmoleculen tegelijkertijd kunnen detecteren.

Als we de meetsnelheid, lage kosten en hoge specificiteit van de ontwikkelde technieken in acht nemen, kunnen ze beschouwd worden als methoden met een hoog klinisch en marktpotentieel. Met deze methoden zou het ook mogelijk zijn een eerste stap te zetten in de richting van het integreren van MIPs in meetapparatuur voor *in vivo* doeleinden. Metingen die namelijk direct in het maagdarmkanaal uitgevoerd worden, leveren een belangrijke bijdrage in het verkrijgen van meer inzicht in het ontstaan van aandoeningen waarin het spijsverteringskanaal een rol speelt. Dit kan leiden tot de ontwikkeling van nieuwe, effectieve behandelmethoden voor dergelijke stoornissen.

.

Chapter 1

Introduction

This first chapter opens with the explanation of the Irritable Bowel Syndrome (IBS). IBS is one of the most common gastrointestinal (GI) disorders, with an estimated prevalence of 10 – 20% of the total population in Western societies. Due to its high economic impact and the significant effect on the quality of life, there is a compelling need to investigate the mechanism of the disease. This is complicated, as the underlying organic cause remains largely unknown, and is very heterogeneous. The possible role of biogenic amines, *e.g.* serotonin and histamine, is elucidated. Then, the state-of-the-art techniques for the detection of these targets are summarized after which an alternative technology, based on Molecularly Imprinted Polymers (MIPs), is presented.

Irritable Bowel Syndrome

Irritable Bowel Syndrome (IBS) is defined as follows [1]:

"Irritable Bowel Syndrome (IBS) is a functional bowel disorder in which abdominal pain or discomfort is associated with defecation or a change in bowel habit."

The most common symptoms include abdominal pain, bloating and altered bowel habit. IBS is a chronic disorder with relapsing symptoms, in the absence of detectable organic causes.

One of the most common misconceptions about IBS is that it is purely a physiological problem, frustrating many people suffering from chronic pain. There is sufficient scientific evidence to prove that IBS is an important medical clinical disorder which has a significant impact on the patient's quality of life. In addition, the burden to society related to direct and indirect health care costs exceeds most gastrointestinal disorders. Therefore, there is a compelling need to investigate the pathogenesis of the disease and to optimize treatment of the symptoms, which is complicated as the exact organic cause of IBS is still largely unknown.

In the following paragraphs we will discuss the diagnosis of IBS, its prevalence, the effect on the quality of life, economic impact and the possible role of the biogenic amines serotonin and histamine in the development of the disorder.

1.1   Diagnosis of IBS

The typical symptoms of IBS, including abdominal pain and change in bowel habit, have already been described in the early 1900s, but it was first named "Irritable Bowel Syndrome" by DeLor in 1967 [2]. At that time there was no exact classification system of the symptoms; Manning *et al.* [3] postulated a list of criteria which can indicate IBS in 1978.

Table 1 : IBS criteria postulated by Manning [3].

1. Onset of stool linked to more frequent bowel movements
2. Looser stool associated with onset of pain
3. Pain relieved by passage of stool
4. Noticeable abdominal bloating
5. Sensation of incomplete evacuation more than 25% of the time
6. Diarrhea with mucus more than 25% of the time

These criteria were proven to lack specificity; therefore at the 13th International Congress of Gastroenterology in Rome in 1988 a group of physicians refined them to improve accuracy of IBS diagnosis. These are known as the "Rome Criteria", with Rome I in 1992, Rome II in 1998 and Rome III defined in 2006. In the Rome II criteria, length of the symptoms is included and pain is issued as a cardinal requirement. Furthermore, "red flag symptoms" are incorporated in order to exclude organic causes for patient's symptoms. The "red flag symptoms" are listed in Table 2 [4].

Table 2: "Red flag" symptoms of IBS according to Rome II.

1. Pain that awakens / interferes with sleep
2. Diarrhea that awakens / interferes with sleep
3. Blood in the stool (visible or occult)
4. Weight loss
5. Fever
6. Abnormal physical examination

More recently, the Rome III criteria were adopted which criticize the differentiation of IBS into various subtypes as the stability over a prolonged period of time is unknown. These subtypes can vary from IBS with diarrhea as predominant symptom (IBS-D), IBS with mainly constipation (IBS-C) and a mixed form (IBS-M).

While the Rome II and III criteria were not developed as guidelines, they are currently considered the "golden standard" for the diagnosis of IBS. In addition to these criteria, laboratory tests should be performed to determine blood count,

basis chemistry panel and erythrocyte sedimentation rate. Diagnostic accuracy for IBS exceeds 98% when laboratory tests are negative and Rome II criteria are met [4].

1.2   Prevalence of IBS

With an estimated prevalence of 10 - 20% in western societies [5], IBS is the most common functional bowel disorder. It also accounts for the majority of gastroenterological outpatients in that region [6]. In developing countries the prevalence is generally lower, while in rapidly developing Asia the percentage is comparable to the Western world [7]. It remains difficult to compare these numbers worldwide, as in different regions other diagnostic criteria are used and not all patients seek medical care (Figure 1).
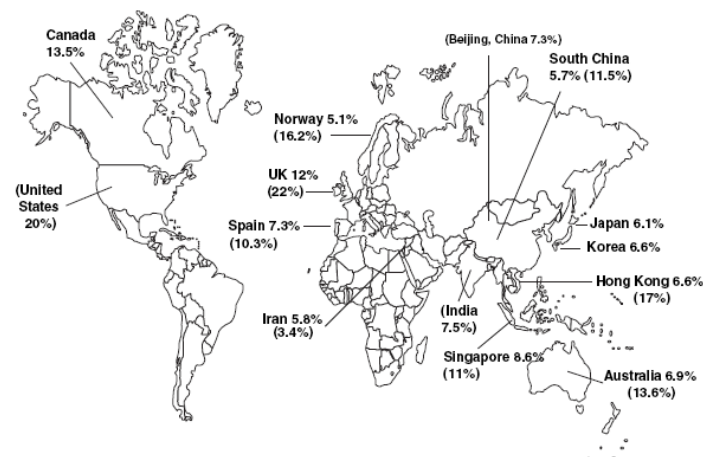
Figure 1: World map of IBS prevalence (2000 – 2004) by Rome II criteria with Manning criteria in parenthesis where available [7].

In the Western world, IBS show female predominance [8] while this is not observed in most eastern countries [9]. The gender distribution is shown in Table 3.

Table 3 : Gender distribution of IBS subjects by Rome criteria in population-based surveys [7].

Country	Year	Female to male ratio
Spain	2001	2.42
Australia	2000	2.01
Canada	2003	1.75
Japan	2004	1.73
Bangladesh	2001	1.35
China	2004	1.25
Singapore	2004	1.21
Taiwan	2003	1.05
Norway	2004	1.04
HK	2002	0.99
Iran	2003	0.93
India	2001	0.85
Korea	2001	0.85

Recently, sex related differences have been investigated due to growing evidence that men and women respond differently to treatments. To explain these differences, a variety of reasons ranging from psychosocial to physiological factors have been suggested [10], however hormonal factors might also be involved. Masculine factors, such as luteinizing hormone and testosterone, could provide some protection against IBS [11], however further research should be conducted to confirm this hypothesis.

1.3 Economic impacts of IBS and effect on quality of life

A majority of IBS patients does not consult physicians; however the cost to society in terms of direct and indirect medical expenses is considerable. A study from the United States compared IBS patients and healthy control subjects and stated the following:

1. Persons with bowel symptoms consistent to IBS miss 13.4 days of work per year compared to 4.9 days for work for persons lacking these. Furthermore, a higher number of patients with IBS symptoms reported to be too sick to go to work [11.3 vs. 4.2 %) [12].

2. In the United States, there are between 2.5 and 3.4 million physician visits for IBS per year [13], during which 2.2 million prescriptions [14] are written.

3. Health costs of $1995 compared to $1340 for those without IBS over one year [15].

In a comprehensive assessment of illness burden for GI disorders in the United States, IBS was associated with €1.6 billion in direct costs and €19.2 billion in indirect costs [16].

Health-related quality of life (HRQL) is an individual's satisfaction or happiness with domains of life insofar as they affect or are affected by health [17]. It incorporates the perception of the patient, experience of illness and functional status. Several self-administered questionnaires to study HRQL now exist for gastrointestinal (GI) disorders and IBS [18]. When compared to having other GI conditions, physical and emotional quality of life for IBS patients was poorer [19]. When looking at non-GI disorders, the HRQL is comparable to diabetes and end-stage renal disease [20], showing a serious impairment in daily life. However, quality of life can be significantly improved related to pain severity and daily function after physiological or antidepressant treatment [21].

1.4 IBS treatments

As the organic cause of IBS remains unknown, clinical treatment is focused on relieving the patient's predominant symptom. Therefore, we will present for the most common symptoms, respectively pain, constipation and diarrhea, its recommended treatments.

Pain:

- Probiotic Bifidobacterium infantis 35624 (one capsule a day) has shown to reduce pain for IBS patients, but is currently only available in the United States [22].

- Tricyclic antidepressants (TCAs) such as amitriptyline, desipramine, paroxetine and selective serotonin reuptake inhibitors (SSRIs). Low

doses of TCA (10- 50 mg per day) rather than full doses used to treat major depression are recommended for treatment of pain and sleep difficulties. Their effect on pain relieve is presumably due to their multiple receptor blocking effect and non-selective monoamine uptake inhibition [23].

Constipation:

- The probiotic strain *Bifidobacterium lactis* DN-173 010 accelerates gastrointestinal transit and increases stool frequency.
- Lubiprostone, marketed under the trade name Amitiza, can be used for women over the age of 18. It is a bicyclic fatty acid that acts on chloride channels of the gastrointestinal epithelial cells, producing a chloride-rich fluid secretion. Due to this, stool is softened and motility is increased which relieves symptoms of constipation within one week. It was approved by the Food and Drug Administration (FDA) in January 2006. In women with symptoms of IBS-C, it was proven to be more effective than placebo [24].
- Tegaserod, marketed under the name Zelnorm or Zelmac, is a 5HT-$_4$ agonist which is used for females with IBS-C. Clinical trials show significant effect of the drug, with a 14% advantage over the placebo in a female population documented with constipation [25]. It was approved for this use by the FDA in July 2002.

Diarrhea:

- Loperamide twice a day does not relief general symptoms of IBS, but is effective for the treatment of diarrhea by reducing stool frequency and improving stool consistency.
- Alosetron hydrochloride, formerly called Lonotrex, is a 5HT-$_3$ antagonist which is used for managing IBS-D of women who experience severe symptoms for longer than 6 months. It is effective in relieving pain and normalizing bowel frequency in female patients, with a 12-15% benefit compared to placebo [26]. Originally it was approved by the FDA in

February 2000, but it was withdrawn in November of that year due to severe gastrointestinal side effects. After further evaluation, the drug was reintroduced in 2002 to be used under restrictive guidelines.

The American College of Gastroenterology (ACG) has a task force to evaluate IBS therapies. According to them, physiological therapies such as cognitive therapy, dynamic psychotherapy and hypnotherapy are more effective than usual care in relieving global symptoms of IBS [27]. This might be because among the IBS patients who seek care, the majority suffers from anxiety and depression. Alternative therapies appeared to show no benefit, except a trial tested with a unique Chinese herbal mixture. However, there were significant concerns regarding the toxicity [28].

There are some new approaches being explored in phase II trial studies such as cilansetron, a 5HT-$_3$ antagonist [29], clonidine [30], buspirone [31] and the SSRI citalopram [32].

1.5 The cause of the Irritable Bowel Syndrome

The exact cause of IBS is unknown, but there are some hypotheses. The immune function of the gut might be altered, which is supported by research done on patients recovering from gastroenteritis. IBS-like symptoms were found in 7 – 30% of them [33], which is classified as Post-Infectious (PI) IBS. The patients with PI-IBS have differences in gut motility, epithelial function and an increased numbers of colonic enterochromaffin cells [34]. Another hypothesis suggests "derailing of the brain-gut axis" and that psychological factors might be important [35]. Recently, the involvement of biogenic amines such as serotonin and histamine has been postulated. In the following paragraphs, we will describe the intestinal function of these amines and their possible role in IBS.

1.5.1 The role of serotonin in the Irritable Bowel Syndrome

Serotonin (5-HT, 5-hydroxytryptamine) is a monoamine neurotransmitter which is primarily (95%) found in the gut. There, it is stored in micro vesicles in the enterochromaffin cells where it is released upon mechanical or chemical stimulation [36]. The released serotonin stimulates the mucosal nerve endings

of the enteric nervous system, thereby coordinating secretory and motor functions of the intestines [37].

Imbalances in serotonin levels in the central nervous system and intestines have been associated with various functional gastrointestinal disorders, such as IBS [38]. In IBS patients, an increased number of enterochromaffin cells and altered mucosal serotonin metabolism has been described which can be beneficially influenced by serotonergic compounds such as Tegaserod and Alosetron[38]. Additionally, research indicates the involvement of $5-HT_3$ receptors in mediating pain sensation [39]. This could partly explain the abdominal pain that IBS patient experience and also their increased susceptibility to the induction of long term depression. In transgenic mice lacking the gene for serotonin transport, symptoms similar to IBS-D are exhibited.

The research into IBS should not purely focus on the functionining of bioamines in the intestines. Serotonin enters the circulation when released from the enterochromaffin cells and therefore, it is more interesting to study its concentration in blood samples.

1.5.2 The role of histamine in the Irritable Bowel Syndrome
A physiologically stressful situation causes the release of the hormone corticotrophin which mediates the interaction and stabilization of the mast cells [40]. Mast cells, present in the circulation but also in the intestinal mucosa, especially after activiation of the immune system, release compounds such as tryptase and histamine. Barbara *et al.* studied the spontaneous release of histamine and tryptase from mucosal biopsy specimens of IBS and healthy patients. In IBS patients, this was significantly increased for histamine (+ 101%) compared to healthy controls (Figure 2) [40]. The same trend was observed for tryptase, with the activity even being higher compared to histamine (3.7 times higher for IBS patients compared to healthy controls).
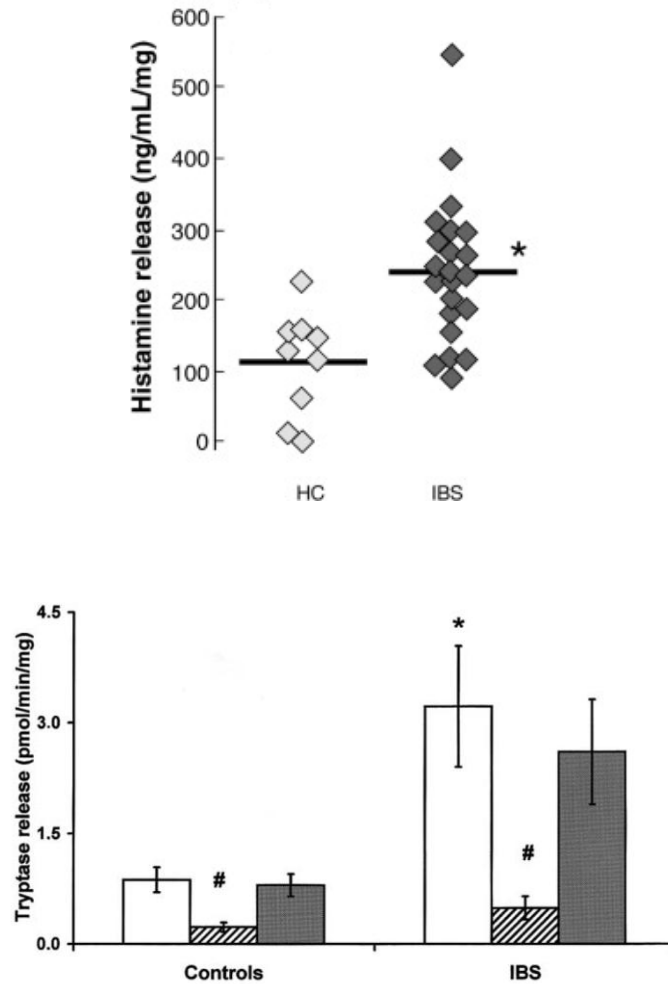
Figure 2: Spontaneous tryptase (above) release from colonic mucosal biopsies in healthy controls (HC) and IBS patients. The release of histamine is shown below. Tryptase and histamine activity was measured in the supernatant obtained after a 25-minute incubation of biopsy specimens in oxygenated buffer using an enzymatic assay [40].

This is a first indication that histamine and tryptase are possibly involved in the pathogenesis of IBS. Mast cells itself are also worth studying, since they play a role in the disturbed sensory-motor function. First, an increased number of mast cells have been detected in the colonic and ileal mucosa of patients with IBS [40, 41]. Second, the results from animal studies have demonstrated that

release of mast cell mediators leads to visceral hypersensitivity and abnormal gut motor function [41].

Therefore, histamine is another interesting biogenic amine to study. Tryptase might be another candidate, however since it is a protein it is more difficult to detect with MIPs.

1.6 Traditional detection techniques of histamine and serotonin

The most common techniques to detect histamine and serotonin are high-performance liquid chromatography (HPLC) [42], gas chromatography (GC) [43] and Enzyme-Linked Immuno Sorbent Assay (ELISA) tests [44]. These techniques ensure low detection limits and have a high specificity; drawbacks are that HPLC and GC are expensive while ELISA tests are laborious. Electrochemical techniques are inexpensive and have therefore been suggested as an alternative. In Table 4, the relevant histamine and serotonin concentrations in biological fluids are summarized.

Table 4: Concentrations of histamine and serotonin in biological samples.

Target	Biological samples		
	Saliva	Urine	Blood
Histamine	-	200 -750 nM	10 – 1000 nM
Serotonin	-	-	10 – 1500 nM

1.6.1 Electrochemical detection of serotonin

For serotonin, Sarada *et al.* [45] were able to measure serotonin in the 10 – 1000 nM range in aqueous media using amperometric detection [45]. Wu *et al.* [46] developed carbon-nanotube-coated glass electrodes suitable for cyclic voltammetry measurements in spiked human blood serum. In cyclic voltammetry, the potential for a small stationary working electrode is changed linearly with the time starting from a point in which no electrode reaction occurs and moving to potentials where reduction or oxidation of the solute takes place. Using the same technique, Kumara Swamy and Venton [47] attempted a first *in vivo* measurement in the striatum of an anesthetized rat (Figure 3 next page).
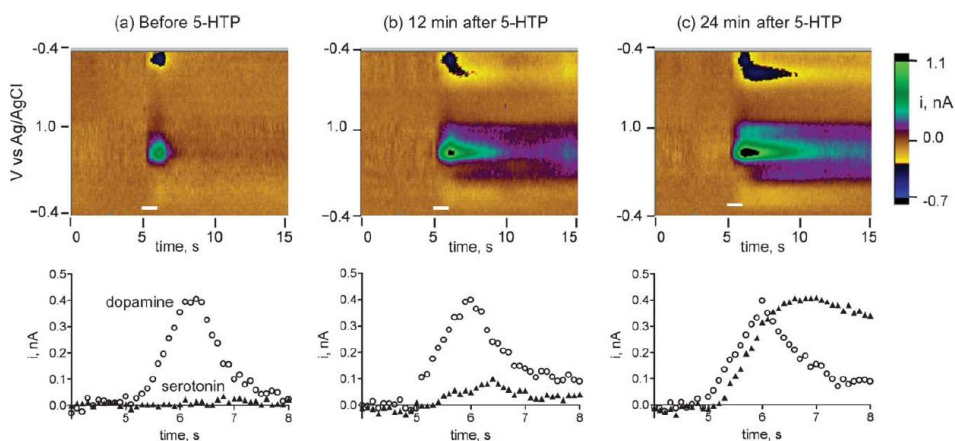
Figure 3: *In vivo* detection of dopamine and serotonin. The duration of the stimulation is marked as white below on the color plot. Plotted below each color are the current vs. time traces for the potentials where reduction peaks for dopamine (open circles) and serotonin (closed triangles) would be detected [47].

Before the serotonin precursor was administered, the plot is characteristic for dopamine release (Figure 3A). Twelve minutes after, reduction peaks for both dopamine and serotonin are observed (Figure 3B). In Figure 3C, the result after twenty-four minutes is plotted, indicating a significant release of serotonin. These results mean that upon administration of 5-HTP a change in the oxidation current is observed due to serotonin release, but this could not be quantified yet.

1.6.2. Electrochemical detection of histamine

In the case of histamine, electrochemical techniques are limited due to its high reduction potential ($\sim$1.2 V). In PBS solutions of pH 7.1, a detection limit of 20 µM was established using amperometric detection [45]. This concentration is well above the physiologically relevant concentration and further on, no tests were performed yet in biological samples. *In vitro* measurements were performed by Bitziou *et al.* [48, 49], who used boron-doped diamond electrodes in amperometric mode to detect histamine release from enterochromaffin like cells from gastric mucosa of the guinea pig stomach (Figure 4).
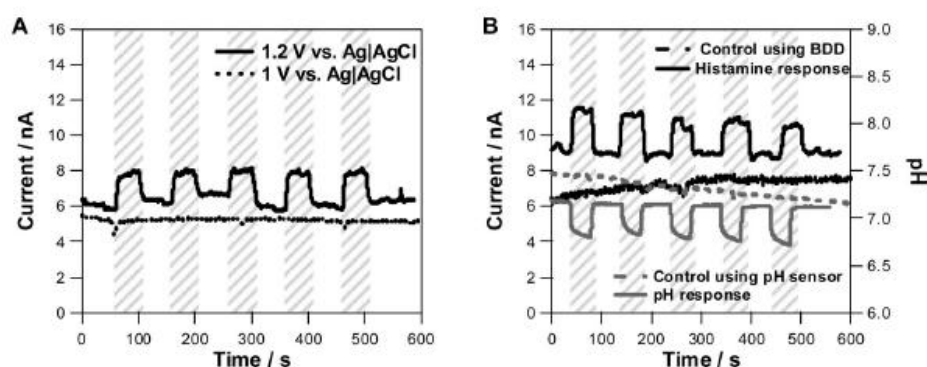
Figure 4: *In vitro* experiments conducted on guinea pig stomach. A) shows the repeated response at 1.2 V, which is sufficient to oxidize histamine, while the dashed line corresponds to 1 V which will oxidize amines such as serotonin B) shows the signal obtained from sensor with and without the tissue. The shaded grey box corresponds to the contact time between stomach tissue and sensor [49].

The sensor was proven to be stable and the signal was not influenced by other electroactive compounds, which enables qualitative measurements *in vitro*. However, quantitative measurements were not performed yet. So far, first attempts of *in vivo* measurements were done by Mochizuki *et al.* [50] and Itoh *et al.* [51]. They could make an estimate of the histamine release in the hypothalamus of anesthetized rats by *in vivo* microdialysis coupled to HPLC equipment with a fluorescence detector (Figure 5).
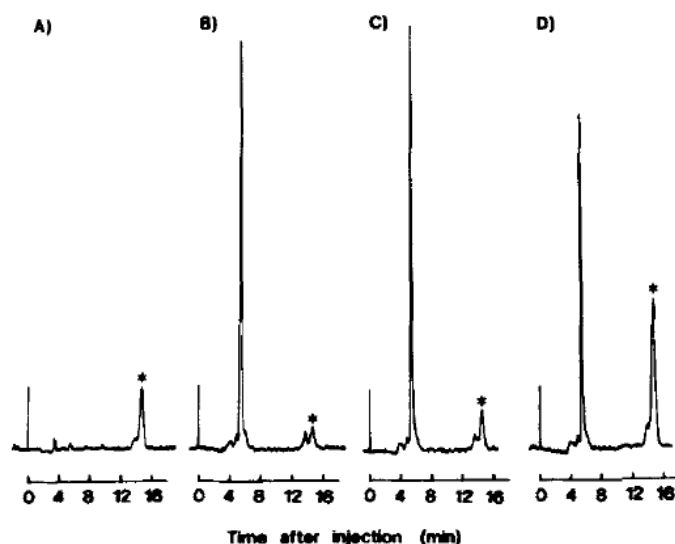
Figure 5: Chromatograms of histamine standard and microdialysates of rat hypothalamus
A) standard solution of histamine in 0.2 M of perchloric acid and one microdialysate
fraction B) before drug treatment and after treatment with C) metoprine and D)
thioperamide. The peaks of histamine are indicated with an asterisk [51].

After drug treatment, an increase in the release rate was observed. However,
this technique cannot be directly transferred to measuring *in vivo* in humans and
furthermore, no reference test with analogous molecules were performed to
demonstrate selectivity of the sensor platform.

Summarizing, HPLC, GC and ELISA tests can detect histamine and serotonin
specifically with a low-detection limit; however, all of the mentioned techniques
are either laborious or expensive. These problems can be overcome by using
electrochemical techniques, which ensure rapid and low-cost detection but are
not able yet to selectively measure histamine in biological samples. Therefore,
an alternative detection technique is proposed which is based on Molecularly
Imprinted Polymers.

1.7 Molecularly Imprinted Polymers (MIPs)

Molecularly Imprinted Polymers (MIPs) are synthetic receptors with imprinted nanocavities that are able to rebind their target molecule as specific and selective as an enzyme [52, 53]. Figure 6 schematically shows their synthesis.
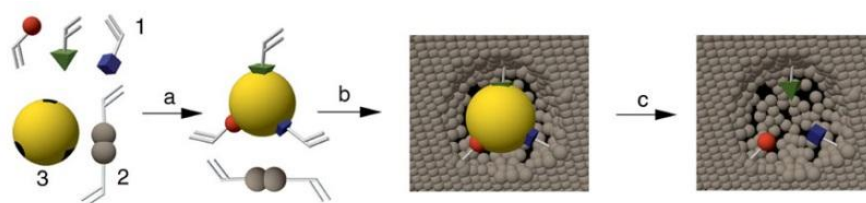
Figure 6: Schematic representation of the MIP synthesis with 1) functional monomers, 2) crosslink monomers, 3) target molecule, a) formation of prepolymerization complex, b) polymerization, c) target extraction [54].

Initially, the template and functional monomers form a prepolymerization complex through covalent or non-covalent interactions (Figure 6). The most common approach is based on non-covalent interactions as these MIPs are re-usable. Examples of non-covalent interactions include hydrogen bonds, π-π interactions, ionic interactions, hydrophobic effects and van der Waals forces. After a pre-polymerization complex is formed, cross-linking monomers are arranged and co-polymerized to form a cast-like shell. Subsequently, the target molecule is extracted by polar solvents. In this way, nanocavities are obtained that are complementary to the template and size, shape and position of the functional groups [55, 56]. Together with the MIPs, Non-Imprinted-Polymers (NIPs) are synthesized according to the same procedure but without the presence of the target molecule. The NIPs do not contain specific nanocavities like the MIP and can therefore serve as a reference material, since binding of the target can only occur in an aspecific manner. Other options to test for the specificity include imprinting with a suitable analogue in order to test the cross selectivity.

The use of MIPs offers several benefits: First, MIPs can be synthesized at a rather low-cost via established polymer-chemical routes [57]. Second, MIPs are robust and can withstand extremes of heat and pH [58, 59]. Third, MIPs

prepared according to the non-covalent approach have the potential of being regenerated [60].

Depending on the application, a different MIP morphology is required which requires some adaptation to the protocol. Traditionally, MIPs have been prepared as bulk polymer monoliths and ground to obtain micrometer-sized particles [55]. This might not be the most elegant approach, but it is commonly used due to its wide applicability and straight-forward synthesis. Monomers, template, crosslinker and initiator are dissolved into an appropriate porogen and polymerized by exposure to UV radiation or heat. The obtained polymer is a rigid block, which is subsequently ground and sieved. The sieved particles have irregular shapes with heterogenic parts due to the lack of control during the polymerization. In Figure 7, a typical Scanning Electron Microscope (SEM) image of bulk polymerized MIPs is shown, demonstrating this phenomena.
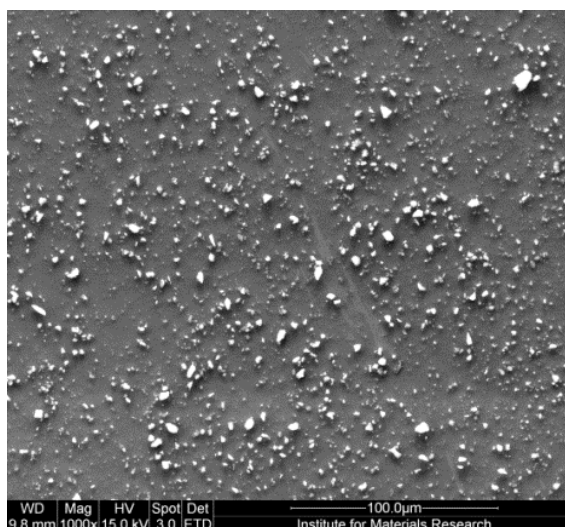
Figure 7: SEM image of bulk MIP particles.

During the past years, increasing research has been done on submicrometer-sized MIPs and thin MIP layers which can be obtained by precipitation polymerization or emulsion polymerization [59, 60]. However, in this thesis we will purely focus on bulk polymerized MIPs as they already showed good results for sensor application.

1.8 Sensor experiments

A variety of MIPs are synthesized and subsequently evaluated by batch rebinding experiments characterized by UV-vis spectroscopy. After optimization, they can be applied into a sensor setup. For separation purposes, MIPs can be readily used by packing them directly into separation columns [61]. However, the integration of MIPs into sensing devices remains challenging. One of the issues is the attachment of the particles and stability during the measurements. In the BIOS group, a method was developed to immobilize MIPs onto the surface by matrix entrapment [62]. A schematic representation is given in Figure 8.
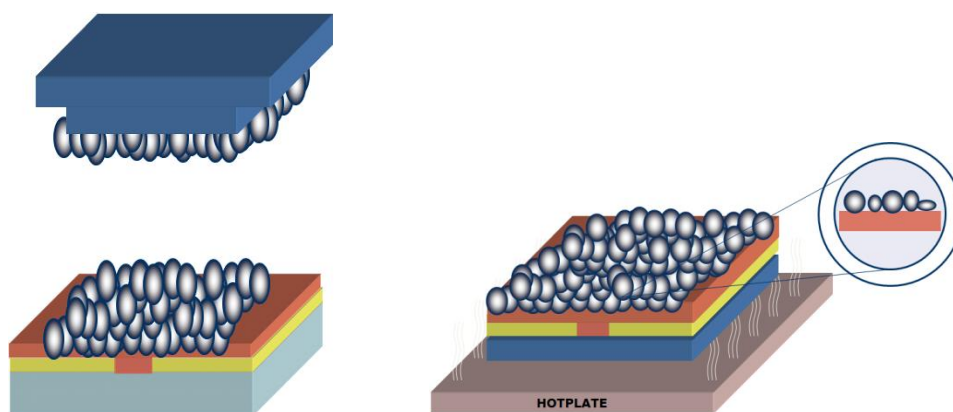
Figure 8: Immobilization method for the MIPs. First, a polydimethylsiloxane (PDMS) stamp with MIP particles is applied to the surface (left). Then, particles will sink into the polymer film layer (demonstrated right) after heating [62].

The particles are applied onto a polydimethylsiloxane (PDMS) and then pressed to the surface. The substrate is covered by an adhesive polymer layer, which will ensure good contact between the MIP particles and the sensor surface. Subsequently, the polymer adhesive layer is heated till above its glass transition temperature (T_g). Above its T_g, the polymer layer will behave more liquid-like which will cause the particles to sink partially into the layer. Thereby, they are firmly fixed into the layer and the excess particles are removed by rinsing with isopropanol.

The use of substrate and the adhesive polymer layer depends on the application. For instance, in this thesis we will present two substrates; 1) glass with aluminum electrodes deposited onto it, 2) pure aluminum. The adhesive polymer layer has to be carefully selected as depending on the detection technique, other requirements should be met. When detection is performed with a gravimetric technique such as the Quartz Crystal Microbalance (QCM), there is no need to have a conductive transducer layer and the commercially available polyvinylchloride (PVC) can be used. In the case of electrochemical and heat-transfer measurements, the semi-conductive polymer OC_1C_{10}-PolyPhenyleneVinylene (PPV) was selected. The structure of this PPV-derivative, better known as MDMO-PPV, is shown in Figure 9. At the organic chemistry group, it was synthesized via the sulfinyl precursor route [63].
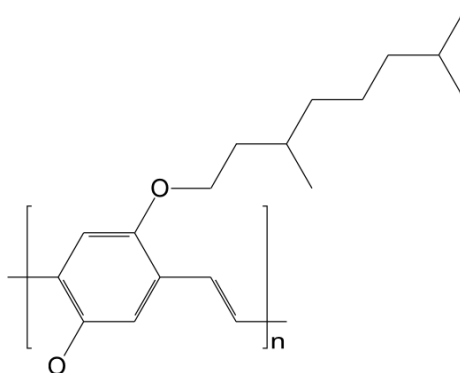
Figure 9: Chemical structure of MDMO-PPV.

When substrates are integrated into a sensor setup, there are various detection techniques. In literature, the majority is based on chromatographic techniques [64], gravimetric detection [65] and electronic read-out platforms [66]. The main drawbacks of chromatographic techniques and gravimetric detection are the often time-consuming measurements and the requirement of expensive equipment. Electrochemical analysis can overcome these problems; therefore first detection based on impedance spectroscopy was investigated. Second, a novel approach based on differential heat-transfer resistance was explored, as this requires only the use of two thermometers and an adjustable heat source.

1.9 Objectives

The main objective of this project was to develop a polymer-type sensor platform for the detection of histamine and serotonin for intestinal -and blood applications. The sensor platform should meet the following criteria:

i) Specific detection of histamine and serotonin at physiologically relevant concentrations in biological samples (Table 4).

ii) The sensor setup should perform measurements at low-cost (~10 euro per material of chip) and with a fast response time (30 – 60 min).

iii) The possibility of performing *in vivo* measurements for intestinal applications.

First, the MIPs were synthesized by bulk polymerization and then batch rebinding experiments were conducted for optimization purposes. In the case of serotonin, there are some examples of existing MIPs in literature, but reports are sparse and very recent. Therefore, a new set of MIPs was synthesized and evaluated, to determine which one was most suitable for electrochemical detection (Chapter 2).

Bongaers *et al.* [67] and Horemans *et al.* [68] presented a MIP for the specific detection of histamine in PBS solutions. However, the response of the MIP was pH dependent due to the different protonation behavior of the template and the methacrylic acid monomers [68]. As the sensor performance in acidic solutions is poor, this complicates measurements of intestinal fluid samples since the pH in the gastrointestinal tract normally varies from pH values 5–8 [69].

Therefore, a new MIP was synthesized with the monomer acrylic acid instead of methacrylic acid, because the acrylic acid monomer is relatively more acidic. This monomer was carefully selected according to a statistical binding analysis model, which will be proposed in Chapter 3.

After optimization, the MIP particles were integrated into a sensor setup. Two different measuring techniques were exploited, respectively impedance spectroscopy (Chapter 2 and 3) and differential heat-transfer resistance (Chapter 4). Furthermore, Chapter 5 is dedicated to future MIP-sensor designs in the field of mass-market consumer products.

1.9.1. The impedimetric approach (Chapter 2, 3)

The impedimetric approach is a well-known technique, which has been previously applied for the detection of L-nicotine [62] and histamine in buffer solutions [67]. With an open addition setup, it was possible to detect in the nanomolar range which is well within the range of physiologically relevant concentrations. The advantage of this open addition cell is the large liquid volume, allowing to measure concentration series rapidly, without changing the liquid, by spiking up to higher and higher concentrations. The impedance signals were measured with a commercial impedance analyzer, Iviumstat electrochemical analyzer from Ivium Technologies B.V. (Eindhoven, The Netherlands). There are some limitations to the open-cell concept with in-plane electrodes, including the contact with ambient oxygen and the relatively long measurement time.

Therefore, a refined sensor cell concept was developed for the measurements of biological samples (Chapter 2). In contrast to the addition setup, this was a flow through setup with an internal liquid volume of only 110 µl. Patient's samples could be safely administered and there is no influence of the ambient air. Furthermore, the cell featured an integrated heating element, enabling strict temperature control and stand-alone operation without the need for temperature regulation in a furnace. The impedance is measured with a homemade setup [70]. AC potentials (~10 mV) were applied in a frequency range of 100 Hz to 100 kHz, covering 10 frequencies per decade with a scanning speed of 5.7 s per sweep. The potential was applied between the MIP-functionalized working electrode and the counter electrode in the liquid. The increased speed of the systems allows electrochemical modeling of the system. With an equivalent circuit model, we could determine that the observed increase in impedance is caused by a capacitance decrease at the interface between the MIP particles and

the fluid. As a next step, biological samples were investigated starting with plasma. When serotonin is released from the enterochromaffin cells in the gut, it enters the circulation where it is taken up by blood platelets [71]. Only a small, but physiologically relevant fraction is present in the plasma as free serotonin. The platelet poor plasma concentration of serotonin will give an important insight into the role of serotonin in heatlh and disease. With spiked samples a calibration curve was constructed, after which initial plasma concentrations could be determined. The determined concentrations showed small uncertainties and are in perfect agreement with HPLC reference tests, as it was illustrated using samples from two different subjects [72]. From a physiological point of view, it bears no relevance to determine serotonin concentrations in intestinal fluid samples. Therefore, the intestinal fluid samples were investigated for its histamine concentration as levels in intestinal fluid samples are associated with gastrointestinal stress (Chapter 3). The same protocol was applied as for the plasma measurements, with first constructing a dose-response curve after which initial concentrations could be determined. Three intestinal fluid samples were measured and the determined histamine concentrations were in nice agreement with ELISA reference tests [73].

1.9.2. The differential heat-transfer resistance approach (Chapter 4)

Impedimetric analysis offers rapid and low-cost detection, however sophisticated equipment is still required. With an approach based on differential heat-transfer resistance, measurements can be performed with only two thermometers and one adjustable heat source. On the other hand, this technique still needs some mathematical operations which can be considered a certain drawback when the system is implemented into a laboratory environment. This concept has been recently applied in the field of DNA mutation analysis [74] and for the selective detection of cancer cells with structural imprinting [75]. To our knowledge, this has not been employed yet for the detection of small molecules with MIP-type receptors.

Proof-of-principle experiments were performed with a MIP for L-nicotine. This MIP was previously used by Thoelen *et al.* [62] to detect L-nicotine in buffer solutions with an addition impedimetric setup. For the thermal resistance experiments, the refined sensor cell was applied which can measure the

impedance signals and the R_{th} simultaneously, providing direct validation of the results. Upon exposing the MIP to L-nicotine concentrations in PBS, we observed an increase in the overall R_{th}. We propose that after binding of the target in the nanocavity, the heat-transfer in the direction of the template is strongly reduced. The more will be bound, the more pronounced this effect will be until a saturation level is achieved [76]. After successful testing of L-nicotine in PBS, it was extended to the molecules serotonin and histamine as these targets are the main interest of this thesis. With these MIPs and templates, the same behavior was exhibited and again an increase of the heat-transfer resistance was seen. Subsequently, with the differential heat-transfer resistance results, the corresponding dose-response curves could be constructed for L-nicotine, histamine and serotonin in buffer solutions.

As first proof-of-application, saliva samples spiked with L-nicotine were evaluated and a dose-response curve is given. This is a first indication for the detection of small organic molecules in complex media, but more experiments with different biological samples should be conducted for this purpose.

1.9.3. Future sensor design (Chapter 5)

The impedimetric and heat-transfer resistance approaches fulfill the requirements of rapid and low-cost detection in biological samples. For commercialization purposes, the design should be further optimized. Important aspects are the miniaturization of the sensor setup and the production in mass quantities. In Chapter 5, some examples are given of future MIP-sensor designs for application in mass-market consumer products or home-diagnostics [77, 78, 79].

1.8 References

[1]   W.G. Thompson, G.F. Longstreth, D.A. Drossman, K.W. Heaton; E.J. Irvine, S.A. Muller-Lissner, *Gut*, 1999, **45**, 1143-1147.

[2]   C.J. DeLor, *Am. J. Gastroenterol.,* 1967, **47**, 427-434.

[3]   A. Manning, A.W. Thompson, K. Heaton, A. Morris, *Br Med J.,* 1978, **2**, 653-654.

[4]   S.J. Vanner, W.T. Depew, W. Paterson, L.R. DaCosta, A.G. Groll, J.B. Simon, M. Djurfeldt, *Am J Gastroenterol.,* 1999, **94**, 2912-2917.

[5]   R. Jones, S. Lydeard, *Br Med J.,* 1992, **304**, 87-90.

[6]   R.F. Harvey, S.Y. Salih, A.E. Read, *Lancet*, 1983, **1**, 632-634.

[7]   K.A. Gwee, *Neurogastroenterol Motil.,* 2005, **17**, 317-324.

[8]   F. Mearin, X. Badia, A. Balboa, *Scand J Gastroenterol.,* 2001, **36**, 1155-1161.

[9]   H. Kumano, H. Kaiya, K. Yoshiuchi, G. Yamanaka, T. Sasaki, T. Kuboki, *Am J Gastroenterol.,* 2004, **99**, 370-375.

[10]   I.O. Olubuyide, F. Olawuyi, A.A. Fasanmade, *Dig Dis Sci.,* 1995, **40**, 938-985.

[11]   L.A. Houghton, N.A. Jackson, P.J. Whorwell, J. Moriss, *Am J Gastroenterol.,* 2000, **100**, 591-595.

[12]   D.A. Drossman, Z. Li, E. Andruzzi, R.D. Temple, N.J. Talley, W.G. Thompson, W.E. Whitehead, J. Janssens, P. Funch-Jensen, E. Corazziari, J.E. Richter, G.G. Koch, *Dig Dis Sci.,* 1993, **38**, 1569-1580.

[13]   J.E. Everhart, P.F. Renault, *Gastroenterology,* 1991, 100, 998-1005.

[14]   R.S. Sandler, *Gastroenterology,* 1990, **99**, 409-415.

[15]   R.L. Levy, M. Von Korff, W.E. Whitehead, P. Stang, K. Saunders, P. Jhingran, V. Barghout, A.D. Feld, *Am J Gastroenterol.,* 2001, **96**, 3122-3129.

[16]   R. Sandler, J.E. Everhart, M. Donowitz, E. Adams, K. Cronin, C. Goodman, E. Gemmen, S. Shah, A. Avdic, R. Rubin, *Gastroenterology,* 2002, **122**, 1500-1511.

[17]   G.H. Guyatt, D.H. Feeny, D.L. Patrick, *Ann Intern Med.,* 1993, **118**, 622-629.

[18]   F.A. Luscombe, *Qual Life Res.,* 2000, **9**, 161-176.

[19]   B.A. Hahn, L.J. Kirchdörfer, S. Fullerton, E. Mayer, *Aliment Pharmacol Ther.,* 1997, **11**, 547-552.

[20]   I.M. Gralnek, R.D. Hays, A. Kilbourne, B. Naliboff, E. Mayer, *Gastroenterology,* 2000, **119,** 655-660.

[21]   E.B. Blanchard, S.P. Schwartz, D.F. Neff, M.A. Gerardi, *Behav Res Ther.,* 1988, **26**, 187-190.

[22]   P.J. Whorwell, L. Altringer J. Morel, Y. Bond, D. Charbonneau, L. O'Mahony, B. Kiely, F. Shanahan, E.M. Quigley, *Am J Gastroenterol.,* 2006, **101**, 1581-1590.

[23]   E. Richelson, *Mayo Clin Proc.,* 2001, **76**, 511-527.

[24]   L.A. Sobrera, J. Castaner, *Drugs of the Future,* 2004, **29**, 336-337.

[25]   S. Müller-Lissner, I. Fumagalli, K.D. Bardhan, F. Pace, B. Nault, E.C. Pecher, *Gastroenterology,* 2000, **116 (Supll 2**), A175.

[26]   M. Camilleri, E.A. Mayer, D.A. Drossman, A.T. Heath, G.E. Dukes, D. McSorley, S. Kong, A.W. Mangel, A.R. Northcutt, *Aliment Pharmacol Ther.,* 1999, **13**, 1149-1159.

[27]   L. J. Brandt, W.D. Chey, A.E. Foxx-Orenstein, L.R. Schiller, B.M. Spiegel, N.J. Talley, E.M.M. Quigley, P. Moayyedi, *Am J Gastroenterol.,* 2009, **104**, S1.

[28]   A. Bensoussan, N.J. Talley, M. Hing, R. Menzies, A. Guo, M. Ngu, *JAMA.,* 1998, **280**, 1585-1589.

[29]   S. Caras, G. Krause, E. Biesenheuvel, C. Steinborn, *Gastroenterology,* 2001, **120**, A217.

[30]   A.E. Bharucha, M. Camilleri, A.R. Zinsmeister, R.B. Hanson, *Am J Physiol.,* 1997, **273**, G997-G1006.

[31]   J. Tack, H. Piessevaux, B. Coulie, B. Fischler, V. De Gucht, J. Janssens, *Gastroenterology,* 1999, **116**, A325.

[32]   D. Broekaert, R. Vos, A.M. Gevers, J. Janssens, J. Vandenberghe, B. Fischler, J. Tack, *Gastroenterology,* 2001, **120,** A641.

[33]   K.R. Neal, J. Hebden, R. Spiller, *BMJ.,* 1997, **7083**, 779-782.

[34]   R.C. Spiller, D. Jenkins, J.P. Thornley, J.M. Hebden, T. Wright, M. Skinner, K. Neal, *Gut,* 2000, **47**, 804-811.

[35]   W.C. Orr, M.D. Crowell, B. Lin, M.J. Harnish, J.D. Chen, *Gut,* 1997, **41**, 390-393.

[36]   M.D. Gershon, J. Tack, *Gastroenterology,* 2007, **132**, 397-414.

[37]   M. Lesurtel, C. Soll, R. Graf, P.A. Clavien, *Cell Mol Life Sci.,* 2008, **65**, 940-952.

[38]   D. Keszthelyi, F.J. Troost, A.A.M. Masclee, *Neurogastroenterol Motil.,* 2009, **21**, 1239-1249.

[39]   S. Ludidi, J.M. Conchillo, D. Keszthelyi, C.J. Koning, S.A. Vanhoutvin, P.J. Lindsey, A.M. Leufkens, J.W. Kruimel, D.M. Jonkers, A.A.M. Masclee, *Neurogastroenterol Motil.,* 2012, **24**, 47-53.

[40]   G. Barbara, V. Stanghellini, R. De Giorgio, C. Cremon, G.S. Cottrell, D. Santini, G. Pasquinelli, A.M. Morselli-Labate, E.F. Grady, N.W. Bunnett, S.M. Collins, R. Corinaldesi, *Gastroenterology,* 2004, **126**, 693-702.

[41]   V.S. Chadwick, W. Chen, D. Shu, B. Paulus, P.B. jr Miner, *Dig Dis Sci.,* 1993, **38**, 1590-1595.

[42]   T. Yoshitake, F. Ichinose, H. Yoshida, K Todoroki, J. Kehr, O. Inoue, H. Nohta, M. Yamaguchi, *Biomed Chromatogr.,* 2003, **17**, 509-516.

[43]   J.J. Keyzer, B.G. Wolthers, F.A. Muskiet, H. Breukelman, H.F. Kauffman, K. De Vries, *Anal Biochem.,* 1984, **139**, 474-481.

[44]   A. Ujike, Y. Ishikawa, M. Ono, T. Yuasa, T. Yoshino, M. Fukimoto, J.V. Ravetch, T. Takai, *J Exp Med.,* 1999, **10**, 1573-1579.

[45]   B.V. Sarada, T.N. Rao, D.A. Tryk, A. Fujishima, *Anal Chem.,* **72**, 1632-1638.

[46]   K. Wu, J. Fei, S. Hu, *Anal Biochem.,* 2003, **318**, 100-106.

[47]   B.E. Kumara Swamy, B.J. Venton, *Analyst,* 2007, **132,** 876-884.

[48]   E. Bitziou, D. O'Hare, B.A. Patel, *Anal Chem.,* 2008, **80**, 8733-8740.

[49]   E. Bitziou, B.A. Patel, *Am J Physiol Gastrointest Liver Physiol.,* 2012, **303**, 396-403.

[50]   T. Mochizuki, A. Yamatodani, M. Okakura, M. Takemura, N. Inagaki, H. Wada, *Naunyn-Schmiedeberg's Arch. Pharmacol.* 1991, **343**, 190-195.

[51]   Y. Itoh, R. Oishi, M. Nishibori, K. Saeki, *J Neurochem.,* 1991, **56**, 769-774.

[52]   K. Mosbach, *Trends Biochem Sci.,* 1994, **19**, 9-14.

[53]   R. Arshady, K. Mosbach, *Chem Phys.* 1981, **182**, 687-692.

[54]   K. Haupt, *Chem Commun.,* 2003, **2,** 171-178.

[55]   K. Haupt, *Anal Chem.,* 2003, **75**, 376-383.

[56]   J.O. Mahony, A. Molinelli, K. Nolan, M.R. Smyth, B Mizaikoff, *Biosens Bioelectron.,* 2006, **21**, 1383-1392.

[57]   G. Wulff, *Trends Biotechnol.,* 1993, **11**, 85-87.

[58]   K. Owens, L. Karlsson, E.S.M. Lutz, L.I. Andersson, *TrAC, Trends Anal Chem.,* 1999, **18**, 146-154.

[59]   B. Sellergren, C.J. Allender, *Adv Drug Delivery Rev.,* 2005, **57**, 1733-1741.

[60]   D.A. Spivak, *Adv Drug Delivery Rev.,* 2005, **57**, 1779-1794.

[61]   E. Benito-Pena, J.L. Urraca, B. Sellergren, M.C. Moreno-Bondi, *J Chromatogr A.,* 2008, **1208**, 62-70.

[62]   R. Thoelen, R. Vansweevelt, J. Duchateau, F. Horemans, J. D'Haen, L. Lutsen, D. Vanderzande, M. Ameloot, M. vandeVen, T.J. Cleij, P. Wagner, *Biosens Bioelectron.,* 2008, **23**, 913-918.

[63]   D. Louwet, D. Vanderzande, A. Gelan, *Synth Met.,* 1995, **69**, 509-510.

[64]   L.I. Andersson, A. Miyabayashi, D.J. O'Shanessy, K. Mosbach, *J Chromatogr.,* 1990, **516**, 323-331.

[65]   M. Avila, M. Zougah, A. Escarpa, A. Rios, *Trends Anal Chem.,* **27**, 54-65.

[66]   S.A. Piletsky, A.P.F. Turner, *Electroanalysis,* 2002, **13**, 317-323.

[67]   E. Bongaers, J. Alenus, F. Horemans, A. Weustenraed, L. Lutsen, D. Vanderzande, T.J. Cleij, F.J. Troost, R.J. Brummer, P. Wagner, *Phys Status Solidi A.,* 2010, **207**, 838-843.

[68]   F. Horemans, J. Alenus, E. Bongaers, A. Weustenraed, R. Thoelen, J. Duchateau, L. Lutsen, D. Vanderzande, P. Wagner, T.J Cleij, *Sens Actuators B.,* 2010, **148***, 392-398.

[69]   D.F. Evans, G. Pye, R. Bramley, A.G. Clark, T.J. Dyson, J.D. Hardcastle, *Gut,* 1988, **29**, 1035-1041.

[70]   B. van Grinsven, T. Vandenryt, S. Duchateau, A. Gaulke, L. Grieten, R. Thoelen, S. Ingebrandt, W. De Ceuninck, P. Wagner, *Phys Status Solidi A.,* 2011, **207**, 919-923.

[71]   M.W. King, M. Berger, J.A. Gray, B.L. Roth, *Annu Rev Med.,* 2009, **60**, 355-366.

[72]   M. Peeters, F.J. Troost, B. Van Grinsven, F. Horemans, J. Alenus, M.S. Murib, D. Keszthelyi, A. Ethirajan, R. Thoelen, T.J. Cleij, P. Wagner, *Sens Actuators B.,* 2012, **171**, 602-610.

[73]   M. Peeters, F.J. Troost, R.H.G Mingels, T. Welsch, B. van Grinsven, T. Vranken, S. Ingebrandt, R. Thoelen, T.J. Cleij, P. Wagner, *Anal Chem.,* 2013, **85**, 1475-1483.

[74]   B. van Grinsven, N. Vanden Bon, H. Strauven, L. Grieten, M.S. Murib, K.L. Jiménez Monroy, S.D. Janssens, K. Haenen, M.J. Schöning, V. Vermeeren, M. Ameloot, L. Michiels, R. Thoelen, W. De Ceuninck, P. Wagner, *ACS Nano,* 2012, **6**, 2712-2721.

[75]   K. Eersels, B. van Grinsven, A. Ethirajan, S. Timmermans, K. J. Monroy, J.F.J. Bogie, S. Punniyakoti, T. Vandenryt, J.A. Hendriks, T.J. Cleij, M.J.A.P. Daemen, V. Somers, W. De Ceuninck, P. Wagner, *submitted to ACS applied materials and interfaces.*

[76]   M. Peeters, P. Csipai, B. Geerets, A. Weustenraed, B. van Grinsven, R. Thoelen, J. Gruber, W. De Ceuninck, T.J. Cleij, F.J. Troost, P. Wagner, *accepted by Analytical and Bioanalytical Chemistry,* DOI: 10.1007/s00216-013-7024-9.

[77]   J. Broeders, S. Duchateau, B. van Grinsven, W. Vanaken, M. Peeters, R. Thoelen, T. J. Cleij, P. Wagner and W. De Ceuninck. *Phys Status Solidi A.*, 2011, **208**, 1357–1363

[78]   J. Broeders, D. Croux, M. Peeters, T. Beyens, S. Duchateau, T.J. Cleij, P. Wagner, R. Thoelen, W. De Ceuninck, accepted by IEEE Sensors Journal. DOI 10.1109/JSEN.2013.2256346

[79]   D. Croux, T. Vangerven, J. Broeders, J. Boutsen, M. Peeters, S. Duchateau, T.J. Cleij, W. Deferme, P. Wagner, R. Thoelen, W. De Ceuninck, *Phys Status Solidi A,* 2012, DOI: 10.1002/pssa.201200743.

Chapter 2

MIP-based biomimetic sensor for the electronic detection of serotonin in human blood plasma

M. Peeters[1], F.J. Troost[2], B. Van Grinsven[1], F. Horemans[1], J. Alenus[1], M.S. Murib[1], D. Keszthelyi[2], A. Ethirajan[1], R. Thoelen[1,3], T.J. Cleij[1] and P. Wagner[1,4]

1)   Hasselt University, Institute for Materials Research, Wetenschapspark 1, B-3590 Diepenbeek, Belgium

2)   Department of Internal Medicine, div. of Gastroenterology – Hepatology, Maastricht University Medical Center, Minderbroedersberg 4-6, 6211 LK Maastricht, The Netherlands.

2)   XIOS University College Limburg, Department of Electronic Engineering, Agoralaan Building H, B-3590 Diepenbeek, Belgium

3)   IMEC vzw – Division IMOMEC, Wetenschapspark 1, B-3590 Diepenbeek, Belgium

2.1 Abstract

Serotonin is an important signaling molecule in the human body. The detection of serotonin is commonly performed by high performance liquid chromatography (HPLC), which is costly and time consuming due to extensive sample preparation. We will show that these problems can be overcome by using molecularly imprinted polymers (MIPs) as synthetic receptors in combination with impedance spectroscopy as read-out technique. The MIPs were prepared with several blends of the underlying monomers and the best performing MIP material was selected by optical batch-rebinding experiments. MIP microparticles were then integrated in an impedimetric sensor cell and dose-response curves were measured in PBS buffer and in non-diluted blood plasma. The sensor provides reliable data in the physiologically relevant concentration regime as an independent validation by HPLC measurements demonstrates. Finally, we show that the impedimetric response upon serotonin binding can be attributed to a capacitive effect at the interface between the MIP particles and the plasma.

2.2 Introduction

Serotonin (5-hydroxytryptamine, 5-HT) is a metabolite of the essential amino acid tryptophan and its role in smooth muscle concentration was already reported in 1951 [1]. The structure of serotonin, its natural metabolite 5-hydroxyindole acetic acid (5-HIAA) and its oxidation product are shown in Figure 1.
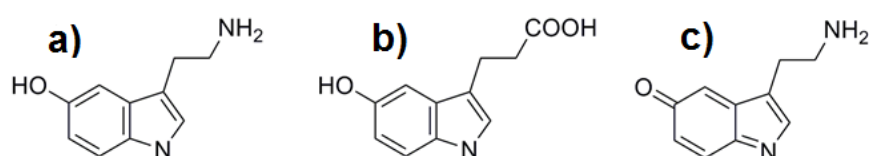
Figure 1: The structure of serotonin (a), its metabolite 5-HIAA (b) and the chemical oxidation product (c).

The role of serotonin in gastrointestinal orders has already been described in section 1.5.1, but the serotoninergic system is also involved in steering numerous behavioural and physiological function including emotions, sleep and appetite [2]. Abnormalities of serotonin-related processes in the central nervous system can lead to severe mental disorders including anorexia, depression, and schizophrenia [2, 3]. Also, anomalous serotonin levels are found in patients with hypertension [4], migraine, fibrotic syndrome, and carcinoid tumors [5, 6]. For diagnostic purposes, serotonin concentrations are usually analysed in portal blood and in the system circulation, where plasma levels of 5 – 20 nM define the typical range for healthy individuals [6, 7].

Serotonin belongs to the class of indoles and this group of aromatic, heterocyclic molecules is sensitive to light, oxygen and changes in pH. Therefore, special precautions must be taken to prevent oxidation during preparation and handling of patient's samples [8, 9]. Techniques such as solvent extraction and ion exchange chromatography require extensive sample preparation and are aspecific with respect to the indole species [10]. These problems can be overcome by HPLC, which can distinguish between different indoles. Therefore, it is currently the most common technique in the field [11], but it is especially

costly and unsuitable for routine tests [2]. Electrochemical techniques are a low-cost alternative, but it not possible yet to measure serotonin specifically and quantitatively in biological samples.

An alternative route to serotonin detection can be found in molecular imprinting. Literature reports on the synthesis of MIPs for serotonin recognition are sparse and very recent: Kitade *et al.* developed a MIP with methacrylic acid (MAA) as functional monomer [12]. Analysis with optical spectrometry allowed a detection limit of 1 µM in water. Okutucu and Telefoncu also used MAA as monomer and packed the MIPs obtained by bulkpolymerization into separation columns. The analysis of plasma platelet samples spiked with serotonin was performed by HPLC [13]. After further optimization, Okutucu and coworkers detected spiked serotonin concentrations in the µM range in human blood [14]. Khurshid *et al.* combined the charged monomer MAA with the neutral monomer methacrylamide to detect 1 mM of serotonin in dimethylformamide with a microplate reader [15].

While the synthesis of the MIPs is low-cost, the aforementioned detection techniques are still not suited for point-of-care applications. This can be solved by combining MIP receptors with electronic read-out strategies. In previous work, first examples were demonstrated with MIP-based impedimetic sensors for L-nicotine [16] and histamine [17, 18]. These sensors have detection limits of 2 nM in buffer solutions, but the functioning in biological media was not yet demonstrated. Other read-out techniques for MIP-based receptors, such as voltammetry and quartz crystal microbalances, have also been reported, but the detectable concentration is generally in the millimolar or micromolar range [18, 19]. Since the serotonin level in human blood plasma is typically 5 – 20 nM, impedance spectroscopy is therefore our method of choice. To our knowledge, there are no previous reports in literature combining the molecular imprinting of serotonin with impedimetric read-out.

The goal of this study was threefold: First, we aimed to optimize the monomer blends and MIP synthesis with respect to affinity and selectivity. Especially, the MIPs should allow discriminating between serotonin, its oxidized form and its

metabolite (5-HIAA). Next, the goal was to develop an impedimetric sensor that can cope with the fast oxidation of serotonin and special care needs to be taken to circumvent non-specific responses from competing molecules in the complex matrix of human blood plasma. To this end, NIPs will be used as a reference channel. Finally, we aimed to set up equivalent-circuit modelling to assist in the understanding in the physical origin of the impedance increase, which is observed upon the molecular recognition of serotonin at the MIP-coated sensor electrodes.

2.3 Materials & Methods

2.3.1 Chemical reagents

Ethylene glycol dimethacrylate (EGDM), methacrylic acid (MAA), acrylamide (AM) and porogen dimethylsulfoxide (DMSO) were purchased from Acros (Geel, Belgium). Prior to polymerization, the stabilizers in the MAA and EGDM were removed by filtration over alumina. The initiator azobisisobutyronitrile (AIBN) was purchased from Fluka (Buchs, Switzerland). The target molecule serotonin and its competitor, the metabolite 5-HIAA, were obtained from Acros. All solvents (Acros) were of analytical grade and used without further purification. The polyphenylenevinylene (PPV) derivative, better known as MDMO-PPV, serves as the immobilization layer on the impedimetric sensor electrodes and was synthesized *via* the sulfinyl precursor route [20]. All chemical and physical properties of this conjugated polymer were in agreement with previously reported data. For the impedance measurements, a home-made 1x PBS solution was used.

2.3.2 MIP polymerization

The MIP synthesis was optimized to achieve a high affinity and specificity for serotonin. The combination of two functional monomers, MAA and AM, was studied by varying the monomer ratios. The following MAA : AM ratios were considered: 1 : 0, 1 : 1, 1 : 3 and 0 : 1. As a measure of the specificity, the imprint factor was selected, which corresponds to the amount of target molecules bound per gram of MIP divided by that of the NIP. The imprint factors were determined by optical batch rebinding experiments at a free target

concentration of 0.3 mM using a Varian Cary 500 UV-vis-NIR spectrophotometer (Leuven, Belgium). The imprint factors are shown in Table 1.

Table 1: The imprint factors (serotonin's C_f = 0.3 mM) depending on the ratio of the monomers MAA/ AM.

MAA ratio	AM ratio	Imprint factor
1	0	0.9
1	1	1.4
3	1	0.9
1	3	3.6
0	1	1.0

Briefly summarized, MIPs composed of solely MAA or AM did not show specific binding properties. Upon mixing MAA and AM in a 1 : 1 ratio, a slightly improved imprint factor (1.4) was achieved. The highest imprint factor was obtained with the MIPs synthesized from the 1 : 3 (MAA : AM) blend. This MIP was prepared as follows: First, a mixture of MAA (2.84 mmol), AM (8.5 mmol), EGDM (22.72 mmol) and AIBN (0.61 mmol) was dissolved into 7 ml of DMSO together with the template molecule serotonin (5.67 mmol). This solution was degassed with N_2 and polymerized in a UV oven for 12 h. After polymerization, the bulk polymer was ground and sieved to obtain microparticles with a size smaller than 25 µm.

Finally, the serotonin was removed from the MIP powders by Soxhlet extraction with methanol (48 h), a mixture of acetic acid / acetonitrile (1/1) (48 h) and again methanol (12 h). The extracted powders were dried in vacuum for 12 h. A non-imprinted polymer (NIP) was synthesized accordingly, but without the presence of the target molecule. These MIP and NIP powders were used in all further bath-rebinding experiments and impedimetric measurements.

2.3.3. Preparation of blood-plasma samples and HPLC characterization
Blood samples were obtained from three healthy subjects, person A, B and C, and divided over 4 ml K_2EDTA tubes in order to prevent coagulation. The blood collection tubes also contained 0.1 ml of ascorbic acid (1.4 g ascorbic acid / 100

ml distilled water). This addition is necessary to prevent the oxidation of serotonin to 5-HIAA by the enzyme monoamine oxidase, which normally occurs within several seconds. It was proven earlier that this treatment guarantees the stability of serotonin [9]. After collection, the tubes were kept at 0°C and subsequently centrifuged with 2000 g for 10 min in order to obtain blood plasma. The as-prepared plasma samples were stored in Eppendorf tubes at -80°C until analysis. For analysis, the plasma samples were divided into six different aliquots. One part was kept as a reference and remained unaltered, while the other parts were spiked with 50, 100, 150, 200 and 250 nM serotonin During handling, the samples were kept at 4°C to minimize enzymatic oxidation prior to analysis. Shortly before measuring, the samples were warmed up to 37 °C.

Reference HPLC measurements were conducted on the plasma samples of person B and C. These measurements were performed according to the protocol described by Danaceau *et al.* [9] in order to verify the native concentrations as obtained by impedimetric read-out. For person B, the serotonin level according to HPLC was 11.2 nM and for person C it was 8.9 nM.

2.3.4. Impedance spectroscopy platforms

Two different impedimetric setups were used. For proof-of-principle experiments concerning the electronic detection of serotonin in PBS buffer, we used an open impedimetric sensor cell which was previously described by Bongaers *et al.* for the detection of histamine [17]. This setup is schematically shown in Figure 2.
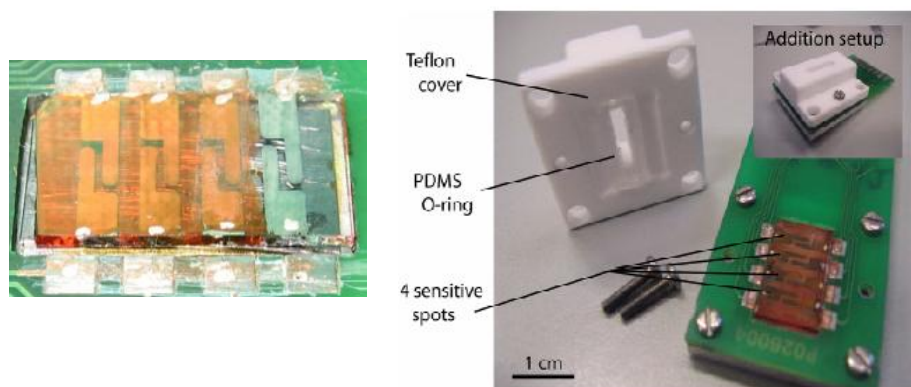
Figure 2: The sample for the open addition setup (left) and the setup containing a Teflon hood (right). Figure adopted from thesis Ronald Thoelen.

The electrode couples, one respectively for the MIP and one for the NIP, have a planar geometry. The particles are loaded onto the electrodes by using MDMO-PPV as adhesive polymer in combination with stamping and thermal treatment. The impedance was measured with the commercially available Iviumstat analyzer from Ivium Technologies B.V. (Eindhoven, the Netherlands).

In order to perform serotonin detection in a complicated medium such as blood plasma, a refined sensor-cell concept was designed (Figure 3). This ensured safe administration of patient's samples and suppressed serotonin's oxidation by ambient air to the widest extend. Furthermore, a heating element was integrated which strictly controlled the temperature at 37 ± 0.02 °C with a homemade PID controller. This eliminates the need for temperature regulation in a furnace, allowing better stabilization of the system.
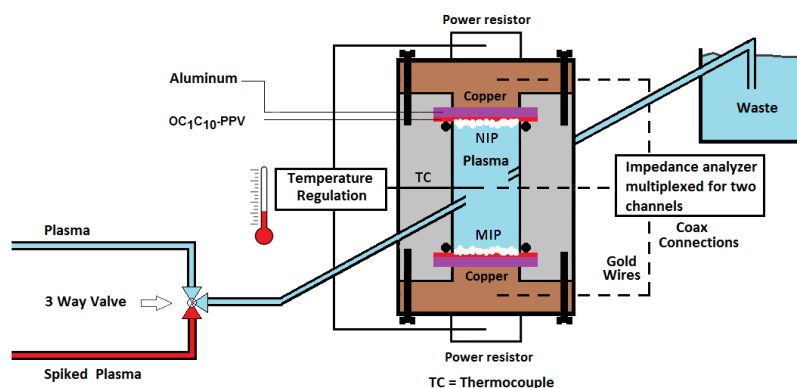
Figure 3: Schematic layout of the impedimetric flow cell for plasma measurements with an active channel (MIP) and a reference channel (NIP). The liquids are sequentially administered by a syringe-driven pump system. The temperature of the liquid is actively regulated for autonomous operation of the setup.

When dealing with a complex matrix such as blood derivatives, the non-specific responses from competing molecules can be stronger than the signals from specific recognition. To identify the specific signal nevertheless unambiguously, the MIP-functionalized electrode and the NIP-coated electrode (reference channel) were installed symmetrically with respect to a gold wire, serving as a common counter electrode. This 'perpendicular' electrode configuration imposes also a well-defined current-flow direction through the MIP-or NIP-coated interface, thus facilitating the equivalent-circuit modeling. The electrodes were constructed from 1×1 cm^2 aluminum substrates, again functionalized with the adhesive MDMO-PPV polymer and loaded with equal amounts of MIP –and NIP powder. The contact area of each electrode with the liquid (28 mm^2) was defined by O-rings and the distance to the gold counter electrode was 1.7 mm. Offset voltages between the gold electrode and the working electrodes could not be detected. The impedance signals were measured with a homemade portable system operating in a frequency range of 100 Hz to 100 kHz with 10 frequencies per decade and a scanning speed of 5.7 per sweep. The amplitude of the AC voltage was fixed to 10 mV [21, 22].

2.4 Results and discussion

2.4.1 Optical batch rebinding experiments

For all the monomer blends mentioned under section 2.3, the performance of the MIPs was analyzed by optical batch rebinding experiments. For these experiments, 50 mg of MIP-or-NIP powder were added to 5 ml of aqueous serotonin concentrations in the range between 0.1 to 1 mM. The resulting suspensions were shaken for 2h on a rocking table at room temperature. After filtration, the free concentration (C_f) of serotonin was measured by UV-vis spectroscopy. Hereafter, the amount of bound serotonin per gram MIP or NIP was calculated (S_b) and the binding isotherms and the corresponding affinity distributions were determined. Figure 4 shows the binding isotherm of the optimized MIP with 1 : 3 ratio between MAA and AM.
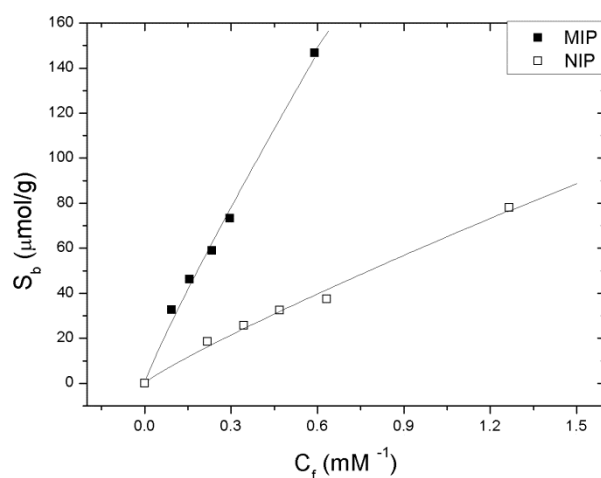
Figure 4: The binding isotherms for MIP (solid squares) and the corresponding NIP (open squares) upon exposure to serotonin. The solid lines are based on an allometric fit, with a R^2 of 0.98 for MIP and NIP.

The solid line is a two-parameter allometric fit (equation 1):

$$S_b = A \ C_f{}^{\nu} \ \text{(equation 1)}$$

This mathematical expression is based on the Freundlich isotherm, which is expected in a MIP system with heterogeneous distribution of the binding sites and affinity constants [23]. There is a clear difference between the MIP -and the NIP isotherm and the imprint factor (IF) (3.6 at C_f = 0.3 mM) is excellent, thereby demonstrating the specific binding. At other concentrations, similar IF values are obtained. This confirms recent findings by Khurshid *et al.,* who reported that a blend of charged and neutral monomers, as used in our study, is crucial for obtaining serotonin MIPs with good affinity properties [15]. In contrast to this, MIPs for the recognition of nicotine or histamine can be synthesized by using MAA as a single, neutral monomer [16, 17].

To determine the Freundlich isotherm, the parameters A and v have to be calculated for the MIP and NIP. These values are given in Table 2.

Table 2: The parameters A and v for MIP as determined by allometric fitting of the binding isotherms.

	R^2	A	N
MIP	0.98	233.4	0.9
NIP	0.98	62.3	0.88

With these parameters, the Freundlich isotherms can be determined (Figure 5).
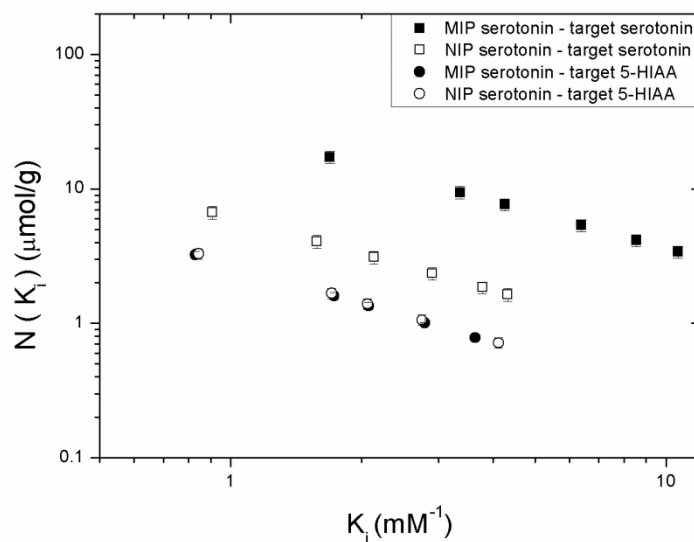
Figure 5: This shows the affinity distribution for MIP (solid squares) and NIP (open squares) according to the Freundlich model. The affinity for the competitor 5-HIAA is negligible both for the MIP (solid circles) and NIP (open circles). The error bars are determined by combining the standard deviations of the individual fit parameters.

With the Freundlich isotherm, the total number of binding sites (N_{tot}) within the range of the affinity constants K_i (1-15 mM^{-1}) can be calculated. In this region, the number of binding sites for the MIP is 26 ± 2 µmol/g and for the corresponding NIP this is 5.6 ± 0.4 µmol/g. This indicates that, within the considered range, the MIP has 4.7 times the amount of binding sites compared to the NIP. A Langmuir interpretation (all binding sites assumed to be equivalent) also confirms the stronger affinity of the MIP (K_i = 3.6 ± 0.1 mM^{-1}) as compared to the NIP (1.2 ± 0.03 mM^{-1}). However, the Scatchard plot clearly indicated heterogeneous behavior and therefore the Langmuir model is not applicable to this system. The Scatchard plot is shown in Figure 6. The binding constant is calculated from the linear part, while after a certain point saturation is observed which shows the heterogeneity of the binding sites.
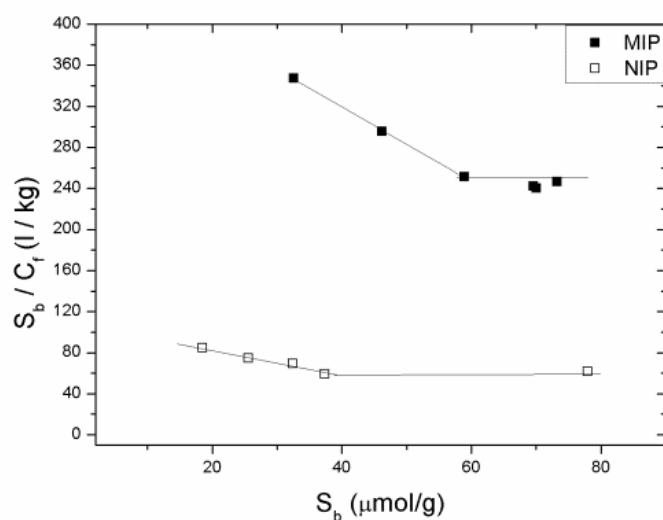
Figure 6: Scatchard plots of the MIP (solid squares) and NIP (open squares) upon
exposure to serotonin. In the low concentration regime, the data is fitted linearly
(R^2=0.98), till saturation occurs.

An alternative is a combination of Freundlich and Langmuir behavior, which also
resulted into a fit with a high linearity coefficient (R^2 =0.97) [24]. We showed
here only the results of the Freundlich model, as this gave an equally good fit
($R^2 = 0.98$) using one parameter less.

2.4.2 Impedance measurements in buffer with open addition setup

MIP-and NIP powders were immobilized on the planar electrode structures. The
results are shown in Figure 7, which is on the next page.

MIP   NIP

MIP

NIP
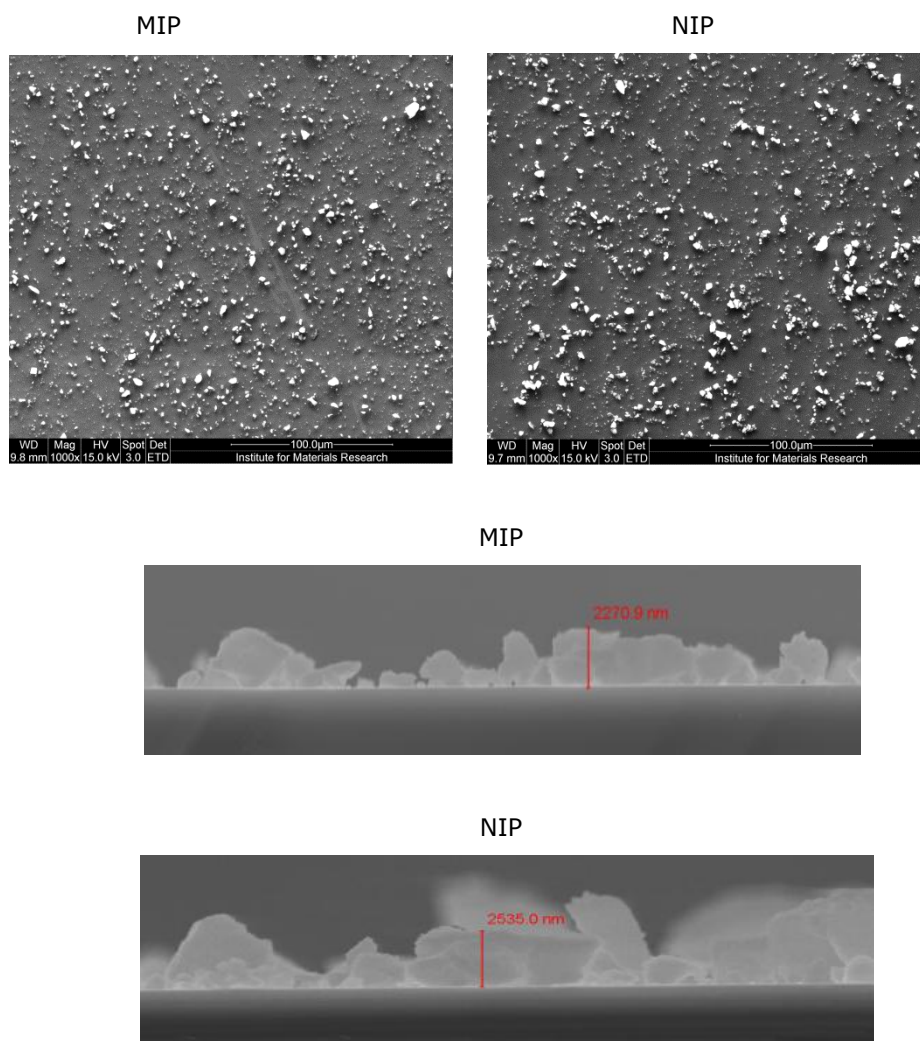
Figure 7: The SEM images of the MIP particles, embedded into the adhesive layer. The top pictures show a top view of the particle distribution for the MIP (left) and for the NIP (right). The bottom view indicates the thickness of the MIP layer and NIP layer.

By optical microscopy in combination with image processing by Image J software, we verified that in the case of the MIP a surface coverage of 28 ± 1 % was obtained, while it was 27 ± 1% for the NIP-loaded electrode (Figure 7). This shows that an almost identical surface coverage can be readily achieved. In

addition, the thickness of the MIP and NIP layers (2.5 ±0.5 µm) is also comparable.

Furthermore, the surface coverage was validated by the change in fluorescence intensity with a Zeiss LSM 510 Meta Axiovert 200 laser scanning confocal microscope using 514-nm argon-ion laser excitation (Figure 8).
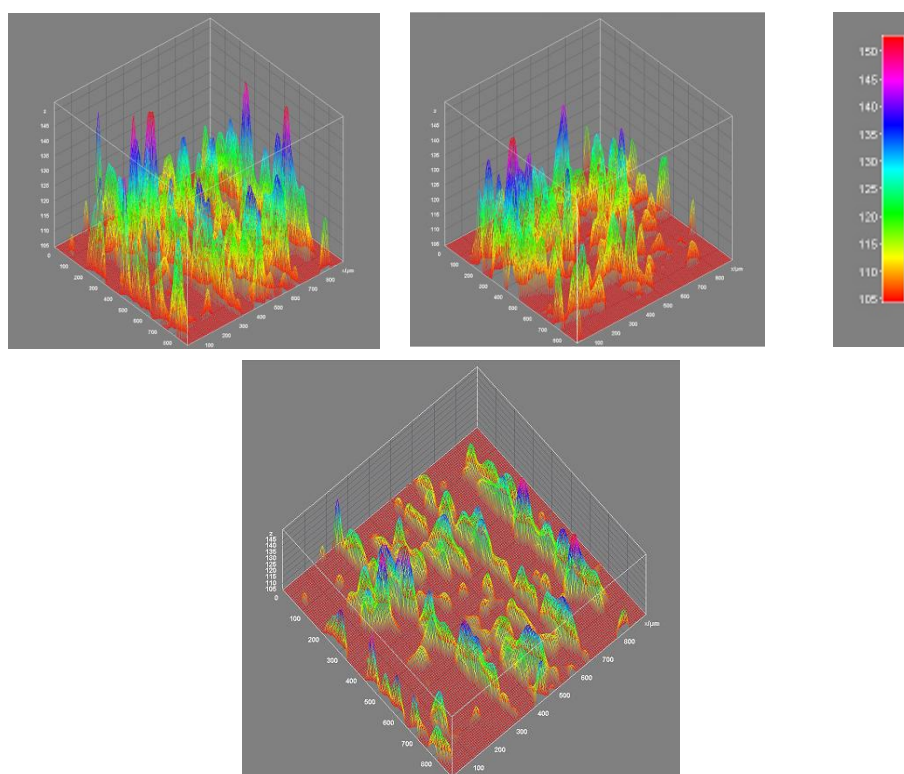
Figure 8: The side view fluorescence images of the MIP (top left) and NIP (top right). The high fluorescence, indicated by the red color, corresponds to the MDMO-PPV layer, when particles are present the signal is strongly quenched to yellow/blue. The bottom picture shows a top view of the MIP, which more clearly indicates where particles are present.

The MDMO-PPV shows strong fluorescence [20], for the MIP and NIP this is not the case and therefore a sharp contrast can be seen between the particles and the background (Figure 8). The scanned sample size was 900 µm x 900 µm.

Subsequently, the fluorescence images processed by Zeiss LSM Image Browser showed a surface coverage of 27 ± 3% coverage for the MIP and 25 ± 3% for the NIP. The error bars were obtained by determining the surface coverage five separate times on the same sample. Therefore, the precondition for differential measurements, having identical particle loadings, is fulfilled.

Next, the sensor cell was filled with PBS buffer in order to simulate the pH and ionic strength of the human body. Also, the physiological temperature conditions of 37 °C were mimicked. After stabilizing for 25 min, increasing concentrations of serotonin were added in a stepwise manner, resulting in a concentration series from 0 to 64.5 nM with an increment of 10.75 nM per step. The results for the NIP and MIP are shown in Figure 9. From this we can directly conclude that for the NIP there is no significant response to addition of histamine, while in the case of the MIP an increase is observed.
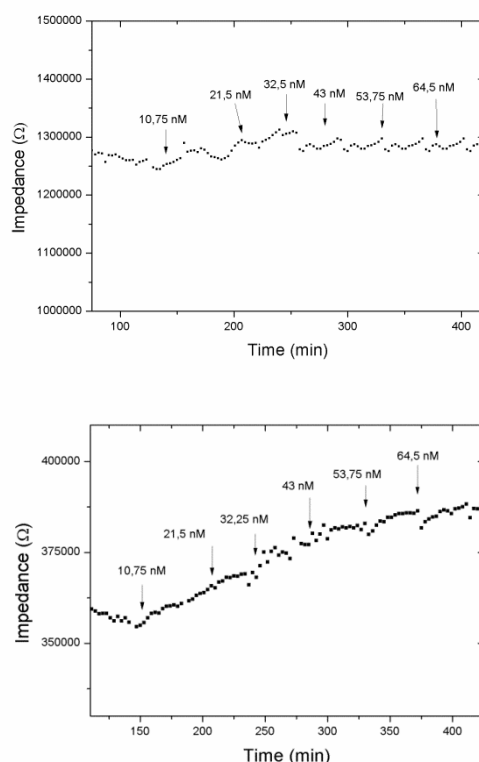
Figure 9: The impedance data (f = 213 Hz) in time when increasing concentrations of serotonin (0 – 64.5 nM) were added to the NIP (above) and MIP (below).

The data presented in Figure 9 is the raw data. To correlate the impedance increase to the serotonin concentration, a dose-response curve should be constructed based on the relative change in impedance at a certain frequency. All data were measured in the entire available frequency range; however we selected a frequency of 213 Hz due to its good signal-to-noise ratio while the frequency is low enough to probe capacitive interface effects. The dose-response curve is shown in Figure 10. For each concentration, the impedance data are normalized with respect to a starting value of 100% for pure, serotonin-free PBS solution. In order to test the selectivity of the sensor, measurements were also performed with PBS solutions containing the oxidized version of serotonin.
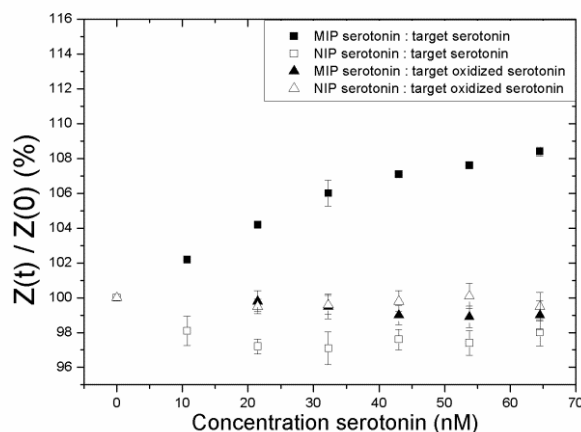
Figure 10: The dose-response curves for MIP and NIP exposed to increasing concentrations of serotonin and its oxidized version in PBS buffer. The error bars are determined by taking the standard deviation of three separate measurements.

The highest serotonin concentration (64.5 nM) resulted in an impedance increase of 8.4 ± 0.4% while physiologically relevant concentrations in the order of 10 nM, see *e.g.* reference [6], also gave an easily measurable increase of 2.5 ± 0.2%. The error at this concentration is used to estimate the detection limit, which is commonly defined as the concentration where the signal amplitude equals three times the standard deviation.

Overall, the data can be excellently represented with an allometric fit (R^2 = 0.98). In the low-concentration regime (0-30 nM), below the concentration at

which saturation is occurring, we can describe the data with a linear fit (R^2 = 0.99). With this obtained fit, we calculated the limit of detection to be 3.2 nM. As this is in the range of physiologically relevant concentrations, the sensor can be used for medical applications. For concentrations higher than 40 nM, the dose-response curve shows a trend towards saturation that can be attributed to the increasing occupation of binding sites. The NIP-based electrode gave no clear impedance change beyond experimental uncertainties. During these measurements, we also took into account that the molecular recognition of the target molecules by MIPs is not instantaneous. After each increase of the serotonin concentration, the sensor cell was allowed to stabilize for 10 minutes and then the impedance was measured with an intermediate waiting time of three minutes. This 'moving average filter' reduces data scattering to a minimum and the total measuring for a specific concentration is still not more than 30 minutes.

To test the selectivity of the sensor, measurements were also performed with PBS solutions containing the oxidized version of serotonin with the same sequence of concentration steps. The chemical structure is similar (Figure 1), however due to oxidation less hydrogen bonds can be formed and therefore binding to the nanocavities is hampered. As shown in Figure 10, neither the MIP –nor the NIP-coated electrode shows a measurable response to the oxidized molecules. Together with the optical batch-rebinding data, proving that the MIP does not bind the metabolite 5-HIAA, we can indeed conclude that the recognition of serotonin is selective. Therefore, the sensor is insensitive towards the most important competitor molecules which are naturally present in patient's samples.

2.4.3. Serotonin detection in human blood plasma with a flow-through impedimetric sensor cell

As a next step, human blood plasma samples were investigated. For these measurements, the refined sensor cell design was used due to its additional benefits when handling biological samples. The cell was first filled with unaltered (non-spiked) plasma of Person A. The sensor cell was allowed to stabilize for 90 minutes and then the impedance spectra of the MIP-and NIP channel were

measured, again with the moving average filter. The resulting impedance values at 213 Hz were used as a nominal sensor baseline, irrespective of the *a priori* unknown concentration c_0 of native serotonin present in the plasma sample. Note that even the lowest of the spiked concentrations, 50 nM, is at least 2.5 times higher than the typical physiological concentrations of 5 – 20 nM [11]. Therefore, the intrinsic c_0 value is expected to be a minor correction to the final dose-response curve. Next, the spiked plasma samples were introduced one by one via the pumping system. After waiting each time for 20 minutes, the impedance spectra of the MIP – and NIP channel were determined before switching to the following higher concentration (Figure 11 next page).

As compared to the studies with the PBS electrolyte, the impedance change of the MIP electrode upon exposure to a given serotonin concentration is less pronounced. This stems possibly from the non-specific adsorption of plasma proteins on the electrode, which result in a partial blocking of the MIP nanocavities. The response of the NIP electrode to serotonin seems stronger as compared to the data in PBS, but we are dealing now with considerably higher serotonin concentrations. Furthermore, this might also be due to the non-specific absorption of proteins from plasma.

The impedance values for the MIP –and the NIP electrode, normalized to the non spiked plasma, are given in Figure 11 on the next page.
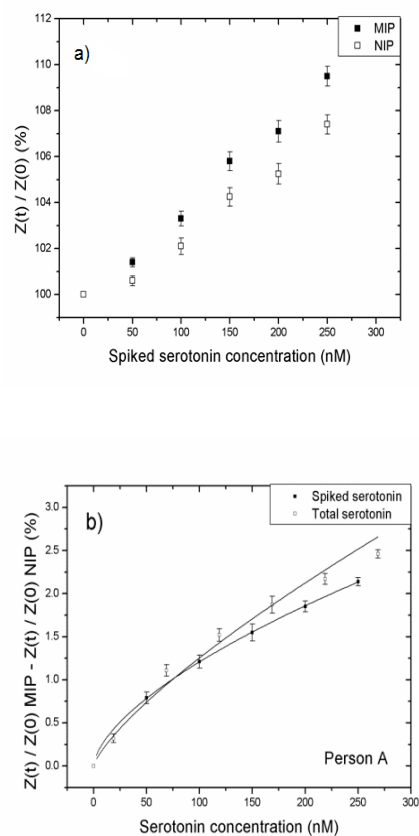
Figure 11: The upper panel (a) shows the normalized impedance response of the MIP and the NIP-based sensor electrode to plasma samples of person A spiked with serotonin. The lower panel (5b) shows the differential signal as a function of the spiked concentration by solid squares. The open squares represent the dose-response data obtained after correction for the native serotonin concentration c_0 (19 nM) present in the person's plasma.

In any case, there is a clear difference between the impedance change of the MIP and NIP channel, which is getting larger when increasing the spiked concentration. The differential signal, the normalized MIP – NIP response, is shown in Figure 11b. This differential dose-response curve can be described with an allometric fit, according to: $y = a\,c^{\,b}$. Hereby, y is the differential impedance change in percent while c is the concentration in nanomolar units. The fit

parameters a and b are given in Table 3. Although we are not discussing in this case a binding isotherm in the strict sense, the similarity with the Freundlich isotherm is obvious.

Table 3: The parameters a and b, as determined by allometric fitting.

R^2	A	B
0.99	0.069	0.62

In the spiked plasma is still some native serotonin present and therefore we do not measure the actual concentration, but a sum of the spiked concentration and the native serotonin concentration. The native concentration c_0 is of interest, as aberrations there might indicate an underlying problem. In order to estimate this, we determined in a second step the sensor baseline more precisely by filling the sensor cell with serotonin-free plasma. For this, 10 mg of MIP powder was added to 3 ml of unaltered plasma and this mixture was shaken for 15 min on a rocking table, allowing the MIP to absorb the native serotonin of person A. According to the binding isotherms, we assumed the serotonin to be extracted completely from the liquid. Subsequently, the particles were removed by filtration. The cell was equipped with freshly-prepared MIP– and NIP electrodes and filled with the serotonin-free and with the unaltered plasma. After stabilization at 37°C for 30 min, the impedance values were determined. The unaltered sample gave a differential-impedance increase (MIP-NIP) of 0.32 ± 0.03%, compared to the starting value with the serotonin-free plasma filling. The increase for the MIP is shown in Figure 12.
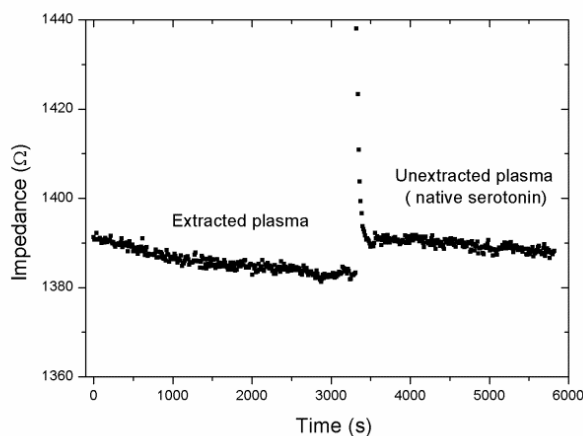
Figure 12: The impedance increase upon addition of the non-extracted plasma to the MIP, which is due to the native concentration of serotonin.

In the sense of the differential dose-response curve, this corresponds well to a native concentration of $c_0 = 19 \pm 1.2$ nM, within the physiologically expected range of a healthy person [11]. Based on the offset values, the dose-response curve shown in Figure 11b was rescaled by adding c_0 to all spiked concentrations and by shifting the differential impedance increases by 0.32%. The resulting data points can be described again with the fit $y = a' \cdot c^{b'}$. The parameters a' and b', respectively after correction for the extracted serotonin, are shown in Table 4. If we compare these parameters to the values obtained before extraction, this corresponds only to a minor shift which is because the spiked serotonin values are significantly higher than the native plasma concentration.

Table 4: Parameters a' and b' after fit.

R^2	a'	b'
0.98	0.061	0.67

The detection limit in plasma was determined as was done for the buffer measurements. The standard deviation was taken at the lowest spiked concentration of 50 nM, which is 0.07%. The data in the low-concentration

regime was fitted linearly (R^2 = 0.94), which resulted in a detection limit of 4.3 nM. This value is slightly higher compared to what was obtained in buffer measurements (3.2 nm), but is still below the physiologically relevant concentration range.

To validate the results, two additional samples of person B and C were measured by our technique and compared with corresponding HPLC tests performed according to the method established by Danaceau *et al.* [9]. First, a calibration curve was constructed for person B by extracting the native concentration from the plasma and then measuring the impedance response to the spiked concentrations of 15, 25, 100, 150 and 200 nM (Figure 13). The dose-response curve can again be described by an allometric fit with the function: $y = a' \cdot c^{b'}$. The brackets here indicate that an extraction step was performed for the baseline correction.
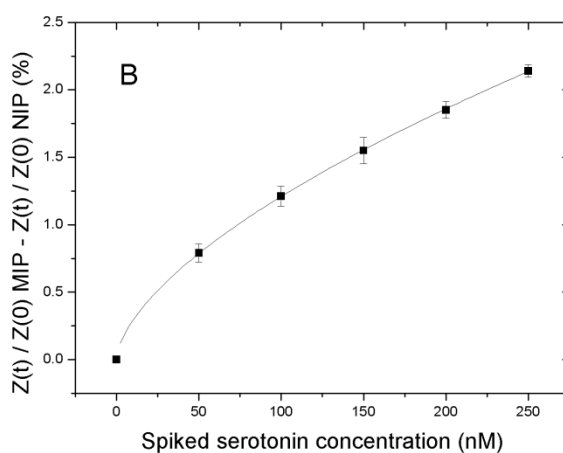
Figure 13: The normalized MIP-NIP impedance response obtained for extracted plasma sample of person B. After extracting, the samples were spiked with serotonin.

Subsequently, a second measurement was performed with an unaltered sample, showing an impedance response of 0.27%. With the obtained calibration curve, the native serotonin concentration of person B was determined to be 13.3 ± 1.3 nM. The HPLC reference indicated a concentration of 11.2 ± 1.0 nM. The same procedure was repeated for person C (Figure 14).
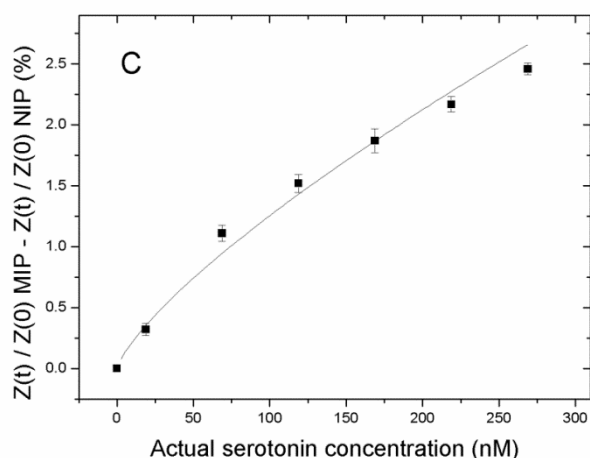
Figure 14: The normalized MIP-NIP impedance response obtained for extracted plasma sample of person C. After extracting, the samples were spiked with serotonin.

When using our technique a concentration of 9.5 ± 1.0 nM was obtained, while the HPLC measured 8.9 ± 0.5 nM. Hereby, it is demonstrated that our sensor indeed provides reliable data in the diagnostically relevant concentration regime.

The drawback of this method is that per person an individual calibration curve should be constructed. Therefore, an attempt was made to construct a universal calibration curve by measuring spiked plasma samples of three new persons (D, E, F). All of the samples were extracted by MIP powder prior to measuring, in order to remove the native serotonin concentration and obtain a reliable baseline. However, no reference HPLC tests were done to validate the results.
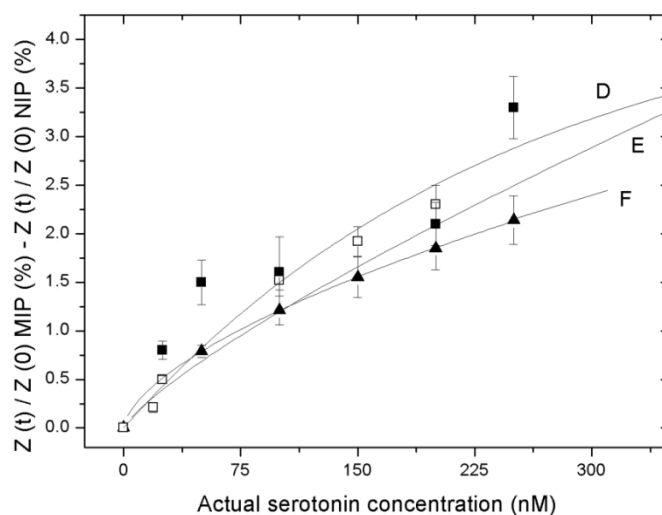
Figure 15: MIP–NIP calibration curve (with extraction for base-line correction) for three healthy volunteers.

To compare the calibration curves, the values of the fit parameters, a' and b', are shown in Table 5.

Table 5: Fit parameters a´ and b´ for volunteers D, E and F.

	R^2	a'	b'
D	0.91	0.2	0.44
E	0.95	0.03	0.8
F	0.99	0.07	0.62

From Table 5, it can be concluded that there are some differences in the calculated fit values for persons D, E and F. However, to determine the native serotonin concentration in plasma, we use only the initial linear slope in the low concentration regime (0 – ~100 nM). The slope is approximately 0,015% per nM for all the three samples (D,E,F), indicating the possibility of constructing a ´universal` calibration curve. Then, there is no need to determine a calibration curve prior to analysis, which will ensure fast measurements and has the additional benefit of requiring a considerably smaller sample volume.

2.4.4 Response modeling of the plasma measurements with equivalent circuits

As a final step, the origin of the impedance increase upon serotonin binding was further analyzed from the plasma samples of person A. Figure 16 shows the Bode plot and Nyquist plot in the frequency regime from 100 Hz to 100 kHz for the MIP electrode when the cell was filled with unaltered plasma. The solid line was calculated with a representative equivalent circuit.
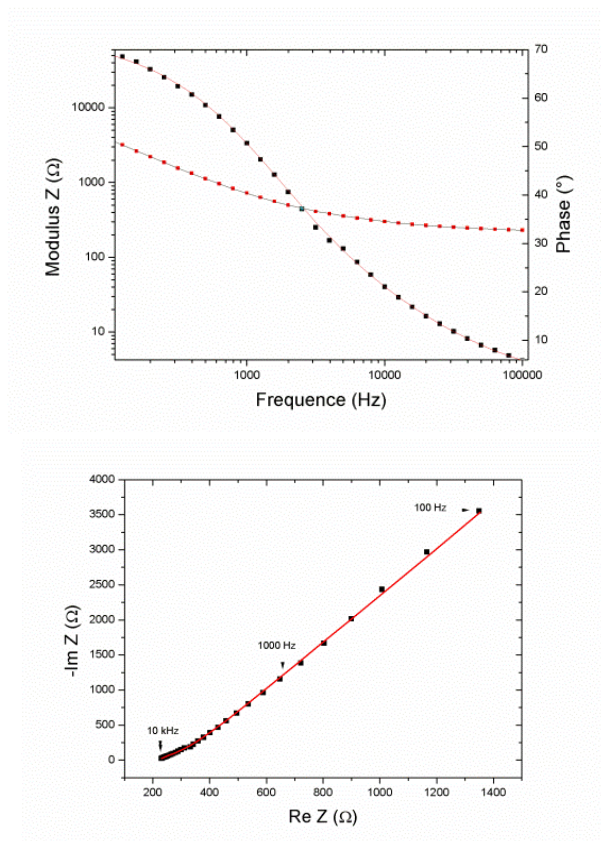
Figure 16: The Bode-plot (op panel) and Nyquist plot (lower panel) with the dots begin the measured values; the straight lines correspond to the calculated values.

The equivalent circuit used for fitting is given in Figure 17. R_f refers to the resistance of the plasma and the counter electrode, elements that are not expected to change upon spiking with higher serotonin concentrations. The adhesive PPV layer and aluminum substrate are in series with R_f and can be represented by an element with a resistor, R_{PPV} and a constant-phase element

(leaking capacitor) CPE_{PPV} in parallel. A leaking capacitor was chosen to take into account roughness and inhomogeneity of the polymer electrode. Finally, also the MIP layer, covering roughly 30% of the electrode's surface, was described as CPE_{MIP} in series. Here, a leaking capacitor is expected due to the intrinsic porosity of the MIP material. The NIP channel was described by a corresponding CPE_{NIP}.
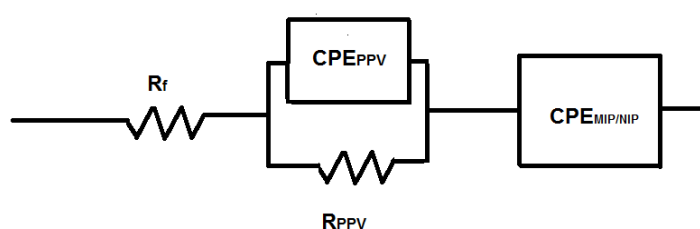
Figure 17 : Equivalent circuit model for our system.

The parameters from the fit were derived by online available ZSimpWin software. The results are summarized in Table 6 and 7 for the MIP and NIP. The high quality of the fit is illustrated by a χ^2 of around 1×10^{-4}. Other equivalent circuit models based on the same number of elements had a χ^2 of 10^{-3} and were clearly less accurate. A more refined modeling of the MIP layer, *e.g.* in terms of a resistor and a CPE in parallel, gave also a χ^2 in the order of 10^{-4}, meaning that the proposed circuit is indeed an excellent description of a the system with a minimum number of elements. The same circuit also describes the behavior of the NIP electrode with a similarly low χ^2 and can still be applied after exposing the MIP-and NIP electrodes to the spiked serotonin concentrations.

Table 6: The influence of the spiked serotonin concentration on the fit parameters of the MIP.

Spiked (nM)	R_f (Ω)	CPE_{ppv} ($\mu S*s^n$)	n_{ppv}	R_{ppv} (Ω)	CPE_{mip} ($\mu S*s^n$)	n_{mip}	χ^2 (10^{-4})
0	212	1.48	0.79	118	**13**	0.62	1.52
50	218	1.41	0.82	88	**7.0**	0.69	1.06
100	220	1.36	0.83	80	**5.3**	0.72	1.49
150	220	1.32	0.84	75	**3.9**	0.75	2.97
200	222	1.30	0.85	71	**2.8**	0.79	4.93
250	228	1.27	0.86	72	**3.4**	0.77	4.93

Table 7: The influence of the spiked serotonin concentration on the fit parameters of the NIP.

Spiked (nM)	R_f (Ω)	CPE_{ppv} ($\mu S*s^n$)	n_{ppv}	R_{ppv} (Ω)	CPE_{nip} ($\mu S*s^n$)	n_{nip}	χ^2 (10^{-4})
0	228	1.71	0.80	132	**54**	0.46	0.82
50	232	1.56	0.81	131	**53**	0.46	0.30
100	232	1.50	0.83	125	**52**	0.46	0.36
150	233	1.46	0.84	109	**45**	0.48	0.40
200	233	1.43	0.85	117	**50**	0.47	0.44
250	234	1.44	0.85	99	**36**	0.51	0.48

When comparing the MIP and the NIP channel for different spiking concentrations, we can observe that the values of the liquid resistance, R_f, the amplitude of the constant phase element CPE_{PPV} and its exponent n_{PPV}, and the resistance R_{PPV} are widely constant. The strongest variation is seen in R_{PPV} where absolute values can differ by a maximum of 50% when comparing the MIP and NIP at a given spiked concentration. The exponent n_{PPV} always stays in the range of 0.79 – 0.86, which is close to the behavior of an ideal capacitor (n = 1). When comparing the CPE behavior of the MIP and NIP element, the difference immediately becomes more striking: the NIP electrode has no serotonin nanocavities and the absolute CPE amplitude is therefore almost insensitive to spiked concentrations. The amplitude of the CPE of the MIP electrode is significantly lower for the non-spiked sample as compared to the NIP electrode

(25%) and this decreases systematically to 10% of its value when exposed to the highest spiked serotonin concentration.

Figure 18 shows the concentration-dependent CPE amplitude of the MIP- and NIP electrode normalized to the initial value obtained in non-spiked plasma.
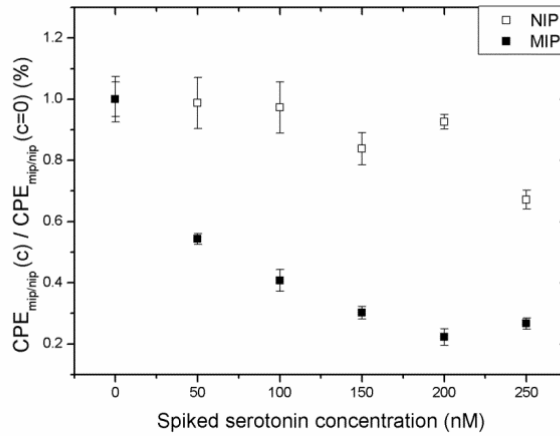
Figure 18: Spiked concentration dependence of the amplitude of CPE_{MIP} and CPE_{NIP}.

The current data do not yet allow interpretation of the resistive and capacitive aspects of the CPE-behavior on morphological or even molecular grounds. A coarse-grain physical interpretation may be as follows; the CPE behavior of the MIP electrode is always more on the capacitive than on the resistive side. The absolute capacity value of the element decreases for increasing serotonin concentrations. This means that the nanocavities in the MIP polymer are more and more filled by serotonin, rather than by water molecules. As a result, the effective contact area between the MIP and the plasma decreases while water, with a high dielectric constant ($\varepsilon = 81$), is replaced by organic molecules with an ε in the range 5-10 [25]. Both aspects, the shrinking of the contact area and the decrease of the dielectric constant at the solid-liquid interface, work into the direction of lowering the interface capacitance. This can be seen in equation 2, if we assume it is a parallel-plate capacitor.

$$C = \varepsilon_0 \, \varepsilon_r \, \frac{A}{d} \qquad \text{(equation 2)}$$

In this formula, C corresponds to the capacitance (F), ε_O is the dielectric constant (~8.85 x 10^{-12} F/m), ε_r is the relative permittivity, A is the area of overlap between the two plates (m^2) and d the distance (m) between the two plates.

The capacitance (C) and impedance (Z) are linked according to equation 3:

$$Z = \frac{1}{j\,\omega\,C} \quad \text{(equation 3)}$$

This proofs that upon capacitance decrease indeed an increase in impedance is observed, thereby validating the obtained experimental results.

2.5. Conclusion

In this work, we have shown that a biomimetic serotonin sensor, based on impedance spectroscopy in combination with MIP-based synthetic receptors, has the potential to become a fast and low-cost alternative to chromatographic techniques. At the receptor side, we have shown that a blend of two functional monomers, methacrylic acid and acrylamide, is essential to achieve selective molecular recognition and the best properties were obtained with a MAA-AM ratio of 1 : 3. Furthermore, we have demonstrated that the sensor response is specific and selective with respect to its competitors, metabolite 5-HIAA and the oxidized version of serotonin. At the sensor side, we developed a symmetrical flow-through cell hosting an active channel (MIP) and a reference channel NIP in order to correct for unwanted side effects such as protein absorption, which naturally occur in a biological matrix. The MIPs as such can also be used to extract the native serotonin from a patient's sample in order to obtain a well-defined sensor baseline in the limit of vanishing serotonin concentration. The detection limit is below the physiologically relevant range and the sensor can operate in non-diluted blood plasma provided that standard precautions are taken to counteract oxidization and enzymatic conversion of serotonin. Furthermore, the determined concentrations show comparatively small uncertainties and are in perfect agreement with HPLC reference tests, as was illustrated for two different persons. This cell allows for the safe and temperature-controlled handling of plasma samples. Moreover, in combination

with a compact impedance analyzer, the sensor setup can be operated as a 'stand-alone device', making it well suited for point-of-care applications, like in a hospital environment.

2.6 Acknowledgements

2.7 References

[1]   V. Esparmer, G. Boretti, *Arch Int Pharmacod.,* 1951, **88**, 296-332.

[2]   I.P. Kema, E.G.E. De Vries, F. Muskiet, *Anal Technol Biomed Life Sci.,* 2000, **747,** 33-48.

[3]   J.E. Blundell, *Am J Clin Nutr.,* 1992, **55**, 155S-159S.

[4]   J.R. Seibold, Serotonin and the cardiovascular system, Raven Press, New York, 1985.

[5]   D.G. Grahame-Smith, *Am J Cardiol.* 1968, **21**, 376-385.

[6]   A.N.M. Wymenga, T.A. Van der Graaf, I.P. Kema, E.G.E. De Vries, N.H. Mulder, *Lancet,* 1999, **353**, 293-294.

[7]   G.M. Anderson, J.M. Stevenson, D.J. Cohen, *Life Sci.,* 1987, **41**, 1777-1785.

[8]   G.M. Anderson, *Adv Exp Med Biol.,* 1991, **294**, 51-61.

[9]   J.P. Danaceau, G.M. Anderson, W.M. McMahon, D.J. Crouch, *J Anal Toxicol.,* 2003, **27**, 440-444.

[10]   D. Tonelli, E. Gattavecchia, M. Gandolfi, *J Chromatogr B Anal Technol Biomed Life Sci.,* 1982, **231**, 283-289.

[11]   B.A. Patel, M. Arundell, K.H. Parker, M.S. Yeoman, D. O'Hare, *J Chromatogr B Anal Technol Biomed Life Sci.,* 2005, **818**, 269-276.

[12]   T. Kitade, K. Kitamura, T. Konishi, S. Takegami, T. Okuno, M. Ishikawa, M. Wakabayashi, K. Nishikawa, Y. Muramatsu, *Anal Chem.,* 2004, **76**, 6802-6807.

[13]   B. Okutucu, A. Telefoncu, *Talanta*, 2008, **76**, 1153-1158.

[14]   B. Okutucu, A. Telefoncu, K. Haupt, *Haceteppe J Biol & Chem.,* 2010, **38**, 79-84.

[15]   S.S. Khurshid, C.E. Schmidt, N. Peppas, *J Biomater Sci, Polym Ed.,* 2011, **22**, 343-362.

[16]   R. Thoelen, R. Vansweevelt, J. Duchateau, F. Horemans, J. D'Haen, L. Lutsen, D. Vanderzande, M. Ameloot, M. vandeVen, T.J. Cleij, P. Wagner, *Biosens Bioelectron.,* 2008, **23**, 913-918.

[17]   E. Bongaers, J. Alenus, F. Horemans, A. Weustenraed, L. Lutsen, D. Vanderzande, T.J. Cleij, F.J. Troost, R.-J. Brummer, P. Wagner, *Phys Status Solidi A.,* 2010, **207**, 837-843.

[18]   F. Horemans, J. Alenus, E. Bongaers, A. Weustenraed, R. Thoelen, J. Duchateau, L. Lutsen, D. Vanderzande, P. Wagner, T.J. Cleij, *Sens Actuators, B.,* 2010, **148**, 392-398.

[19]   M.C. Blanco-López, M.J. Lobo-Castañón, A.J. Miranda-Ordieres, P. Tuñón-Blanco, *TrAC Trends Anal Chem.,* 2004, **2**, 36-48.

[20]   D. Louwet, D. Vanderzande, A. Gelan, *Synth Met.,* 1995, **69**, 509-510.

[21]   B. van Grinsven, T. Vandenryt, S. Duchateau, A. Gaulke, L. Grieten, R. Thoelen, S. Ingebrandt, W. De Ceuninck, P. Wagner, *Phys Status Solidi A.,* 2011, **207**, 919-923.

[22]   B. van Grinsven, N. Vanden Bon, L. Grieten, M. Murib, S. Janssens, K. Haenen, E. Schneider, S. Ingebrandt, M.J. Schöning, V. Vermeeren, M. Ameloot, L. Michiels, R. Thoelen, W. De Ceuninck, P. Wagner, *Lab Chip.,* 2011, **11**, 1656-1663.

[23]   R. J. Umpleby, S.C. Baxter, A.M. Rampey, G.T. Rushton, Y.Z. Chen, K.D. Shimizu, *J Chromatogr B: Anal Technol Biomed Life Sci B.,* 2004, **804**, 141-149.

[24]   G. Sener, L. Uzun, R.I. Say, A Denizli, *Sens Actuators, B. Chemical ,* 2011, **160**, 791-799.

[25]   R.C. Weast et al., Handbook of Chemistry and Physics, 53 ed., CRC Press, Cleveland, 1972.

Chapter 3

Impedimetric detection of histamine in bowel fluids using synthetic receptors with pH-optimized binding characteristics

M. Peeters[1], F.J. Troost[2], R.H.G. Mingels[1], T. Welsch[3], B. van Grinsven[1], T. Vranken[1], S. Ingebrandt[3], R. Thoelen [1,4], T.J. Cleij[1] and Patrick Wagner [1,5]

1) Hasselt University, Institute for Materials Research, Wetenschapspark 1, B-3590 Diepenbeek, Belgium

2) Department of Internal Medicine, div. of Gastroenterology – Hepatology, Maastricht University Medical Center, Minderbroedersberg 4-6, 6211 LK Maastricht, the Netherlands

3) University of Applied Sciences Kaiserslautern, Department of Informatics and Microsystems Technology, Amerikastrasse 1, D-66482 Zweibrücken, Germany

4) XIOS University College Limburg, Department of Electronic Engineering, Agoralaan Building H, B-3590 Diepenbeek, Belgium

5) IMEC vzw – Division IMOMEC, Wetenschapspark 1, B-3590 Diepenbeek, Belgium

3.1 Abstract

Histamine is a biogenic amine that is indispensable in the efficient functioning of various physiological systems. In previous work, a molecularly imprinted polymer (MIP) based sensor platform with impedimetric read-out was presented which could rapidly and at low-cost determine histamine concentrations in buffer solutions within pH 7-9 [1,2]. For diagnostic applications, this target should be detectable in a wider pH range as is it mostly occurs in mildly acidic environments. To understand the pH-dependent response of the MIP sensor, we propose a statistical binding analysis model. Within this model, we predict the theoretical performance of MIP based on acrylic acid in the required pH range and verify these results experimentally by UV-vis spectroscopy, microgravimetry and impedance spectroscopy. Using impedimetric read-out, specific and selective detection of histamine in the physiologically relevant nanomolar concentration range is possible in neutral and mildly acidic phosphate buffer. Finally, this platform was used to analyse the histamine concentration of mildly acidic bowel fluid samples of several test persons. We show that this sensor provides reliable data in the relevant concentration regime, which was validated independently by Enzyme-Linked Immuno Sorbent Assay (ELISA) tests.

Keywords: biomimetic sensors, histamine, molecularly imprinted polymers (MIPs), impedance spectroscopy, microgravimetry, combinatorial affinity model, bowel diseases.

3.2 Introduction

3.2.1 General introduction

Histamine is an organic nitrogen compound which was first described by Henry H. Dale and P.P. Laidlaw in 1910 [3] (Figure 1).
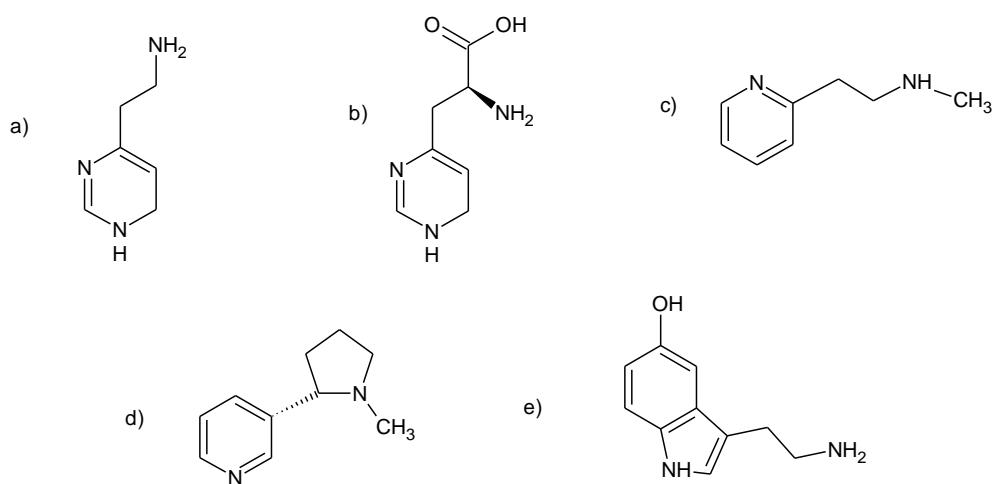
Figure 1: The structure of histamine (a) and its competitor molecules, b) histidine, the precursor c) betahistine d) nicotine e) serotonin.

It is produced from the decarboxylation of the amino acid histidine by the enzyme histidine decarboxylase. This reaction takes place in the mast cells and basophils [4,5] where histamine is detained in intracellular granules [6]. In mast cells isolated from the lung, skin and the small intestine, approximately 3-8 pg histamine/cell is found [7]. When mast cells are exposed to allergens, histamine is released and the local concentration is increased resulting in an allergic reaction [8]. Another important site of histamine storage and release are the enterochromaffin-like cells in the stomach and intestines. There, histamine is involved in regulating the physiological function of the gut [6]. Furthermore, a high concentration of histamine (1 – 6 µmol/kg) is present in the brain where it acts as a neurotransmitter [9].

Histamine is naturally present in many fruits, vegetables, beer, red wine, cheese and fish [10]. The concentration is relatively low, however when food is spoiled the amount can increase to toxic levels up to 50 mg per 100 g of product,

causing food poisoning [10]. Histamine detection is therefore of great importance for the food industry and food safety. Another area of substantial interest is biomedical research since histamine plays a pivotal role in IBS [11, 12], allergies [8], asthma [13], rheumatoid arthritis and related diseases [14]. For this type of medical applications, the detection limit should be considerably lower than in the case of food analysis: in *e.g.* blood the normal physiological concentration ranges from 200-600 nM [15].

Molecularly Imprinted Polymers (MIPs) present an interesting alternative to the more traditional detection techniques, *e.g.* HPLC and ELISA, since measurements can be performed rapidly and at low-cost. Until now, there are only a few reports in literature about MIPs for histamine recognition; Tong *et al.* reported on a MIP-based sensor where zinc (II)-protoporphyrin (ZnPP) was used as fluorescent monomer and detection was in the millimolar range [16]. Allender *et al.* studied various MIPs for pharmaceutical applications, including a MIP for histamine with methacrylic acid as monomer. Subsequently, MIPs were packed into separation columns and measurements were performed with HPLC as detection method [17]. Pietrzyk *et al.* synthesized a MIP by electropolymerizing polypyrrole and a detection limit of 20 µM was reached in phosphate buffer with an amperometric sensor [18]. The first MIP sensor capable of measuring in the physiologically relevant nanomolar range has been developed recently by Bongaers *et al.* and Horemans *et al.* [1,2]. They performed all their measurements in buffer solutions, while for future applications biological samples are considerably more interesting. The MIP used in these publications was composed of MAA as functional monomer, EGDM as crosslinker and DMSO as porogen. After bulk polymerization, particles were ground and fixated into electrodes using a polymer adhesive. Subsequently, detection down to the nanomolar concentration range could be performed by impedance spectroscopy. In the micromolar range, the quartz crystal microbalance (QCM) [19] proved to be most useful. While histamine could be measured specifically and selectively at pH 7, at mildly acidic pH values no binding was observed which is due to the protonation behaviour of the target molecule and the MIP. Besides Bongaers *et al.* [1], this pH dependence was also reported by Trikka *et al.* who performed histamine measurements with a MIP with exactly the same composition but as detection

method, a colorimetric assay was used [20]. In section 3.2.2 of the Introduction, we will now propose a statistical binding model to explain this pH-dependent sensor response.

3.2.2. Statistical binding analysis model

We are interested in measuring histamine in the gastro-intestinal tract, where the pH of the fluids varies between pH values of 5-8 [21]. The functional monomer MAA, which was used by Bongaers *et al.* and Horemans *et al.,* is present in the neutral (COOH- and deprotonated form (COO⁻), depending on the pH of the solution [1,22]. At pH 5, which is well below the pKa (6.5) of MAA, the acid occurs mostly in the neutral form [22]. The target, histamine, occurs in three natural forms (HisN), the single protonated state (His$^+$) and the double protonated state (His^{++}). Up to a pH of 10 the protonated states are abundant, at higher pH values the neutral form will demonstrate. These results for histamine, adopted from Bongaers *et al.* [1], are given in Table 1.

Table 1: Relative abundance of His^{++}, His$^+$ and HisN from pH 1-14.

pH	His $^{++}$	His $^+$	HisN
1	100	0	0
2	100	0	0
3	100	0	0
4	100	0	0
4.5	100	0	0
5	99	1	0
6	91	9	0
6.5	67	33	0
7	44	56	0
8	7	93	0
9	1	95	4
9.5	0	88	12
10	0	24	76
11	0	20	80
12	0	2	98
13	0	0.2	99.8
14	0	0	100

In Figure 2, the results for the abundance of the states of histamine and the various situations of the MIP, *A-D*, are shown.
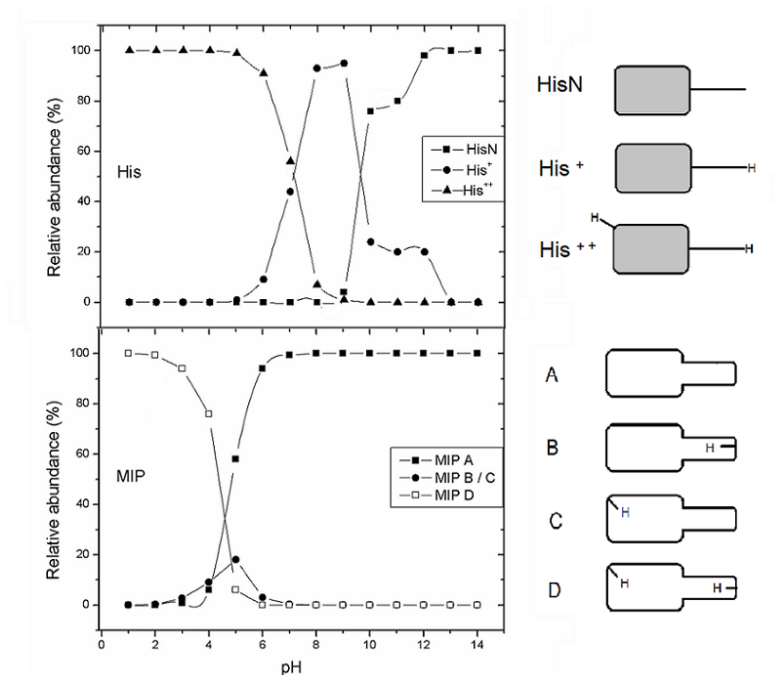
Figure 2: Schematic representation of the protonation states of histamine (above) and MIP conformations *A-D* (below) in the pH range 1-14.

The driving force between MIP and template interaction is hydrogen bond formation. To form a hydrogen bond, there should be a hydrogen bond donor and a hydrogen bond acceptor. In the case of the functional monomer, the neutral methacrylic acid (COOH) is a donor. The protonated histamine also acts as donor and therefore, no hydrogen bonds can be formed which makes binding to the target unlikely at pH 5. For binding to occur, the monomer should be an acceptor, which is the case in the deprotonated (COO⁻) state. If we wish that the functional monomer is mostly in the deprotonated state at pH 5, it should be more acidic than MAA and have a lower pKa value. Therefore, acrylic acid (AA) was selected, with a pKa value of approximately 4.5 [23]. Furthermore, the only difference in chemical structure is that methacrylic acid contains one extra methyl group. This ensures that the difference in pH behavior is due to the acidity of the monomers and is not somehow linked to its chemical structure.

With the following calculations, we will demonstrate that MIPs based on AA monomers are able to bind histamine at mildly acidic pH which is not possible to achieve with MAA as monomers.

Histamine contains two functional sites for hydrogen bond formation, namely the amine group and the nitrogen in the ring next to the double bond. To correct for these two binding sites, already during the synthesis twice the amount of monomer compared to the target was used. The monomer can be either in the neutral and the deprotonated state and, since per target molecule two monomers are available, this results into four possible MIP conformations. They are labeled from *A* to *D* (Figure 2). Situation *A* represents two functional monomers in the deprotonated state, while for situation *D* both monomers are in the neutral form. In the case of *B* and *C*, there is one monomer in the neutral and the other in the deprotonated state. In total, the sum of the situations *A*, *B*, *C* and *D* is 100%. The relative abundance of the states is determined by the Henderson – Hasselbalch equation (equation 1).

$$pH = pKa - \log\frac{[\text{COOH}]}{[COO^-]} \quad \text{(equation 1)}$$

As derived from this formula, situation *B* and *C* can be calculated by multiplying the percentage of COOH present by that of COO⁻. Directly resulting from this, *A* and *D* correspond to the squared percentage of COO⁻ or COOH, respectively. As an example, we calculate the values at pH 5. At pH 5, the percentage of COO⁻ is 76% and of COOH is 24%. The occurence of MIP *A* is then equal to 76% squared, which is 58%. For MIP *D*, this corresponds to 6%. The other remaining 36% is equally divided over MIP *B* and *C*, with both of them being present at 18%. The results for pH 1-14 are given in Table 2.

Table 2: Relative occurence (%) of MIP A, B, C and D for the monomer AA in the pH range 1-14.

pH	MIP A	MIP B	MIP C	MIP D
1	0	0	0	100
2	0	0.3	0.3	99.4
3	0	3	3	94
4	6	18	18	58
4.5	25	25	25	25
5	58	18	18	6
6	94	3	3	0
6.5	97	1.5	1.5	0
7	99.4	0.3	0.3	0
8	100	0	0	0
9	100	0	0	0
9.5	100	0	0	0
10	100	0	0	0
11	100	0	0	0
12	100	0	0	0
13	100	0	0	0
14	100	0	0	0

For histamine to bind to the MIP, at least one, but preferably two, hydrogen bonds should be formed. The situations in which two hydrogen bonds, one hydrogen bond and no hydrogen bonds are established are demonstrated in Figure 3.
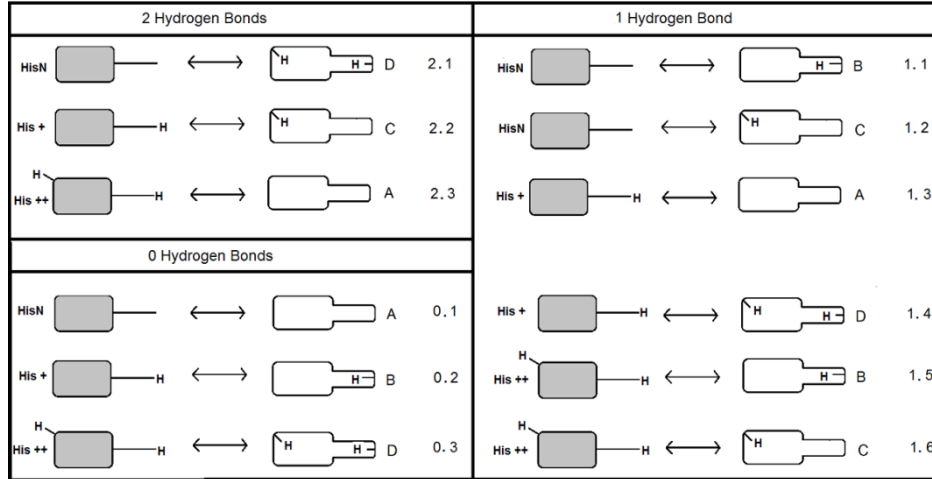
Figure 3: Overview of situations in which 0, 1 and 2 hydrogen bonds can be formed.

To estimate the probability of hydrogen bond formation, the probability of the independent events needs to be multiplied and subsequently summed up. We will now show the steps, which ultimately lead to a formula for the calculation of the probability of hydrogen bond formation.

Let $n\ (i, j)$ be the number of hydrogen bonds if His { HisN, His$^+$, His^{++} } is in state i and MIP { A, B, C, D } is in state j. Moreover, for n = 0, 1, 2 let S_n be (equation 2) :

$$S_n = \{\ (\ i, j\ )\ |\ n\ (\ i, j) = n\ \}\ \text{(equation 2)}$$

S_n corresponds to the situations in which, respectively, S_0 (0), S_1 (1) and S_2 (2) hydrogen bonds are formed. S_0 and S_2 are composed of three elements, while for S_1 there are six different combinations. These are shown in Figure 3.

Finally, we define (equation 3 and 4)

$$P_{His}\ (i\ |\ k) = \text{prob (His is in state } i \text{ if pH} = k)\ \text{(equation 3)}$$

$$P_{MIP} = (j\ |\ k) = \text{prob (MIP is in state } j \text{ if pH} = k)\ \text{(equation 4)}$$

In this formula, P_{His} is the probability of HisN, His^+ and His^{++} at pH = k. These probabilities are listed in Table 1. P_{MIP} is the probability of MIP A, B, C and D at pH = k which can be found in Table 2.

Then for n = 0, 1 and 2, we have that (equation 5):

$$\text{prob } (n \text{ hydrogen bonds} \mid pH = k) = \sum_{(i,j) \, \in \, S_n} = P_{His} (i \mid k) \, P_{MIP} (j \mid k)$$

(equation 5)

The probability of hydrogen bond formation from pH 1-14 is shown in Table 3 for both the new MIP, based on AA monomers, and the previously used MIP with MAA monomers. As an example, we calculate the probability of the formation of two hydrogen bonds at pH 6. At this pH, histamine is for 91% in the His^{++} state, 9% in the His^+ state and HisN is not encountered. Therefore, option 2.1, 0.1, 1.1 and 1.2 (Figure 3) do not have to be taken into account. The probability of the formation of two hydrogen bonds is equal to 2.2. and 2.3 summed up. For option 2.2., the probability of His^+ (9%) needs to be multiplied by the probability of MIP C (3%), resulting in a 0.3% probability. For option 2.3, His^{++} (91%) is multiplied by A (94%), which leads to a 85.5% probability and, in total, of 85.8%. Subsequently, the probability of one hydrogen bond formation is 13.9% and the probability of zero hydrogen bonds is 0.3%.

Table 3: The probability of hydrogen bond formation for the MIP with AA monomers and the MIP with MAA monomers. The data are given in the pH range 1-14.

pH	0 H-bonds	1 H-bond	2 H-bond	% bound Monomer AA	% bound Monomer MAA
1	100	0	0	0	0
2	100	0	0	0	0
3	94.6	5.4	0	5.4	0
4	57.2	36.8	6	24	0.6
4.5	25	50	25	75	2
5	6	36.8	57.2	94	7
6	0	14	86	100	46
6.5	0	34	66	100	75
7	0	44	56	100	89
8	0	7	93	100	98
9	4	95	1	96	96
9.5	12	88	0	88	88
10	76	24	0	24	24
11	80	20	0	20	20
12	98	2	0	2	2.4
13	100	0	0	0	0
14	100	0	0	0	0

We assume that if one or two hydrogen bonds are formed, binding will occur. The probability of binding for the MIPs is now shown in Figure 4.
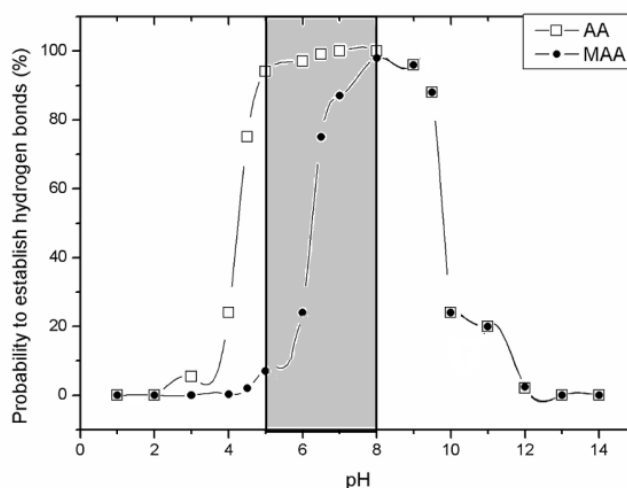
Figure 4: The percentage of histamine bound by MIP synthesized from MAA and AA monomers as calculated by the combinatorial affinity model. The grey area corresponds to the typical pH range in the intestinal tract (pH 5 – 8) [21].

With both the MIPs, it is not possible to perform measurements in strongly basic environments; however this is outside the scope of our research. Around neutral pH, they show a high theoretical binding probability. As previously mentioned, the MAA MIP has a very low binding capacity at pH < 7 and is therefore not suitable for detection of histamine in acidic environments. In contrast, the newly developed MIP based on AA monomers has a theoretical binding probability of still 94% at pH 5, which is a significant improvement. We will now also demonstrate experimentally that histamine can be bound with a high affinity and selectivity at both neutral and mildly acidic pH with the AA MIP. Furthermore, when combined with a refined sensor setup, we will show that it is possible to detect histamine in bowel fluids from the small intestines.

3.3 Experimental section

3.3.1 Chemical reagents

Ethylene glycol dimethacrylate (EGDM), methacrylic acid (MAA), acrylic acid (AA) and dimethylsulfoxide (DMSO) were purchased from Acros (Geel, Belgium). Prior to polymerization, the stabilizers in the MAA and EGDM were removed by filtration over alumina. Azobisisobutyronitrile (AIBN) was purchased from Fluka

(Buchs, Switzerland). The target molecule histamine was obtained from Sigma Aldrich. Histidine, L-nicotine, serotonin and betahistine, analogues of histamine, were used to test the selectivity. They were obtained from Fluka (Buchs, Switzerland). All solvents were of analytical grade and purchased from Acros (Geel, Belgium). They were used without further purification. The polyphenylenevinylene (PPV)derivative, OC_1C_{10}-PPV, which served as the immobilization layer on the impedimetric sensor MIP and NIP electrodes, was synthesized via the sulfinyl precursor route [24]. Besides MIP sensors, this PPV derivative can also be used for other bioanalytical applications, *e.g.* as an immobilization layer for antibodies [25]. All chemical and physical properties of the conjugated polymer were in agreement with previously reported data. A home-made 1× PBS solution was used for the impedance measurements. The human histamine ELISA test was obtained from Gentaur Molecular Products (Kampenhout, Belgium, product number CSB E07042h).

3.3.2 MIP synthesis

As mentioned in the Introduction (section 3-2), it is necessary to use a monomer with a lower pKa to detect histamine in acidic environments. Therefore, acrylic acid (AA) with a pKa value of 4.5 was selected [43]. The corresponding MIP was synthesized according to the following procedure: First, a mixture of AA (18 mmol), EGDM (72 mmol) and AIBN (0.61 mmol) was dissolved in 7 ml DMSO together with the template molecule histamine (9.0 mmol). This solution was degassed with N_2 and polymerized in a UV oven for 12 h. After polymerization, the bulk polymer was ground and sieved to obtain microparticles with a size smaller than 25 µm. Finally, the histamine was removed from the MIP powders by Soxhlet extraction with methanol (48 h), a mixture of acetic acid/acetonitrile (1/1) (48 h) and again methanol (12 h). The extracted powders were dried in vacuum for 12 h at room temperature. A NIP was synthesized in the same way, but without the presence of the target molecule. The selectivity of the MIP was tested by optical batch rebinding experiments using chemically similar structures of histamine, such as betahistine and histidine. Furthermore, serotonin and nicotine were used because they are similar in size (Figure 1). For the impedimetric measurements, a MIP was developed that was imprinted with betahistine, as an alternative test for the

selectivity. The MIP was synthesized with the same procedure and same molar ratios, but instead of histamine, betahistine was used as the template molecule. The MIP and NIP powders mentioned here were used for all further batch-rebinding and impedimetric measurements.

3.3.3 Preparation of bowel fluid and ELISA test

Bowel fluid samples from the duodenum were obtained from three healthy volunteers, Person 1, 2 and 3, and divided over 1 ml Eppendorf tubes. After collection, the tubes were centrifuged with 2000 g to obtain a clear fluid. The samples were stored at -80˚C to prevent degradation. Prior to analysis, the samples were heated up to 37˚C and divided into different aliquots. One part remained unaltered, while from the other parts the native histamine was removed by extraction. This was done by adding 10 mg of MIP powder to 3 ml of the bowel fluid. The fluid mixture was shaken for 30 min to allow full absorption of the native histamine, followed by filtration to remove the MIP particles. The resulting extracted bowel fluid served as a reference and furthermore, upon adding of spiked concentrations of 2.5, 5, 7.5, 25 and 50 µM, it was possible to construct a dose-response curve. Subsequently, the impedance response of the unaltered sample was measured with freshly prepared MIP- and NIP electrodes. With the dose-response curve, the native histamine concentration could be calculated.

With the unaltered samples, ELISA reference tests were performed with the human histamine ELISA test from Gentaur Molecular Products. All samples were measured in triplo and the histamine concentration was calculated by comparing the optical density of the sample to that of the standard curve (Figure 5).
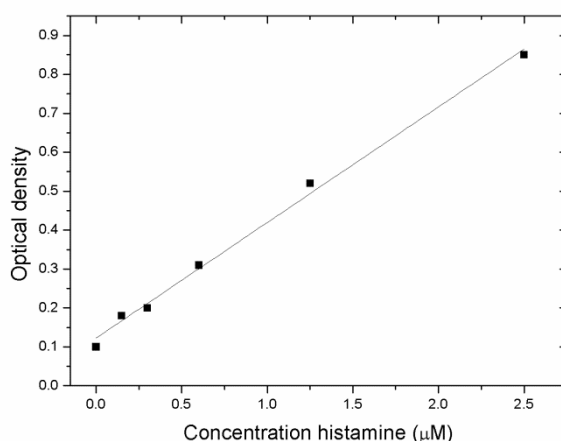
Figure 5: Calibration curve for the ELISA test, where the histamine concentration is plotted vs the optical density.

For calibration, known histamine concentrations (0.15, 0.3, 0.6, 1.25, 2.5 µM) were used and the optical density at 450 nm was determined. The data can be excellently fitted with a linear fit (R^2 = 0.99), with an intercept of 0.14 and a slope of 0.29 μM^{-1}. According to the calibration, the histamine concentration was determined to be 870 nM ± 60 for Person 1. For Person 2, this was found to be 500 nM ± 50 nM and for Person 3, respectively 460 ± 60 nM.

3.3.4 Impedance-spectroscopy platforms

In previous work, we have introduced a differential sensor cell offering several benefits for biological measurements [26]. With this setup, native serotonin plasma concentrations were measured with relatively small uncertainties and the obtained results were in full agreement with HPLC reference tests [27]. The flow-through cell is made of Perspex and has an internal volume of 110 µl. During the measurements, the temperature was fixed to 37 ± 0.02°C using a homemade proportional-integral-derivative (PID) controller (P = 10, I = 5, D= 0.1). The MIP -and NIP-coated electrodes (reference channel) were installed symmetrically with respect to a gold wire serving as a common counter electrode. To construct the electrodes, 1 × 1 cm^2 aluminum substrates were spincoated with conductive OC_1C_{10}-PPV. Equal amounts of the MIP -and NIP powder were embedded into the layer by heating up the PPV above its glass

transition temperature. The contact area of each electrode with the liquid (28 mm²) was defined by O-rings and the distance to the gold counter electrode was 1.7 mm. The impedance signals were measured with a home-made, portable system operating in a frequency range of 100 Hz to 100 kHz with 10 frequencies per decade and a scanning speed of 5.7 s per sweep [26]. The amplitude of the AC voltage was fixed to 10 mV under open circuit conditions.

3.4 Results and discussion

3.4.1 Optical binding rebinding experiments

Batch rebinding experiments were performed with a Varian Cary 500 UV-vis-NIR spectrophotometer (Leuven, Belgium). The performance and selectivity of the synthesized MIPs were analyzed under varying pH conditions. Furthermore, at pH 5 the selectivity was evaluated with the analogues nicotine, serotonin, histidine and betahistine (Figure 1).

For the batch rebinding experiments, 20 mg of MIP or NIP powder was added to 5 ml of aqueous histamine concentrations in the range between 0.1 to 1.0 mM. The pH of the aqueous solutions was adjusted between pH 4 – 9 by the addition of a hydrochloric acid solution or a sodium hydroxide solution. The resulting suspensions were shaken for 1 h on a rocking table at room temperature. After filtration, the free concentration (C_f) of histamine was determined by UV-vis spectroscopy. Hereby, the amount of bound histamine per gram of MIP or NIP was calculated (S_b) and the binding isotherms were constructed. The binding isotherms for the MIP and NIP of AA for pH 4 to 9 are demonstrated in Figure 6 a,b. Furthermore, the IF at a given concentration (C_f = 0.05 mM) was calculated. This corresponds to the amount of target molecules bound per gram of the MIP divided by that of the NIP and is a measure of the specificity (S_b MIP / S_b NIP). To calculate the IF for each pH value, the binding isotherms were fitted allometrically and with the obtained fit, the values at the correct concentration could be determined. These results, in the pH range 4 – 9, are plotted in Figure 6c.
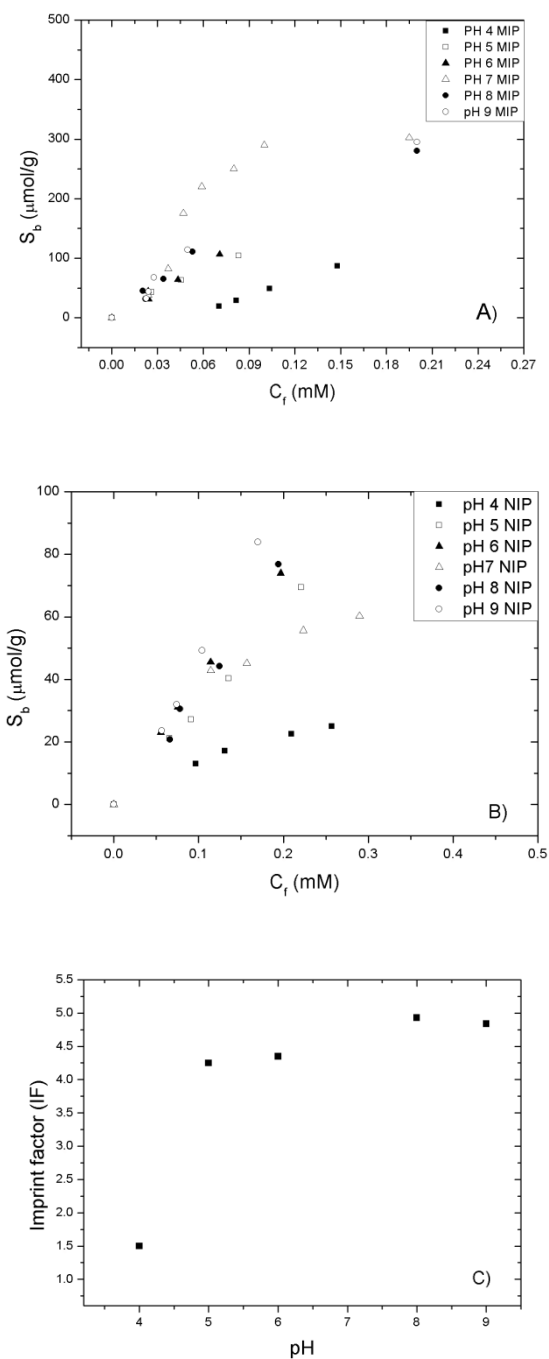
Figure 6: Binding isotherms for the MIP (A) and NIP (B) at pH 4-9. To directly compare the MIP and NIP, the imprint factor (C_f = 0.05 M) are given in the pH range 4 – 9 (C).

The binding isotherms of the MIP (Figure 6a) and NIP (Figure 6b) show that at pH 4 the binding is mostly aspecific, while from pH 5 – 9 histamine can be detected specifically. This can be explained by the statistical binding analysis model. At pH 4, there is only a low probability (24%) of hydrogen bond formation. The theoretical probability of binding in the pH region 5 – 9 is above 90%, which indicates that the MIPs are able the bind the target specifically as indeed is observed from experiments. This is confirmed by Figure 6c, which shows the imprint factor that is significantly lower at pH 4 (1.5) than at pH 5 – 9 ($\sim$ 4.5).

There are several models to describe such binding isotherms. The Langmuir model assumes that all the binding sites are homogeneous, which is clearly not the case with MIPs as there are both aspecific and specific affinity sites. To correct for these heterogeneous binding sites, the Langmuir-Freundlich or Freundlich model can be applied [28]. These models resulted both in a fit with a high linearity coefficient ($R^2 = 0.98$) at pH 5, however there was chosen to show the results of the Freundlich model as this uses one parameter less than the Langmuir-Freundlich model (Figure 7). In this Figure also the Freundlich isotherm of the MIP based on MAA monomers is shown, to give a direct comparison of the different behavior at pH 5.
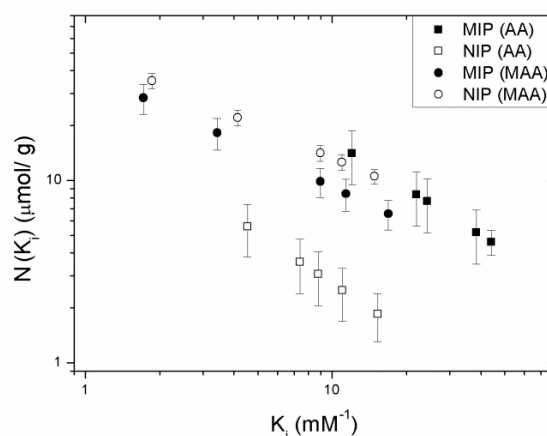
Figure 7: The Freundlich isotherm of the AA MIP and NIP when exposed to histamine concentrations in PBS of pH 5. As a comparison, the results are also given for a MIP based on MAA monomers.

These isotherms show the distribution of the affinity sites by plotting the binding energy (K_i) versus that of the number of sites present ($N(K_i)$). The sites with a low binding affinity correspond to the aspecific binding, while the high affinity binding sites represent the specific binding. The total number of binding sites for the MIP with AA monomers was 114 ± 0.9 µmol/g, while that of its reference NIP is considerably lower with 21 ± 0.4 µmol/g (i.e., an imprint factor of 5.4). As a comparison, the MIP based on MAA monomers had a total number of binding sites of 20 ± 0.3 µmol/g, which was 13 ± 0.6 µmol/g for its NIP. Hereby it is proven that the MIP synthesized from acrylic acid, in contrast to the MIP synthesized from methacrylic acid, can specifically detect histamine at pH values as low as 5.

To further test the selectivity, the binding of a number of related molecules was investigated. Histidine was used as an analogue in previous articles [1,2] due to its biological relevance, it is the natural precursor of histamine. In its chemical structure, however, there is a significant difference: histidine is an acid while histamine acts as a base. Therefore, we also studied the response of betahistine, which is chemically more similar to histamine. The only difference is that the amine group of the histamine molecule is substituted by a methyl group (Figure 1). The binding isotherms obtained with histamine and the analogues are presented in Figure 8.
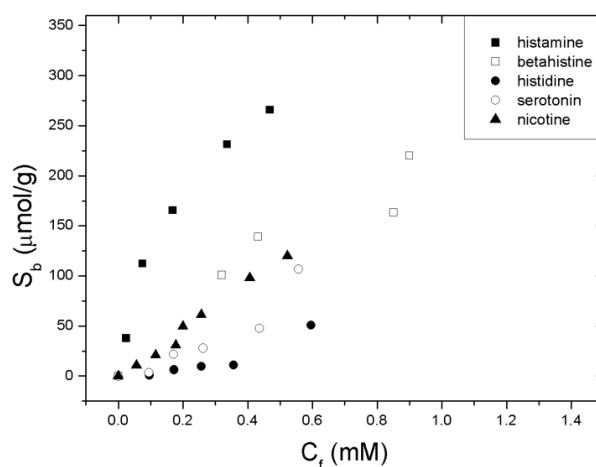
Figure 8: Binding isotherm of the analogues molecules betahistine, histidine, serotonin and nicotine to the MIP compared to that of histamine. The measurements were performed in PBS solutions of pH 5.

From Figure 8, we can observe that the MIPs bind no more of the chosen analogues than the reference NIP binds histamine and therefore, the selectivity of the MIP is proven. Furthermore, as betahistine binds relatively the most to the MIP, this was chosen as an analogue for the impedance measurements.

3.4.2 Impedimetric measurements in PBS buffer

Histamine occurs mostly in acidic fluids such as saliva, stomach fluid and intestinal fluid. It is of clinical relevance to measure in intestinal fluid, as an increase in concentration could be a possible marker of IBS [11, 12]. The normal histamine concentration ranges from 500 – 1000 nM, which was determined by ELISA tests. The pH lies between pH 5 – 8, meaning that it can vary from slightly acidic to slightly basic [21]. Before directly measuring biological fluids, the specificity and selectivity was tested in PBS solutions. To cover the entire pH range of bowel fluids, measurements were performed at pH 5 and 7.

MIP and corresponding NIP particles were immobilized onto the aluminum electrodes with the procedure described by R. Thoelen *et al.* [29]. By optical microscopy in combination with image processing (Image J software), the surface coverage was determined to be 27%   ± 2.0 for the MIP and

26% ± 3.0 for the NIP –loaded electrode.   Therefore, the precondition for differential measurements, having identical particle loadings, is fulfilled. Next, the flow-through cell was filled with PBS buffer. After stabilizing the cell with PBS (respectively, pH 5 or 7) for 45 min, increasing concentrations (50 – 1000 nM) of histamine were added. The raw impedance data in time, for a frequency of 316 Hz, is shown for the NIP and MIP at pH 5 (Figure 9).
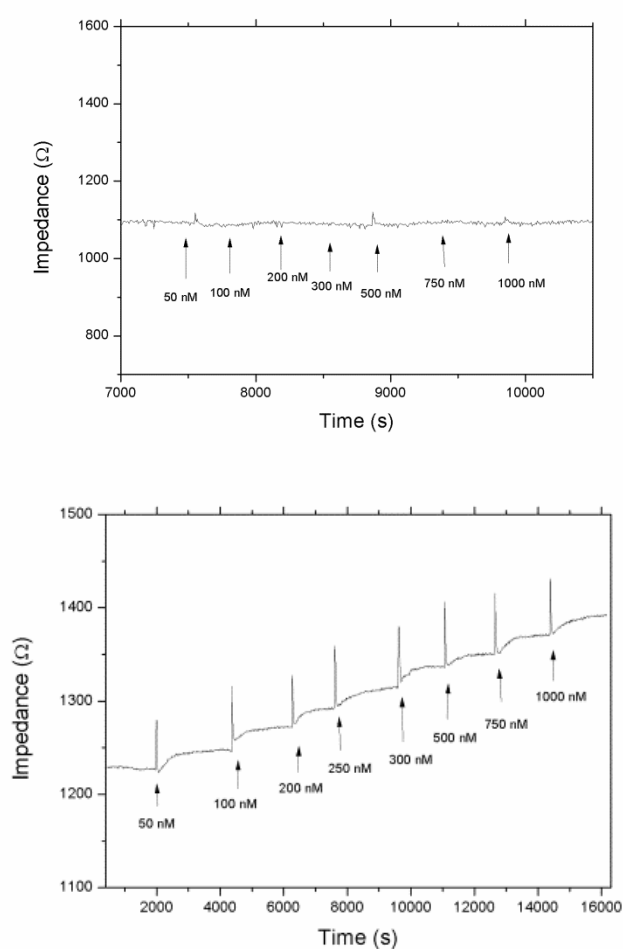
Figure 9: The impedance in time, at a frequency of 316 Hz, is shown for the NIP (above) and MIP (below) when increasing concentrations of histamine (50-1000 nM in PBS pH 5) were added.

The MIP and NIP were exposed to the same concentrations of histamine; however there is a clear difference between their responses. For the MIP,

directly after addition the impedance increases till a plateau level is reached. After the next addition, this process is repeated until the sensor is fully saturated. In the case of the NIP, upon addition a minor peak is observed due to the temperature difference of the added fluid and the sensor cell, but after stabilization the signal goes back to the base level.

From the raw data, the corresponding dose-responses can be constructed (Figure 10). This was done at a frequency of 316 Hz, which was selected for two reasons. First, the signal was very stable with only a standard deviation of 0.1% on the impedance. This ensures a high signal to noise ratio ($\sim$ 10) at a concentration of 50 nM in PBS of pH 5. Additionally, we can make an estimation of the detection limit. The limit of detection is commonly defined as three times this standard deviation. Hereby, a detection limit of 15 nM is achieved in buffer solution. This is well below the physiologically relevant concentration, which is 500 nM or higher. Secondly, it was previously demonstrated that the effect upon binding is mainly capacitive [28] and therefore, especially the low frequency regime should be investigated.
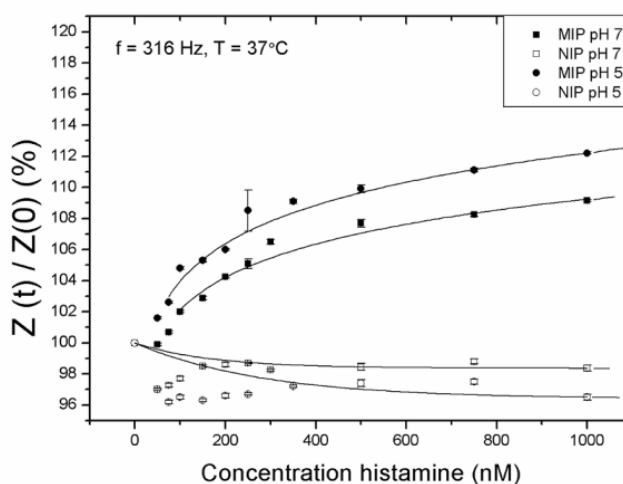
Figure 10: Dose-response curve for MIP and NIP exposed to increasing concentrations of histamine in PBS of pH 5 and 7. The error bars are indicated, but if applicable, they can be smaller than the symbol size. The used fit was allometric (y = a x^b, with R^2 = 0.98).

The impedance data for each concentration were normalized with respect to a starting value of 100% pure PBS, prior to addition of the target molecule. After the addition step, the sensor was left to stabilize for 10 min. The response value was then obtained by averaging five data points with an interval of one minute. Hereby, the measuring time was not significantly prolonged and impedance data scattering was reduced to a minimum.

The impedance results confirmed that the MIP based on AA monomers can detect histamine at pH 5. In the 0 – 400 nM range of histamine in PBS with a pH 5, the dose-response results can be represented well with a linear fit (R^2 = 0.99). For the physiologically relevant concentration range (500-1000 nM), the data is best represented with an allometric fit (R^2 = 0.98) which is due to an increasing occupation of the binding sites. However, there is still a significant difference between the impedance response at 500 nM (109.9 % ± 0.2) compared to 1000 nM (112.2 % ± 0.1), which allows discrimination between normal and elevated values of histamine.

To test the selectivity, impedance measurements were performed within the same concentration range for betahistine (0 – 1000 nM) as was done for histamine. Additionally, histamine measurements in the presence of an excess of 1000 times serotonin were performed, which did not significantly alter the obtained results. To test the cross selectivity, a MIP was synthesized using betahistine as the template molecule. The protocol was kept the same as for histamine; for the exact recipe we refer to section 3.3.2. This MIP was also incorporated into the sensor setup and subsequently, impedimetric measurements were performed with increasing betahistine concentrations (0 – 750 nM). The obtained results at a frequency of 316 Hz are shown in Figure 11.
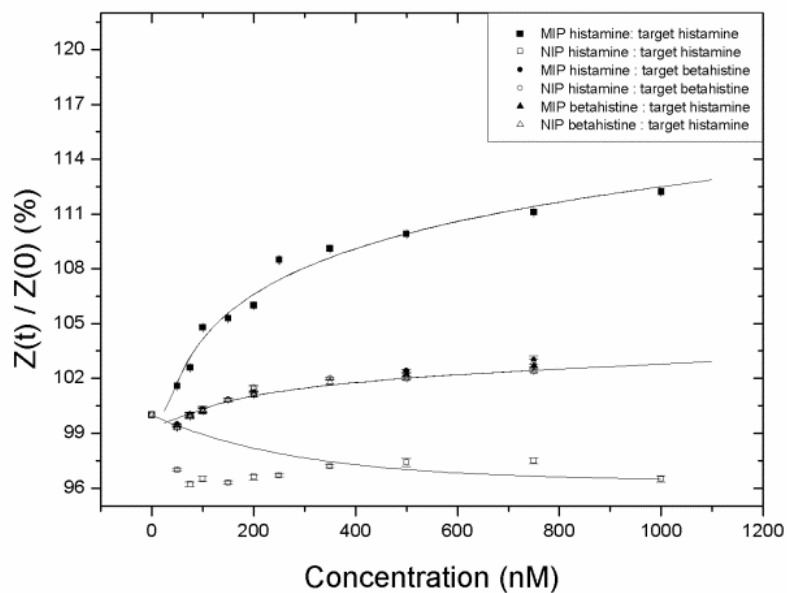
Figure 11:Dose-response curve for the histamine MIPs and NIPs exposed to increasing concentrations of histamine and betahistine in PBS of pH 5.To test the cross selectivity, a MIP with betahistine as template was developed to which histamine was added. The used fit is allometric (y=a x^b, with R^2=0.98).

This is a first indication of specific recognition by the MIP receptors. However, normally in biological samples histamine is in the presence of various biogenic amines which are possible competitors. Therefore, the measurements were performed in PBS (pH 7) solutions with not only histamine, but also an excess of serotonin. At each histamine concentration, an additional 100 µM concentration of serotonin was present.
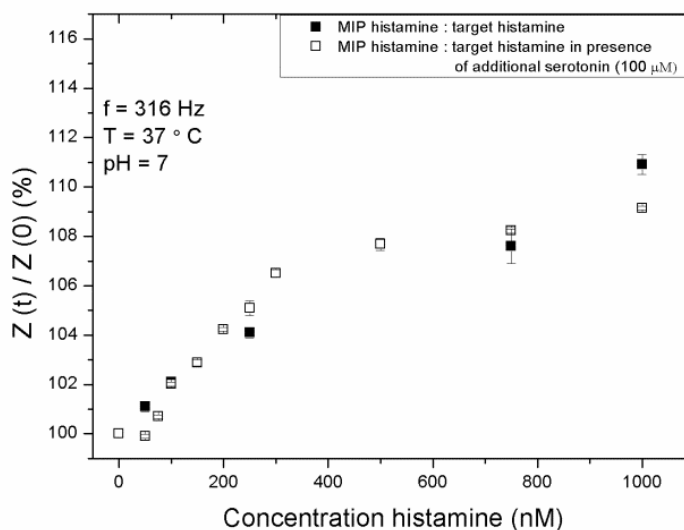
Figure 12: The dose-response curve for MIP-NIP signal exposed to increasing concentrations of histamine in PBS of pH 7. The open squares correspond to Figure 10, the solid squares were performed in the presence of 100 μM serotonin.

Hereby, we conclude that histamine can be measured in a specific manner, even when interfering compounds are present. It is possible to cover the entire desired pH range (5 - 8) of biological samples. In the rare case that the pH of the patient's sample is lower than 5, one can think of adjusting the pH by sodium hydroxide (NaOH) addition or by dilution in order to perform the analysis within the specified pH-range of the sensor. For measurements in highly acidic samples, one may also consider MIPs synthesized from a monomer with a lower pKa value.

3.4.3 QCM measurements in MilliQ water of pH 5

QCM was selected as a second read-out technique since it can be used to determine histamine concentrations in the micromolar range. With this additional technique, we ensure detection in buffer in a wide concentration range from nanomolar (impedance spectroscopy) to micromolar (QCM) to millimolar (UV-vis spectroscopy).

Horemans et *al.* [2] investigated the fluid of canned tuna for its histamine content with a QCM sensor platform. For the measurements with histamine in Milli Q water of pH 5, the same design was adopted. The method of detection is based on the piezoelectric properties of quartz crystals. When target molecules bind to the nanocavities, its oscillation frequency will change according to the mass increase. This relationship is described by the Sauerbrey equation.

The measurements were performed with a PLO-10 phase-lock oscillator from Maxtek Inc (Cypress, USA). The crystals were standard AT-cut, 5 MHz, Tiu/Au polished with an active oscillation region of 34.19 mm^2. The pump was a NE-500 syringe pump from Prosense B.V (Oosterhout, The Netherlands). The quartz crystals were spincoated with a 0.7% wt PVC solution in tetahydrofuran (THF). Subsequently, the MIP and NIP particles were embedded into the polymer layer similar to the stamping method used for the impedimetric measurements. The surface coverage was assessed to be 27 ± 0.5 % for the NIP and 28 ± 0.7 % for the MIP. For the actual measurements, crystals were placed in the crystal holder, which was connected to the syringe pump on one side and on the other side to the addition reservoir. At the start of the measurements, Milli Q water was pumped through the crystal holders with a flow rate of 0.1 ml/min. After stabilization, the flow was stopped and concentrations of histamine were pumped into the cell (rate = 0.1 ml/min). The concentration range for both the MIP and NIP was 75 – 1000 µM in Milli Q with pH adjusted to 5 with a hydrochloric acid (HCl) solution. In the dose-response curve, the histamine concentration is plotted versus the frequency shift of the MIP–NIP signal.
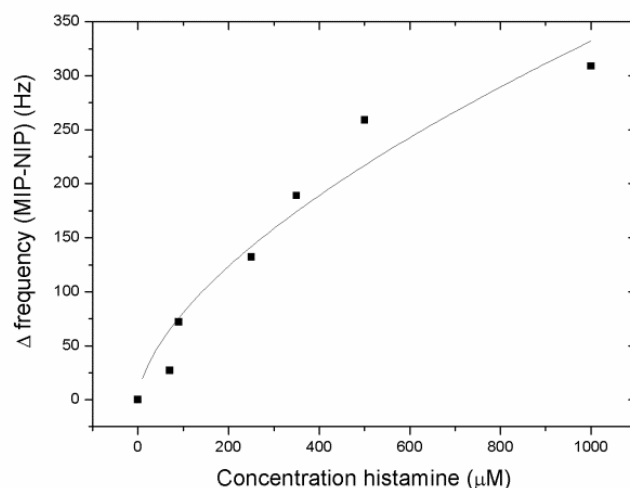
Figure 13: QCM dose-response (MIP–NIP) signal for histamine in water of pH 5. The data is again represented by an allometric fit (R^2 =0.95).

With this sensor platform, histamine could be detected in the micromolar range (70 – 1000 µM in water of pH 5) with a maximum frequency shift of 309 ± 5 Hz. Although these concentrations are too high for biomedical purposes, this range of detection is perfectly suitable for food safety analysis, since the concentration of histamine in rotten fish, due to the breakdown of histidine, can be up to 1000 µM [10].

3.4.4 Determination of histamine content in bowel fluid, validated by ELISA tests

As a final step, the histamine concentration of intestinal fluid samples was investigated. Patient samples from the duodenum were collected and prepared according to paragraph 3.3.3. To perform the measurements, the cell was first filled with the extracted (non-spiked) bowel fluid of Person 1. The cell was allowed to stabilize for 90 min until a 0.1% noise ratio was achieved. Subsequently, spiked plasma samples were introduced one by one via a pumping system. After waiting each time for 20 min, the impedance results were determined of the MIP and NIP and averaged over 5 data points. The impedance values of the MIP–NIP response, normalized to non-spiked extracted plasma at 316 Hz, are given in Figure 14.
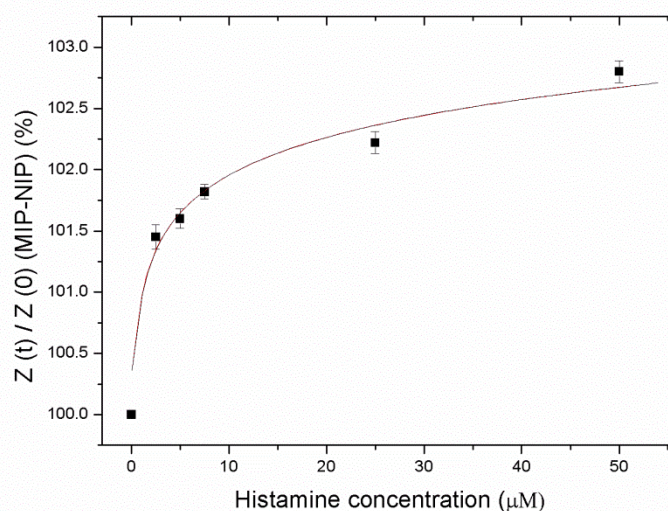
Figure 14: The normalized MIP-NIP response of the extracted bowel fluid of person 1 spiked with 2.5, 5, 7.5, 25 and 50 µM of histamine. The graph is fitted with an allometric function ($y = a\,x^b$) with parameters a = 1.14, b = 0.22 and R^2 = 0.97. Unextracted bowel fluid resulted in an increase of 0.86%, which corresponds to a value of 800 ± 90 nM. With ELISA reference tests, a value was found of 870 ± 60 nM.

The impedance change upon exposure to a given histamine concentration is less pronounced than the measurements performed in PBS buffer. A possible explanation for this could be the non-specific absorption of proteins and bile acids onto the electrode, which partially block the nanocavities. However, there is still a clear MIP–NIP difference with increasing concentrations, as the differential (MIP–NIP) signal in Figure 14 shows. This can be excellently described with an allometric fit. With this experimental dose-response curve, initial (unextracted) bowel fluid concentrations can be measured and the corresponding histamine concentrations were determined for Person 1, 2 and 3 (Table 4). As an example, in the case of Person 1 an impedance increase of 0.86 % ± 0.09 was found which corresponds to an initial concentration of 800 nM ± 90. For Person 2 and Person 3, the histamine concentrations were, respectively, 570 nM ± 70 and 500 nM ± 60.

To validate the results, reference ELISA tests were performed. As Table 4 demonstrates, the results obtained by the sensor and the ELISA tests are nicely within the statistical error range. The pH was estimated by using universal pH paper, which indicates that the samples are, as was expected, mildly acidic.

Table 4: The pH of the bowel fluid samples and the histamine concentration as determined by the sensor setup and reference ELISA tests of Person 1, 2 and 3.

Persons	pH	Sensor histamine concentration (nM)	ELISA histamine concentration (nM)
P1	5	800 ± 90	870 ± 60
P2	6	570 ± 70	500 ± 50
P3	6	500 ± 60	460 ± 60

3.5 Conclusions

Histamine is a biogenic amine which mainly occurs in acidic fluids, such as saliva and gastric fluid. Commonly, detection is performed by techniques such as HPLC or ELISA. Sensor platforms with MIPs as synthetic receptors present a fast and low-cost alternative to these traditional techniques, however, previously developed MIPs exhibited a pH dependent binding behavior which complicated binding in acidic environments. We have proposed a statistical binding analysis model to explain this pH dependent response and, based on theoretical calculations, developed a MIP able of detecting histamine at acidic pH. These theoretical calculations were supported by UV-vis batch rebinding experiments, which demonstrated specific and selective detection of histamine in the required pH range. With impedance spectroscopy as read-out technique, detection could be performed in the physiologically relevant concentration range. Three intestinal fluid patient samples were measured and the determined histamine concentrations were in nice agreement with ELISA reference tests. Summarizing, we have developed a fast and low-cost method to detect histamine selectively in bowel fluids with the possibility of transferring the techniques to other analytes in an array format.

3.6 Acknowledgements

3.7 References

[1]   E. Bongaers, J. Alenus, F. Horemans, A. Weustenraed, L. Lutsen, D. Vanderzande, T.J. Cleij, F.J. Troost, R.-J. Brummer, P. Wagner, *Phys Status Solidi A.,* 2010, **207**, 837-843.

[2]   F. Horemans, J. Alenus, E. Bongaers, A. Weustenraed, R. Thoelen, J. Duchateau, L. Lutsen, D. Vanderzande, *Sens Actuators, B.,* 2010, **148**, 392-398.

[3]   H.H. Dale, P.P Laidlaw, *J Physiol.,* 1910, **41**, 318-344.

[4]   W. Paul, *Fundamental Immunology,* 2nd ed.; Raven Press: New York, 1984, 716-720.

[5]   D. Metcalfe, D. Baram, Y. Mekori, *Physiol Rev.,* 1997, **77**, 1033-1079.

[6]   H. Rang, M. Dale, J. Ritter, P. Gardner, *Pharmacology,* 3rd ed.; Churchill Livingstone, New York, 1995, 226-229.

[7]   L.G. Jr. Harsing, H. Nagashima, D. Duncalf, E.S. Vizi, P.L. Goldiner, *Clin Chem.,* 1986, **32**, 1823-1827.

[8]   R.Y. Lin, L.B. Schwartz, A. Curry, G.R. Pesola, H.S. Hee, L. Bakalchuk, C. Tenenbaum, R.E. Westfal, *J Allergy Clin Immunol.,* 2000, **106**, 65-71.

[9]   J.C. Schwartz, H. Pollard, T.T. Quach, *Neurochem.,* 1980, **35**, 26-33.

[10]   L. Lehane, J. Olley, *Int J Food Microbiol.,* 2000, **58**, 1-37.

[11]   G. Barbara, V. Stanghellini, R. De Giorgio, C. Cremon, G.S. Cottrell, D. Santini, G. Pasquinelli, A.M. Morselli-Labate, E.F. Grady, N.W. Bunnett, S.M. Collins, R. Corinaldesi, *Gastroenterology,* 2004, **126**, 693-702.

[12]   J.D. Wood, *Gut,* 2006, **55**, 445-447.

[13]   Y.Z. Chhabra, H. Li, A.E. Alkhouri, Q. Blake, C.L. Armour, J.M. Hughes, *Eur Respir J.,* 2007, **29**, 861-870.

[14]   M. Adlesic, M. Verdrengh, M. Bokarewa, J. Dahlberg, S.J. Foster, A. Tarkowski, *Scan J Immunol.,* 2007, **65**, 530-537.

[15]   J.A. Jackson, H.D. Riordan, B.S. Neterhy, *J Orthomol Psychiatry,* 1998, **13**, 236-240.

[16]   A. Tong, H. Dong, L. Li, *Anal Chim Acta.,* 2002, **466**, 31-37.

[17]   C.J. Allender, C. Richardson, B. Woodhouse, C.M.. Heard, K.R. Brain, *Int J Pharm.,* 2000, **195**, 39-43.

[18]   A.S. Pietrzyk, S. Suriyanarayanan, W. Kutner, R. Chitta, F. d'Souza, *Anal Chem.,* 2009, **81**, 2633-2643.

[19]   M. Jenik, R. Schirhagl, C. Schirk, O. Hayden, P. Lieberzeit, D. Blaas, G. Paul, F. Dickert, *Anal Chem.,* 2009, **81**, 5320-5326.

[20]   F. Trikka, K. Yoshimatsu, L. Ye, D. Kyriakidis, *Amino Acids*, 2012, **43,** 2113-2124.

[21]   D.F. Evans, G. Pye, R. Bramley, A.G. Clark, T.J. Dyson, J.D. Hardcastle, *Gut,* 1988, **29**, 1035-1041.

[22]   E.K. Izumrudov, S.A. Sukhishvili, *Biomacromolecules,* 2005, **6**, 1782-1788.

[23]   M. Fujiwara, R. Grubbs, J.D. Baldeschwieler, *J Colloid Interface Sci.,* 1997, **185**, 210-216.

[24]   D. Louwet, D. Vanderzande, A. Gelan, *Synth Met.,* 1995, **69**, 509-510.

[25]   P. Christiaens, V. Vermeeren, S. Wenmackers, M. Daenen, K. Haenen, M. Nesládek, M. vandeVen, M. Ameloot, L. Michiels and P. Wagner, *Biosens Bioelectron.,* 2006, **22**, 170 – 177, 2006.

[26]   B. van Grinsven, N. Vanden Bon, L. Grieten, M. Murib, S. Janssens, K. Haenen, E. Schneider, S. Ingebrandt, M.J. Schöning, V. Vermeeren, M. Ameloot, L. Michiels, R. Thoelen, W. De Ceuninck, P. Wagner, *Lab Chip,* 2011, **11**, 1656-1663

[27]   M. Peeters, F.J. Troost, B. van Grinsven, F. Horemans, J. Alenus, M.S. Murib, D. Keszthelyi, A. Ethirajan, R. Thoelen, T.J. Cleij, P. Wagner, *Sens Actuators, B.,* 2012, **171**, 602-610.

[28]   R.J. Umpleby, S.C. Baxter, A.M. Rampey, G.T. Rushton, Y.Z. Chen, K.D. Shimizu, *J Chromatogr B: Anal Technol Biomed Life Sci B.,* 2004, **804**, 141-149.

[29]   R. Thoelen, R. Vansweevelt, J. Duchateau, F. Horemans, J. D'Haen, L.
        Lutsen, D. Vanderzande, M. Ameloot, M. vandeVen, T.J. Cleij, P. Wagner,
        Biosens Bioelectron., 2008, **23**, 913-918

Chapter 4

Heat-transfer based detection of L-nicotine, histamine, and serotonin using molecularly imprinted polymers as biomimetic receptors

M. Peeters[1], P. Csipai[1,2], B. Geerets[1], A. Weustenraed[1], B. van Grinsven[1], J. Gruber[2], W. De Ceuninck[1,3], T.J. Cleij[1], F.J. Troost[4] and P. Wagner[1,3].

1) Hasselt University, Institute for Materials Research IMO, Wetenschapspark 1, B-3590 Diepenbeek, Belgium.

2) Universidade de São Paulo, Instituto de Química, Av. Prof Lineu Prestes, 748 CEP 05508-000 São Paulo, SP, Brazil.

3) IMEC vzw, IMOMEC, Wetenschapspark 1, B-3590 Diepenbeek, Belgium

4) Department of Internal Medicine, div. of Gastroenterology – Hepatology, Maastricht University Medical Center, Minderbroedersberg 4-6, 6211 LK Maastricht, The Netherlands.

4.1 Abstract

In this work, we will present a novel approach for the detection of small-molecules with Molecularly Imprinted Polymers (MIP)-type receptors. This heat-transfer method (HTM) is based on the change in heat-transfer resistance imposed upon binding of target molecules to the MIP nanocavities. Simultaneously with that technique, the impedance is measured to validate the results. For proof-of-principle purposes, aluminum electrodes are functionalized with MIP particles and L-nicotine measurements are performed in phosphate buffered saline (PBS) solutions. To determine if this could be extended to other templates, histamine and serotonin samples in buffer solutions are also studied. The developed sensor platform is proven to be specific for a variety of target molecules, which is in agreement with impedance spectroscopy reference tests. In addition, detection limits in the nanomolar range could be achieved, which is well within the physiologically relevant concentration regime. These limits are comparable to impedance spectroscopy, which is considered one of the state-of-the-art techniques for the analysis of small molecules with MIPs. As a first demonstration of the applicability in biological samples, measurements are performed on saliva samples spiked with L-nicotine. In summary, the combination of MIPs with HTM as novel read-out technique enables fast and low-cost measurements in buffer solutions with the possibility of extending to biological samples.

4.2 Introduction

Molecularly Imprinted Polymers (MIPs) are synthetic receptors which can bind their target as specific and selective as an enzyme [1, 2]. In recent years, the interest from the bio-analytical field has increased rapidly because MIPs are extremely suitable for the detection of chemical targets in complex matrices such as urine, blood and saliva [3]. For separation purposes, MIPs can be readily used by packing them directly into separation columns [4]. The main drawbacks of chromatographic techniques are the often time-consuming measurements and the requirement of expensive equipment [5,6]. The incorporation of MIPs into sensing devices remains therefore challenging. In literature, the majority of the sensor platforms is based on gravimetric detection [7] and electronic read-out platforms [8, 9]. In contrast to gravimetric detection, electrochemical techniques are inexpensive but the analysis is often complicated. There are a few examples of MIP measurements in biological samples such as in human blood plasma [10], intestinal fluid [11], blood serum [12, 13] and urine [13]. These measurements are all *in vitro*; until now little has been reported about their application in living organisms. Hoshino *et al*. [14] studied the behavior of molecularly imprinted polymer nanoparticles for mellitin *in vivo.* With fluorescent labeling of the target, they could determine that the nanoparticles could effectively capture the mellitin from the blood stream of mice. Furthermore, the particles were demonstrated to be nontoxic to cultured cells (fibrosarcoma cells) over a concentration range of 3 – 3000 µg/ml. This is a very promising result for future *in vivo* measurements, but the fluorescent technique is costly and not label-free.

In this article, we will focus on detection by means of differential heat-transfer resistance. For the Heat-Transfer Method (HTM) only two thermocouples, a proportional-integral-derivative (PID) controller and an adjustable heat source are required, ensuring a straightforward sensor platform and low-cost detection. This approach has been recently applied for the screening of single nucleotide polymorphisms in DNA fragments [15], which makes it a valuable tool in mutation analysis. To our knowledge, HTM has not been employed yet for small-molecule detection with MIP receptors. There are some examples of thermometric MIP sensors in literature, but they are based on the reaction heat developed upon binding and not on the heat-transfer properties of the MIP-layer

[16, 17, 18]. As a proof-of-principle experiment, we studied the detection of L-nicotine (Figure 1) with the HTM concept.
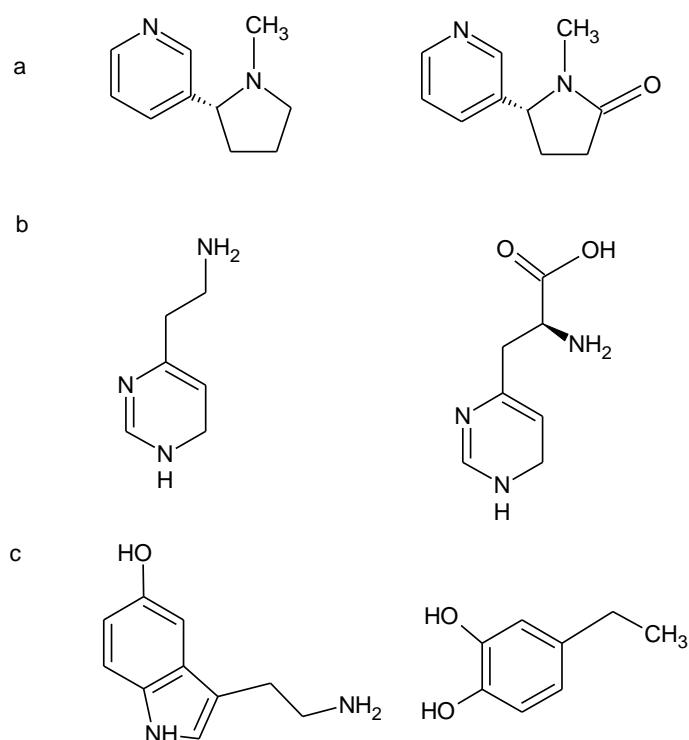
Figure 1: Chemical structures of A) L-nicotine and its metabolite cotinine B) histamine and its precursor histidine C) serotonin and its competitor dopamine.

L-nicotine is the major addictive substance in tobacco [19]. Consumption of tobacco has proven to result in a higher risk for the development of cancer [20, 21] and disorders *e.g.* pulmonary disease [22] and atherosclerosis [23]. Thoelen *et al.* [24] integrated MIP particles for L-nicotine into an impedimetric sensor setup and measured a series of concentrations in PBS solutions. This MIP, based on the monomer MAA, will be used for further measurements described within this article.

The detection of histamine and serotonin in biological fluids has been reported previously with MIP receptors in combination with impedimetric read-out [10, 11]. With some modifications to the setup (Figure 2), we can simultaneously

measure the impedance signals and heat-transfer resistance for direct validation of the results. First, proof-of-principle measurements are conducted with L-nicotine in PBS. Subsequently, similar experiments are performed with histamine and serotonin to show the principle for a variety of targets. For the applicability of the sensor platform in biological samples, spiked L-nicotine samples in saliva were studied and a dose-response curve was constructed. In summary, we will demonstrate the fast and low-cost detection of small molecules in buffer solutions with MIP receptors in combination with the HTM. Since this method has the possibility of extending to biological samples, it offers a huge potential for analytical research.

4.3. Experimental

4.3.1. Materials

Ethylene glycol dimethacrylate (EGDM), methacrylic acid (MAA), acrylic acid (AA), acrylamide (AM) and dimethylsulfoxide (DMSO) were obtained from Acros (Geel, Belgium). Prior to polymerization, the stabilizers in EGDM, MAA and AA were removed by filtration over alumina. The initiator azobisisobutyronitrile (AIBN) was purchased from Fluka (Buchs, Switzerland). As templates, L-nicotine, histamine and serotonin (Figure 1 A, B and C) were used. L-nicotine was obtained from Acros, while serotonin and histamine were purchased from Alfa Aesar (Karlsruhe Germany). All solvents were of analytical grade and used without further purification.

4.3.2 MIP synthesis

The MIP L-for nicotine was synthesized as follows: First, a mixture of 12.5 mmol MAA (Acros), 72 mmol EGDM (Acros) and 0.61 mmol AIBN (Fluka) was dissolved in 7 ml hexane together with 6.41 mmol of the template molecule L-nicotine (Acros). The solution was degassed with N_2 and polymerized in a thermostatic water bath at 60 °C for 72 h. After polymerization, the polymer was ground and the L-nicotine was removed by Soxhlet extraction with methanol (48 h), a mixture of acetic acid/acetonitrile (1/1) (48 h) and again methanol (12 h). A NIP was synthesized according to the same procedure, but without the presence of

the target molecule. The synthesis procedure for the MIPs for serotonin and histamine are described in detail in ref [10] and [25].

4.3.3. Electrode preparation for the thermal resistance and impedance measurements

For the heat-transfer resistance and impedance measurements, 1 x 1 cm^2 aluminum substrates were spincoated with conductive MDMO-PPV. This PPV derivative, serving as an adhesive layer, was synthesized via the sulfinyl precursor route [26]. Subsequently, MIP –and NIP particles were applied to the surface with a PDMS stamp. By heating above the T_g of 120 °C, the powder is allowed to sink partially into the adhesive layer. After cooling, the surface is rinsed with isopropanol to remove excessive powder and ensure that the particles are strongly fixated into the layer [24]. To demonstrate an equal load of the MIP –and NIP electrode, the sensor surface was studied with an Axiovert 40 inverted optical microscope (Carl Zeiss). With optical microscopy in combination with image processing (software by Image J of National Institute of Health, Bethesda, USA), the MIP (25 ± 2 %) and NIP (24 ± 3 %) were found to have nearly identical particle loadings which is necessary to perform differential measurements.

4.3.4 Design of sensor-setup

The general concept for the measuring setup is shown in Figure 2.
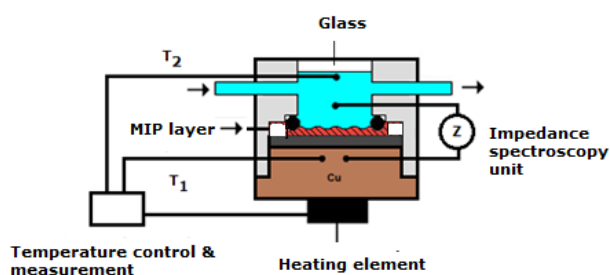
Figure 2: Schematic illustration of the general concept of the measuring set-up. The temperature of the copper block, T_1, is strictly controlled at 37.00 ± 0.02 °C. The heat flows from the copper block through the MIP layer to the liquid, where T_2 is measured. Simultaneously with the temperature, the impedance is monitored.

The aluminum substrates, functionalized with MIP and NIP particles, were horizontally mounted into a Perspex flowcell with an internal volume of 110 µl. Silver paste ensured good thermal contact between the copper and the substrate. Two miniature thermocouples (type K, diameter 500 µm, TC Direct, the Netherlands) monitored the temperature of the copper backside contact (T_1) and the temperature of the fluid (T_2) 1.7 mm above the chip surface. The temperature T_1 was strictly controlled at 37.00 ± 0.02°C with a home-made PID controller (parameters: P = 10, I = 5, D = 0.1). Hereby, the temperature inside the human body is mimicked. For the generated heat flow, a power resistor (22 Ω, MPH20, Farnell, Belgium) was used which was mechanically attached to the copper block with heat-conductive paste. Simultaneously with the temperature, the impedance response was measured in a frequency range of 100 Hz to 100 kHz with 10 frequencies per decade and a scanning speed of 5.7 s per sweep. The amplitude of the AC voltage was fixed to 10 mV under open circuit conditions. All measurements were performed under static conditions [15].

4.3.5. Sample preparation in phosphate buffered saline (PBS) solutions for L-nicotine, histamine and serotonin

For a proof-of-principle experiment, the detection of L-nicotine was performed in PBS buffer (pH = 7.4). PBS buffer was used to simulate the ionic strength of biological samples. The L-nicotine concentrations were varied from 100 nM to 1.0 mM to ensure a wide concentration regime is analyzed. To test the selectivity, the same concentrations were prepared with cotinine in PBS. This procedure was repeated for histamine and serotonin. In the case of histamine, histidine served as an analogue while for serotonin its competitor dopamine was selected.

4.3.6 Sample preparation of spiked saliva samples

As a next step, saliva samples were analyzed. To collect the saliva, a non-smoker test person deposited saliva in a sterilized Falcon tube. The saliva was centrifuged immediately for 10 min with a speed of 10,000 rpm and the supernatant subsequently filtered with a 1 µm syringe filter. The obtained saliva samples were split into several aliquots. One aliquot was kept unaltered, thereby

serving as a control fluid. The other aliquots were spiked with L-nicotine concentrations of 0.25, 0.5, 1.0, 2.5 and 10.0 mM.

4.4. Results and discussion

4.4.1 Proof-of-principle: L-nicotine measurements in buffer

The MIP –and NIP functionalized aluminum chips were mounted into the flow cell, which was subsequently filled with PBS of pH 7.4. The flow-cell was placed in an environment with a stable ambient temperature of 19.00 ± 0.02 °C. The temperature of the copper, T_1, was strictly controlled at 37 ± 0.02 °C by the PID controller. When T_2 reached a stable level, increasing concentrations of L-nicotine in PBS (0.05 – 10 μM) were added. Between each addition, the sensor was left to stabilize for at least 15 min. The time-dependence of T_2 for a measurement with the MIP functionalized electrode is shown in Figure 3.
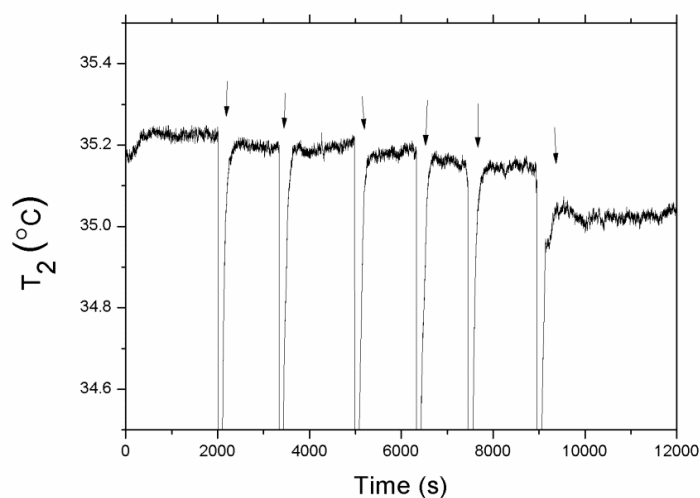
Figure 3: The temperature of the fluid (T_2) in time when the MIP is exposed to increasing concentrations of L-nicotine (0.05 -10.0 μM in PBS buffer, pH 7.4). The additions are indicated by arrows. The temperature of the copper block, T_1, is strictly controlled at 37.00 ± 0.02 °C.

In PBS, T_2 stabilizes at 35.2 ± 0.02 °C. After adding increasing concentrations of L-nicotine, a drop in the temperature T_2 is observed. However, to analyze the layer properties before and after binding of the target exactly, we should not only study the effect on temperature T_1 and T_2 but also the power (P). Therefore, we propose to investigate the thermal resistance (R_{th} in °C/W), as was done previously for the detection of point mutations in DNA [22]. This is defined as follows:

$$R_{th} = \frac{(T_1 - T_2)}{P} \quad \text{(equation 1)}$$

In this formula, (T_1 - T_2) corresponds to the temperature difference (°C) and P is the required heating power (W) of the adjustable heat source in order to keep T_1 constant. With these parameters, the time dependent R_{th} data can be calculated. These results are shown for the MIP functionalized electrode (Figure 4A) and the electrode with only the adhesive MDMO-PPV (Figure 4B) on the next page. The NIP electrode was also measured, but not included in Figure 4 since the results were very similar to the electrode with only the adhesive polymer. To all the data, a percentile filter (50% of 50 points) was applied.
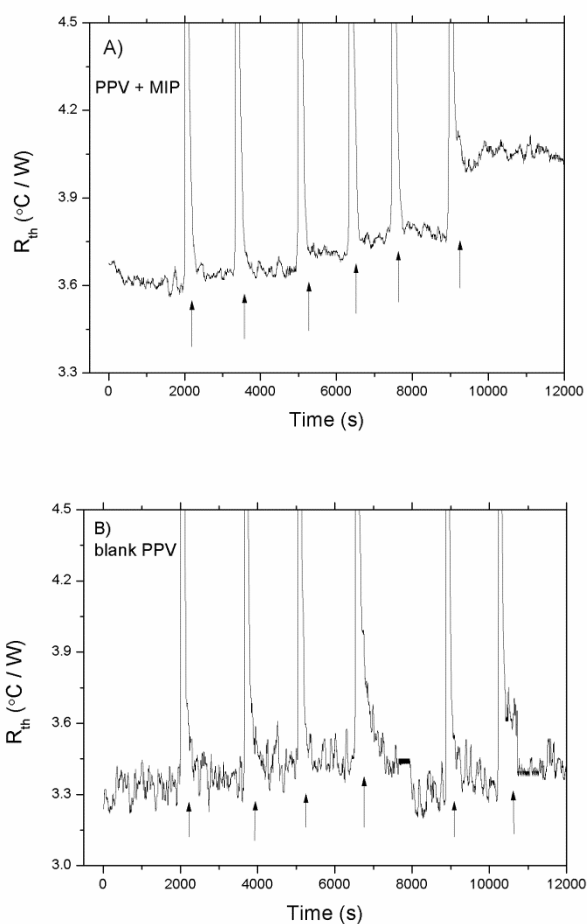
Figure 4: Time-dependence of the heat-transfer resistance R_{th} upon exposure to increasing L-nicotine in PBS (0.05, 0.1, 0.2, 0.5, 1.0 and 10.0 µM) for A) the MDMO- PPV-spincoated aluminum electrode functionalized with MIP particles by thermal treatment B) the aluminum electrode spincoated with MDMO-PPV and subsequently heated above its glass transition temperature.

Upon introducing a concentration of 10 µM L-nicotine in PBS (pH 7.4), no response in R_{th} is observed for the reference system. Surprisingly, the electrode functionalized with MIP particles showed a significant increase of ~0.4 °C/W.

This can be explained qualitatively by the "pore-blocking model". MIPs contain nanopores which can specifically rebind their target based on its size and

functionality. Upon rebinding, the heat flux through one cavity is strongly reduced due to the presence of the template. As a result, the total heat-transfer will be increased. The more L-nicotine will be bound, the more cavities will exhibit this behavior leading to an ultimately higher effect size. This "pore-blocking model" is schematically shown in Figure 5.
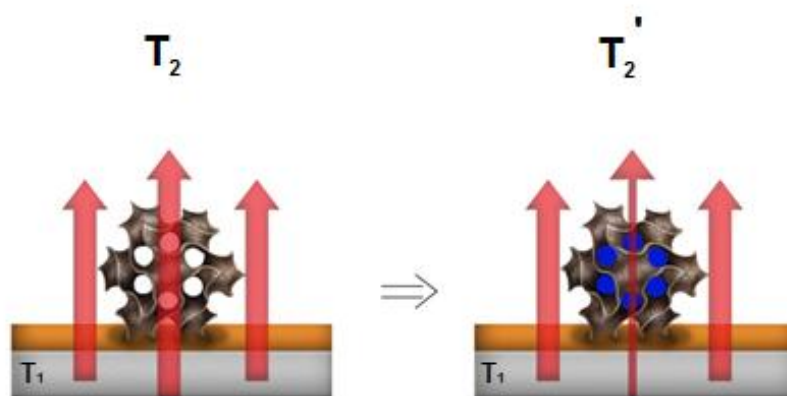
Figure 5: Artist's impression of the "pore-blocking model". The MIP particle, embedded in the surface, contains various pores where binding sites are present for its template. When these channels are filled by target molecules (indicated by blue dots), heat flux through the MIP layer is strongly reduced.

In PBS, the R_{th} stabilizes at 3.6 ± 0.1 °C/W and increases to 4.0 ± 0.1 °C/W upon addition of 10 µM of L-nicotine (Figure 4B). The effect size of ~11.0% is significantly higher than the noise on the signal (3%), thereby directly proving the binding of the target to the nanocavities of the MIP. These experiments were now performed with freshly prepared electrodes in the concentration regime 0 – 100 µM L-nicotine in PBS. In order to demonstrate specificity of the sensor platform, the same measurements were also conducted with the NIP-functionalized electrode. Additionally, the effect of cotinine (Figure 1A) additions on the MIP was analyzed. This was done in order to address the selectivity, as cotinine is similar in chemical structure and L-nicotine's natural metabolite. The R_{th} data can be represented as a dose-response curve, where the difference in R_{th} versus the concentration of the target is plotted. These results are

summarized in Figure 6. The asterisk corresponds to an estimate of the detection limit.
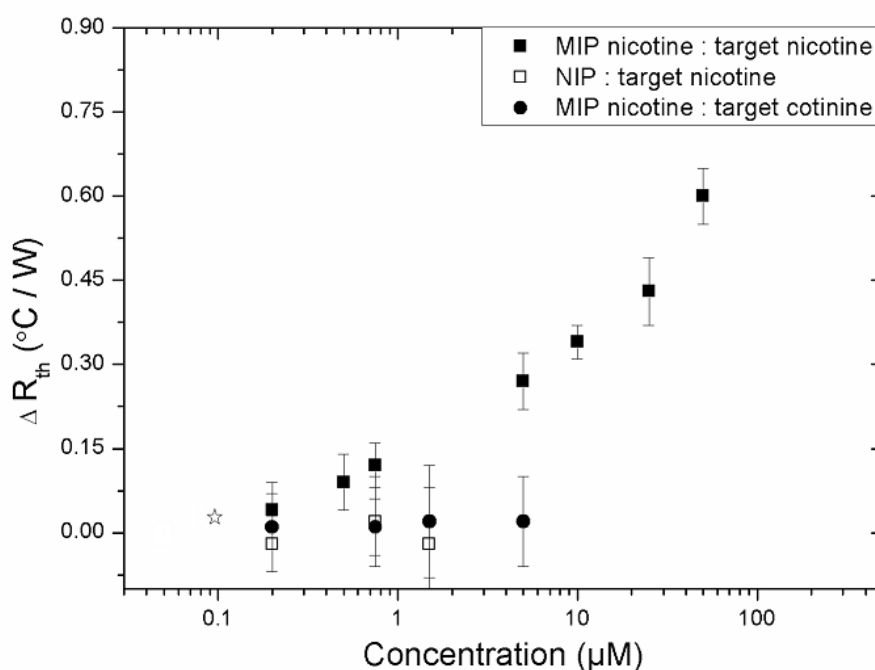
Figure 6: Dose-response curve for the MIP (solid squares), NIP (open squares) and MIP with cotinine (solid circles). The measurements were performed in threefold with T_1 strictly controlled at 37.00 ± 0.02 °C. The asterik corresponds to an estimate of the detection limit.

The measurements were performed in threefold; each measurement was conducted with a freshly functionalized electrode. The error bars given in Figure 6 correspond to the standard deviation on the three separate experiments, showing excellent reproducibility of the samples. We could measure in a wide concentration regime, from 0.2 µM (ΔR_{th} = 0.07 ± 0. 01 °C/W) to 50 µM (ΔR_{th} = 0.60 ± 0. 03 °C/ W). The standard deviation at baseline level, when no L-nicotine is present (0.01 °C/W) is used to estimate the detection limit, which is commonly defined as the concentration where the signal amplitude is three times the standard deviation. In the low concentration regime, 0.2 – 0.75 µM, the dose-response results can be represented well with a linear fit (R^2 = 0.97). With this fit, the limit of detection was calculated to be approximately 125 nM as is indicated in Figure 6 by an asterisk. This is within the physiologically relevant

range, the L-nicotine saliva concentration can vary from 0 – 500 µM [27]. The sensing platform was also determined to be specific, since the NIP with L-nicotine and the MIP with cotinine did not show a significant response in R_{th}.

4.4.2 L-nicotine in buffer : validation by impedance spectroscopy

After stabilizing in PBS, increasing concentrations of L-nicotine and cotinine were added (0 – 1000 µM). Between the addition steps the sensor was left to stabilize for 10 min. Subsequently, the response value was obtained by averaging five impedance data points with an interval of one minute. All the obtained impedance data were normalized with respect to a starting value of 100 % pure PBS. The corresponding dose-response curves at a frequency 316 Hz are shown in Figure 7. This frequency was selected because it is low enough to probe capacitive effects and ensures a high signal to noise ratio [24]. The impedance was measured simultaneously with the heat-transfer resistance, meaning Figure 6 and Figure 7 show the results of the same experiments but obtained with a different read-out technique. The concentration varies from 0 – 1000 µM of L-nicotine or cotinine in PBS (pH 7.4). The measurements were performed three times at T_1 of 37.00 ± 0.02 °C. The error bars are indicated, but might be smaller than the symbol size.
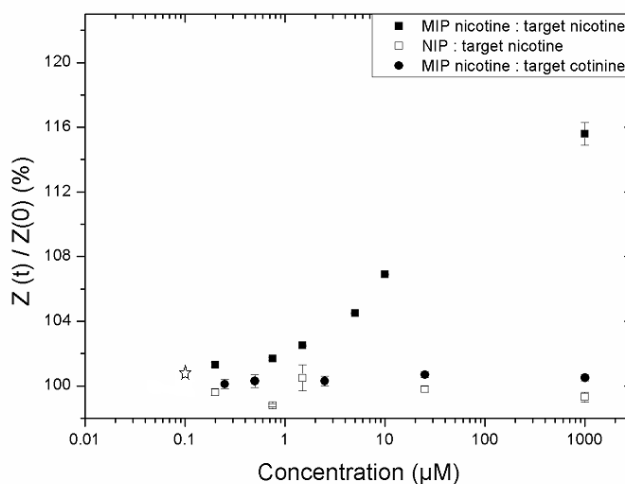
Figure 7: Dose-response curve at 316 Hz for the MIP (solid squares), NIP (open squares) and MIP with cotinine (solid circles), where the normalized impedance is plotted versus the logarithm of the target concentration.

Without the presence of L-nicotine, the standard deviation on the signal was 0.2%. This would correspond to a detection limit of approximately 100 nM, which is comparable to what was achieved with HTM. For the MIP, a linear response in R_{th} is observed from 0.1–2.5 μM L-nicotine. At higher concentrations saturation is gradually occurring, the maximum response of 115.6 ± 0.7 % is obtained at 1000 μM. For comparison, the NIP signal did not significantly change upon exposure to concentrations of L-nicotine while the increase of the MIP to 25 μM cotinine was only 100.7 ± 0.2%. This corroborates the heat-transfer results, validating that the sensor platform can be applied for the specific detection of L-nicotine in buffer solutions.

4.4.3 Histamine and serotonin measurements in buffer

To demonstrate the applicability of the sensor platform for a variety of target molecules, additional histamine and serotonin measurements (0 – 1000 μM in PBS of pH 7.4) were performed with MIP materials presented in previous work [10, 25]. As analogues, we selected for histamine its precursor histidine (Figure 1B) and for serotonin its natural competitor dopamine (Figure 1C). The dose-response curves are shown in Figure 8. In all measurements, T_1 was strictly controlled at 37.00 ± 0.02 °C.
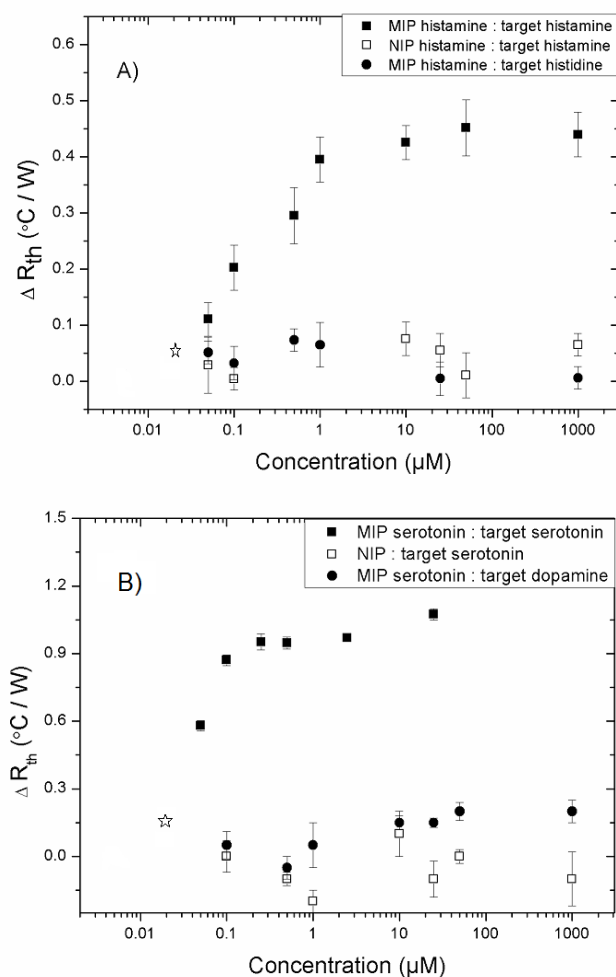
Figure 8: A) Dose-response curve for the MIP of histamine (solid squares), NIP (open squares) and MIP with histidine (solid circles) B) Dose-response curve for the MIP of serotonin (solid squares), NIP (open squares) and MIP with dopamine (solid circles).

Figure 8A shows the dose-response curve for histamine. At a maximum concentration of 1000 µM histamine, the ΔR_{th} of the MIP increased with 0.4 ± 0.04 °C/W. Its references, the NIP with histamine and the histamine MIP with histidine as target, showed no significant response at this concentration range. Thereby, it is proven that the sensing platform can detect histamine in a specific manner. Furthermore, we estimated the detection limit to be approximately 30

nM, which is within the range as it was obtained previously with impedance spectroscopy.

From Figure 8B can be determined that upon addition of 50 µM serotonin, the R_{th} of the MIP goes up by 1.07 ± 0.03 °C/W. There was no effect on the NIP, some minor increases occurred for the serotonin MIP in combination with the competitor dopamine (0.20 ± 0.05 °C/W). However, the signal ratio between target versus competitor is approximately 5, which ensures a selective detection of serotonin with the sensor platform. The estimated limit of detection is 20 nM, low enough to measure in the physiologically relevant concentration range [10].

4.4.4 Investigation of the immobilization layer

For impedance measurements, a conductive immobilization layer is required and therefore MDMO-PPV was used. It was studied if for the R_{th} measurements this was also the case, or if a non-conductive layer could be applied as for the QCM measurements. To this end, experiments were performed with electrodes spincoated with a thin layer of PVC (0.35 wt% in THF) and functionalized with histamine MIP particles [10] by thermal treatment. The electrodes were subsequently exposed to increasing concentrations of histamine in PBS buffer (0.05 – 1000 µM) at pH 7.4. The absolute R_{th} values for the measurement are shown in Figure 9. The arrows denote where solutions were added.
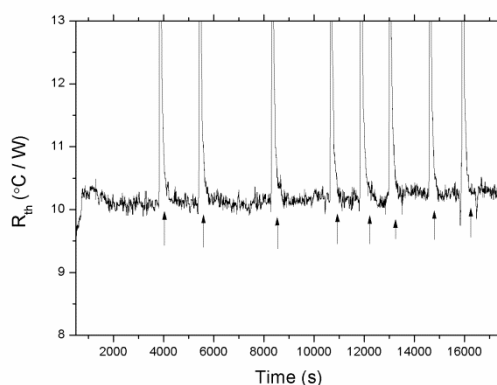
Figure 9: The absolute R_{th} values when exposing the histamine MIP to increasing concentrations of histamine (0.05-1000 µM) in PBS. In contrast to previous experiments, commercially available PVC was used as an immobilization layer instead of the conductive MDMO-PPV.

With PVC as immobilization layer, the R_{th} stabilizes at 10.2 ± 0.4 °C/W. This absolute R_{th} value is significantly higher compared to the measurement with PPV (4.0 ± 0.1 °C/W), indicating the PVC has a strong insulating effect on the layer. Furthermore, the error (0.4 °C/W to 0.1 0.1 °C/W) is larger, showing that the MIP-layer with PVC is less stable.

Upon exposure to histamine, no significant effect in R_{th} is observed. This might be because of the insulating properties of the PVC and therefore, we can conclude that for the moment it is necessary to keep using MDMO-PPV as immobilization layer.

4.4.5 Washing and rebinding of samples
MIPs prepared by the non-covalent approach are in principle reusable if they are properly washed. The washing steps with polar solvents are normally over a prolonged period of time, *e.g.* the Soxhlet extraction is performed for one week. The MIP layer is in principle stable during that time frame; however, our immobilization layer MDMO-PPV degrades within several days. This complicates the repeating of experiments with the same functionalized electrodes and therefore for each measurement, a new MIP sample is prepared.

To test the washing, a proof-of-principle experiment was performed with the L-nicotine MIP. First, the sample was stabilized in PBS and then a high concentration (1.0 mM) of the target molecule was added. Subsequently, the effect of washing with PBS and methanol was studied. Furthermore, it was analyzed if after successful washing L-nicotine could rebind to the MIP (Figure 10).
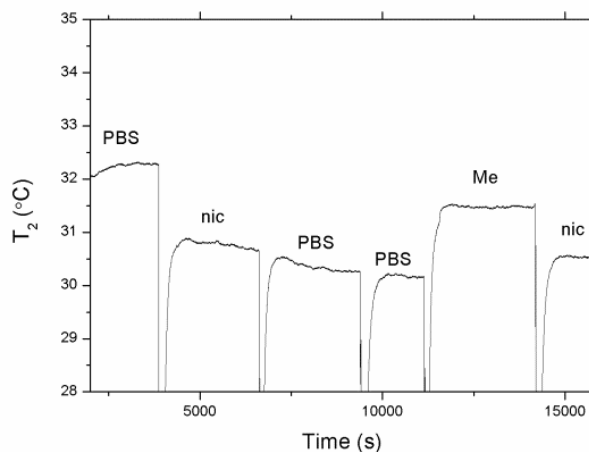
Figure 10: The washing and rebinding of the L-nicotine MIP.

Upon addition of 1.0 mM of L-nicotine, a large drop in the temperature is observed as seen in previous experiments. The washing steps with PBS, performed twice, seem to have no significant effect besides some drift of the signal. This is as expected, since PBS will not interfere with the hydrogen bonds between MIP and target. Methanol on the other hand will disturb these bonds, therefore we observe a release of the target from the MIPs and the temperature will increase slightly. The washing with methanol only once is not sufficient to go back to the base level, but we have to take into account that normally washing steps are performed over a longer period of time. Furthermore, with Soxhlet extraction not only methanol is used but also a mixture of acetic acid with acetonitrile which is more effective in breaking the hydrogen bonds. After adding 1.0 mM of L-nicotine again, we see rebinding to the MIP which is a first indication of the re-usability of the MIPs. However, it is recommended to perform further experiments before we can draw any final conclusions.

4.4.6. Proof of application: detection of L-nicotine in spiked saliva samples

In order to assess the applicability of the sensor platform in biological media, saliva samples spiked with L-nicotine (0.25, 0.5, 1.0, 2.5 and 10.0 mM) were evaluated. For these measurements there was no need for dilution, thereby further simplifying the sample preparation. The absolute R_{th} values for the MIP

and NIP after exposure to increasing spiked concentrations of L-nicotine are shown in Figure 11.
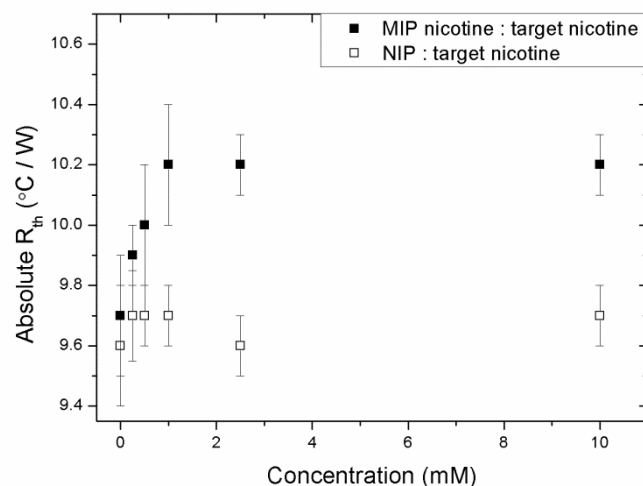
Figure 11: The dose-response curve for the concentration of L-nicotine in spiked saliva (0, 0.25, 0.5, 1, 2.5, 10.0 mM) versus the differential heat-transfer resistance (ΔR_{th}). This curve represents the absolute values of the R_{th} of MIP and NIP.

The absolute R_{th} values in saliva are higher than for the L-nicotine MIP in PBS. This can be due to two reasons; first, the absorbed proteins act as an additional insulating layer, increasing the total thermal resistance and second, the viscosity of the saliva is much higher which limits the heat transport and prolongs measurement time.

Figure 11 shows that there was no significant response of the NIP to increasing concentrations of spiked L-nicotine. For the MIP, in the regime from 0.25 to 1.0 mM the increase in ΔR_{th} is linear ($R^2 = 0.97$) with a maximum of 0.50 ± 0.01 °C/W. For concentrations higher than 1.0 mM, saturation is occurring due to increasing occupation of the binding sites. The sensitive regime of the sensor is between 0.25 to 1.0 mM and these concentrations are within the relevant range of biological samples [34]. Therefore, the applicability of the sensor platform for measurements in biological samples is demonstrated.

In the case of saliva, no reference impedance tests could be conducted. This is due to the absorption of proteins, resulting in an extremely high electrical resistance beyond the measuring limit. While we could not directly validate the results, this might be an additional benefit for the R_{th}-based sensor platform as we can also measure in complicated viscous solutions.

4.5 Conclusions

In this article, we presented the heat-transfer method (HTM) for the specific detection of L-nicotine. This is the first time that detection of small molecules based on MIP-type receptors in combination with the HTM concept has been reported. The principle of the technique can be explained by the "pore-blocking model"; upon binding of the target to the nanocavities present in the MIP, heat transport in that direction is strongly reduced resulting in a total increase of the heat-transfer resistance. For proof-of-principle measurements, L-nicotine concentrations in PBS solutions were analyzed. The detection could be performed in a specific manner, which was validated by reference tests with impedimetric read-out. In addition, a similar detection limit was achieved compared to the impedance spectroscopy tests. This detection limit is surprising low, it is in the nanomolar range which is well within the physiologically relevant regime. Furthermore, it was possible to extend this method to other small molecules, which was proven for histamine and serotonin samples in buffer solutions. As a first proof-of-application experiment, saliva samples spiked with L-nicotine were evaluated. The constructed dose-response curve showed sensitivity in the physiologically relevant regime, demonstrating the applicability of the sensor platform in biological media. Summarizing, the novel approach HTM enables the fast, straightforward, and low-cost detection of small molecules with MIP-receptors which makes it of great interest for biosensing and analytical applications.

4.6 Acknowledgements

4.7 References

[1]   K. Mosbach, *Trends Biochem Sci.* 1994, **19**, 9-14.

[2]   R. Arshady, K. Mosbach, *Chem Phys.* 1981, **182**, 687-692.

[3]   K. Haupt, K. Mosbach, *Chem Rev.* 2000, **100**, 2495-2504.

[4]   E. Benito-Pena, J.L. Urraca, B. Sellergren, M.C. Moreno-Bondi, *J Chromatogr A.,* 2008, **1208**, 62-70.

[5]   L.I. Andersson, A. Miyabayashi, D.J. O'Shanessy, K. Mosbach, *J. Chromatogr A.,* 1990, **516**, 323-331.

[6]   S. Vidyasankar, M. Ru, F.H. Arnold, *J Chromatogr A.,* 1997, **775**, 51-63.

[7]   M. Avila, M. Zougagh, A. Escarpa, A. Rios, *Trends Anal Chem.* 2008, **27**, 54-65.

[8]   S.A. Piletsky, A.P.F. Turner, *Electroanalysis,* 2002, **13**, 317-323.

[9]   Y. Mao, Y. Bao, S. Gan, F. Li, L. Niu, *Biosens Bioelectron.* 2011, **28**, 291-297.

[10]   M. Peeters, F.J. Troost, B. van Grinsven, F. Horemans, J. Alenus, M.S. Murib, D. Keszthelyi, A. Ethirajan, R. Thoelen, T.J. Cleij, P. Wagner, *Sens Actuators, B.,* 2012, **171-172**, 602-610.

[11]   M. Peeters, F.J. Troost, R.H.G. Mingels, T. Welsch, B. van Grinsven, T. Vranken, S. Ingebrandt, R. Thoelen, T.J. Cleij, P. Wagner, *Anal Chem.* 2013, **85**, 1475-1483.

[12]   A.K. Patel, P.S. Sharma, B.B. Prasad, *Thin Solid Films,* 2010, **10**, 2847-2853.

[13]   B.B. Prasad, S. Srivastava, K. Tiwari, P.S. Sharma, *Biochem Eng J.* 2009, **44**, 232-239.

[14]   Y. Hoshino, H. Koide, K. Furuya, W.W. Haberaeker III, S.H. Lee, T. Kodama, H. Kanazawa, N. Oku, K.J. Shea, *J Am Chem Soc.* 2010, **132**, 6644-6645.

[15]   B. van Grinsven, N. Vanden Bon, H. Strauven, M.S. Murib, K.L. Jiménez Monroy, S.D. Janssens, K. Haenen, M. Schöning, V. Vermeeren, M.

Ameloot, L. Michiels, R. Thoelen, W. De Ceuninck, P. Wagner, *ACS Nano.* 2012, **6**, 2712-2721.

[16]   U. Athikomrattanakul, N. Gajovic-Eichelmann, F.W. Scheller, *Anal Chem.* 2011, **83**, 7704-7711.

[17]   K. Lettau, M. Katterle, A. Warsinke, F.W. Scheller, *Angew Chem Int Ed.,* 2006, **45**, 6986-6990.

[18]   R. Rajkumar, M. Katterle, A. Warsinke, H. Möhwald, F.W. Scheller, *Biosens Bioelectron.* 2008, **23**, 1195-1199.

[19]   L.B. Neal, *Prev Med.* 1997, **26**, 412-417.

[20]   R. Schrek, L.A. Baker, G.P. Ballard, S. Dolgoff, *Cancer Res.* 1950 **10**, 49-58.

[21]   R. Doll, R. Peto, *JNCI.* 1981, **66**, 1191-1308.

[22]   A.S. Mayer, L.S. Newman, *Respir Physiol.* 2001, **128**, 3-11.

[23]   J. Bergström, *Odontology,* 2004, **92**, 1-8.

[24]   R. Thoelen, R. Vansweevelt, J. Duchateau, F. Horemans, J. D'Haen, L. Lutsen, D. Vanderzande, M. Ameloot, M. vandeVen, T.J. Cleij, P. Wagner, *Biosens Bioelectron.* 2008, **23**, 913-918.

[25]   F. Horemans, J. Alenus, E. Bongaers, A. Weustenraed, R. Thoelen, J. Duchateau, L. Lutsen, D. Vanderzande, *Sens Actuators B.* 2010, **148**, 392-398.

[26]   D. Louwet, J. Vanderzande, A. Gelan, *Synth Met.* 1995, **69**, 509-510.

[27]   M.A. Russell, C. Wilson, C. Feyerabend, C. Cole, Y. Salojee, *Br Med J.* 1976, **6017,** 1043-1046.

Chapter 5

Future design of MIP-based sensor platforms

In Chapter 5, a number of future designs of MIP-based platforms are discussed.

Adopted from:

J. Broeders, S. Duchateau, B. van Grinsven, W. Vanaken, <u>M. Peeters</u>, R. Thoelen, T. J. Cleij, P. Wagner and W. De Ceuninck. *Phys. Status Solidi A*, 2011, **208**, 1357–1363.

D. Croux, T. Vangerven, J. Broeders, J. Boutsen, <u>M. Peeters</u>, S. Duchateau, T.J. Cleij, W. Deferme, P. Wagner, R. Thoelen, W. De Ceuninck, *Phys. Status Solidi A,* 2012, DOI: 10.1002/pssa.201200743.

J. Broeders, D. Croux, <u>M. Peeters</u>, T. Beyens, S. Duchateau, T.J. Cleij, P. Wagner, R. Thoelen, W. De Ceuninck, *accepted by IEEE Sensors Journal,* DOI 10.1109/JSEN.2013.2256346.

5.1. Introduction

While the technique of molecular imprinting is rapidly developing, commercialization remains a challenge. In the field of solid phase extraction (SPE) there are some commercially available products. For instance, SupelMIP^{TM} cartridges from Acros can be used for the selective extraction of beta-agonists, beta-blockers, pesticides and clenbuterol [1, 2]. In other areas, examples are sparse.

Besides extraction purposes, biomimetic sensing offers a huge potential for the food industry. One can think of scombroid poisoning, an illness that occurs within several hours after eating spoiled fish [3]. This is commonly reported when tuna is not adequately refrigerated or preserved after being caught. The main toxin involved is histamine, which concentration can go up to 1000 μM due to the breakdown of histidine [4]. In previous research, Horemans *et al.* determined histamine concentrations in canned tuna fluid with a MIP-based QCM sensor platform [5]. While this proofs that MIPs are a very interesting candidate for these types of applications, the drawback is that the sensor platform still requires sophisticated equipment. Therefore, we will propose in Chapter 5 some alternative MIP-based sensor platforms. These sensor platforms have in common that they are straightforward and easy to use, can be produced in mass quantities, and are miniaturizable.

Electrochemical impedance spectroscopy was selected since it can be applied in a variety of sensors. Usually, the impedimetric changes in the sensor are monitored by bulky and expensive equipment. To this end, we will first present a minituarized, low-cost impedance analyser which can be used for biological measurements [6]. As a next step, a new method is introduced for smartphone-based impedimetric spectroscopy [7]. This system works with disposable test strips and is a first step towards the direction of home-diagnostics biosensing applications.

The second technique works by inductive coupling with a resonating LC circuit, similar to the humidity sensor presented by Tan *et al.* [8]. Disposable wireless packaging sensors tags were developed and as a proof-of-principle, histamine concentrations were studied.

5.2 Examples of MIP-based sensor platforms

5.2.1. Miniaturized impedance setup: BioZ analyzer

A minituarized low-cost impedance analyzer, the BIOZ analyzer, was developed. This system can measure quasi-simultaneously the impedance on eight different channels in the frequency range 10 Hz to 1000 kHz (Figure 1).

Figure 1: The BIOZ analyzer, adopted from Broeders *et al.* [6].

First, the accuracy and stability of the device were tested. The results show that the impedance could be measured accurately in a broad range and that experiments could be performed over intervals of several days. To demonstrate the applicability in biological setups, a MIP sensor for histamine was studied. The detailed synthesis procedure of the MIP is described in ref [5].

The aluminum electrodes are spincoated in order to obtain a thin adhesive layer (~100 nm) of MDMO-PPV. To these substrates, a PDMS stamp with MIP and NIP particles was applied. After thermal treatment, the particles are immobilized into the polymer layer. Next, the functionalized electrodes are mounted into an open addition setup and the cell is filled with PBS. During the measurement, the temperature was kept constant at 37.00 ± 0.02 °C with a programmable hot plate. After 2.5 h of stabilization, a concentration of 2 nM histamine in PBS was added. The normalized MIP-NIP impedance response is shown in Figure 2. As frequency 150 Hz was selected, since the binding effect is the most pronounced in the first decade.
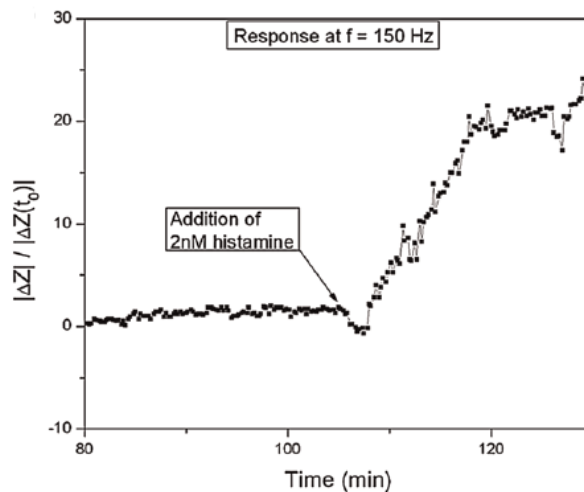
Figure 2: The normalized MIP-NIP impedance response before and after addition of 2 nM of histamine [6].

The addition of a 2 nM concentration of histamine resulted in a significant increase of the MIP-NIP signal due to the binding of the target molecules. This is a first indication the setup can be applied for biological samples.

5.2.2. Mobile application for impedance based biomimetic read-out

The BIOZ analyzer is a low-cost and miniaturized device, which is a great benefit compared to the often bulky and expensive traditional impedance equipment. For the first tests, the analyzer was used in combination with an open addition setup which is not very user friendly. Therefore, a novel impedimetric read-out of biomimetic sensors via smartphones and tablet PC's is presented which works with disposable test strips. The disposable test strips, compared to what is used for the glucose sensor, are a first step into the direction of home-diagnostics applications.

Electrodes were printed with a semi-automated Isimat 1000P screen-printing machine. Their size was 2 mm by 20 mm with a thickness of approximately 100 µm. Subsequently, the electrodes are glued to a 3 mm thick Teflon strip (Figure 3).
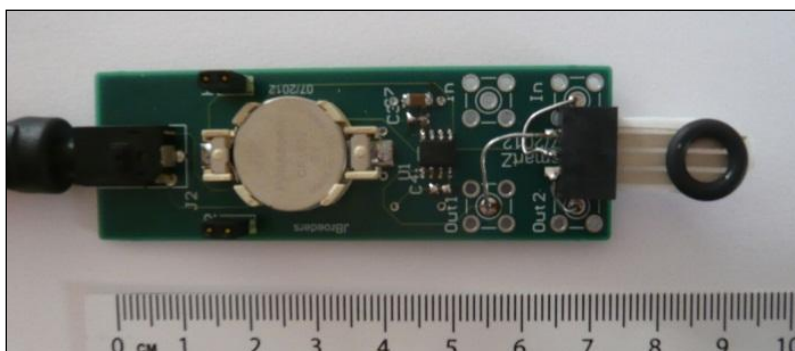
Figure 3 : Hardware interfaced to the smartphone with test strip mounted (right side) [7].

Next, a thin layer (~100 nm) of MDMO-PPV was spincoated to the test strips. MIP and NIP particles for histamine were embedded into the layer by thermal treatment. The detailed synthesis procedure of the MIPs is given in ref 5. In contrast to the electrodes, the counter electrode was not functionalized and could therefore serve as the common counter electrode. A 2 mm thick O-ring with a diameter of 7.3 mm was attached to function as a liquid reservoir. Since the liquid reservoir is very small, samples of only 60 µl have to be applied.

As a first test, the system was stabilized in PBS after which a concentration of 1 µM of histamine was added. The results for MIP and NIP are shown in Figure 4.
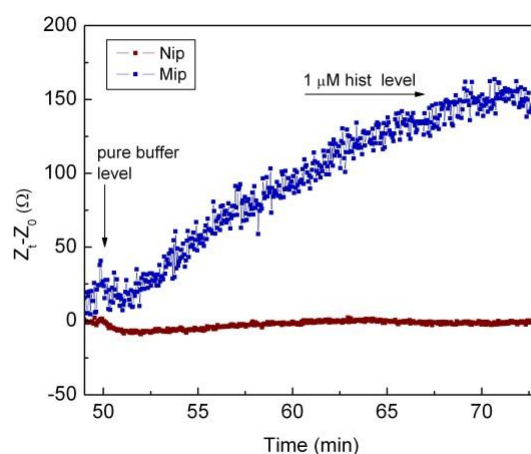
Figure 4: The impedance response of MIP and NIP after addition of 1 µM of histamine
Figure adopted from: Broeders *et al.* [7].

From Figure 4 is directly clear that while the impedance of the MIP directly increases after histamine addition, the NIP shows no significant response. The difference in magnitude of 150 Ωm is easily detectable; however for biomedical purposes it is more interesting to investigate the nanomolar concentration regime. This is possible if fluctuations are filtered using a reference electrode or the NIP sensor, by which the detection limit could be lowered to 20 nM. To verify this, more experiments should be conducted.

5.3.3. MIP films on Radio Frequency Identification (RFID) tags

We will present here a disposable wireless MIP-based packaging sensor tag for histamine detection. The sensor principle is based upon inductive coupling with a resonating LC circuit. The RFID tags are screen-printed, which allows extremely fast and low-cost mass-production. They were produced with an Isimat 1000 P, a semi-automatic screenprinting machine. Conductive silver patterns are deposited onto a flexible poly(ethylene terephthalate) (PET) substrate with a thickness between 2 and 5 μm. The layer is then covered with a new layer of PET-foil, with two holes for interconnects and a central opening for MIP deposition. The circuit is then shorted by printing a small bridge between the pads as both ends of the circuit. The capacitance was spincoated with a PVC solution (0.7 wt % in THF) to obtain a layer thickness of 100 nm. Subsequently, MIP and NIP particles were applied on the surface by a PDMS stamp and embedded into the adhesive layer by heating it above the glass transition temperature of PVC. For proof-of-principle experiments, a MIP for histamine was used [5]. The step-by-step construction process of the sensor cell is shown in Figure 5.
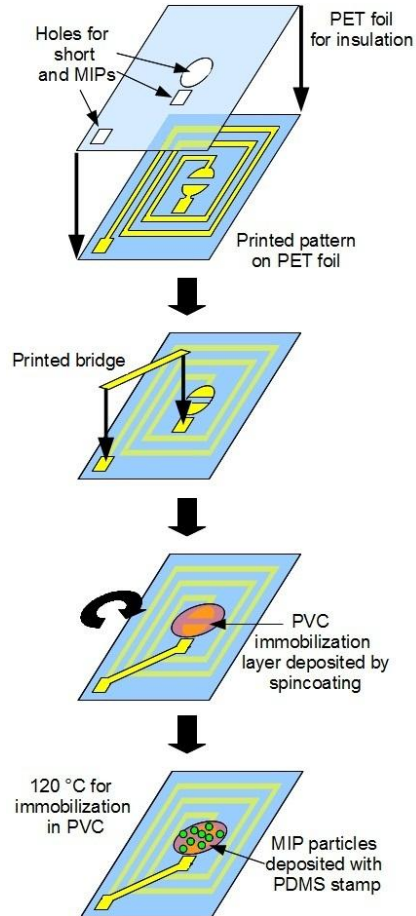
Figure 5: Step-by-step construction of the MIP film on a RFID tag. Adopted from Croux *et al.* [9].

The constructed sensor can be described with a parallel LC circuit. This circuit, often used in filters and tuners, exhibits a self-resonance at a certain frequency (equation 1).

$$f = \frac{1}{2\pi \sqrt{LC}} \quad \text{(equation 1)}$$

In this formula, f corresponds to the frequency, L to the inductor and C to the capacitor. If binding to the MIP layer occurs, the dielectric properties of the capacitor will change and thus the resonance frequency. As proof-of-principle experiments, the tags were submerged into PBS after which increasing

concentrations of histamine (0 – 1000 nM) were added. The dose-response curves for the MIP and NIP are demonstrated in Figure 6.
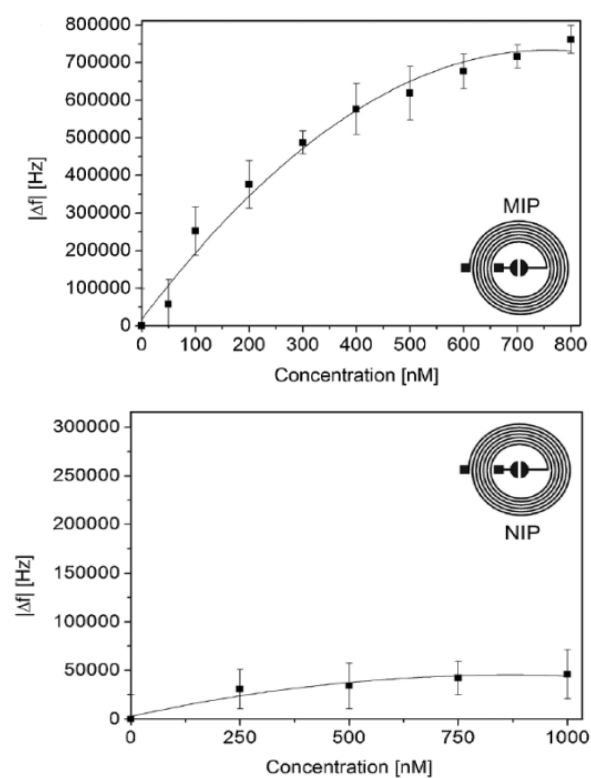
Figure 6: Dose-response curve for the MIP (above) and NIP (below), when exposed to increasing concentrations of histamine in PBS (0 – 1000 nM). Figure adopted from Croux *et al.* [9].

The dose-response curves show histamine detection starting from 50 nM for the MIP. The response is linear till concentrations of 700 – 800 nM, then a saturation level is reached. The response time is extremely fast, the signal can be detected within 1 min after additions and reaches a new-steady state in less than 5 min. The tag is also very specific for histamine, since the NIP shows only a minor response caused by the change in permittivity of the surrounding liquid. The noise level and limit of detection have found to vary between 50 nm and 300 nm, depending on the quality of the MIP and PVC layer. This makes it a very

promising sensor platform for commercial applications, but further research has to been done on other target molecules and on improving the reproducibility.

5.3 References

[1]   A. Blomgren, C. Berggren, A. Homberg, F. Larsson, B. Sellergren, K. Ensing, *J Chromatogr A.,* 2002, **975**, 157-164.

[2]   C. Widstrand, F. Larsson, M. Fiori, C. Civitareale, S. Mirante, G. Brambilla, *J Chromatogr B Analyt Technol Biomed Life Sci.,* 2004, **804**, 85-91.

[3]   R.F. Clark, S.R. Williams, S.P. Nordt, A.S. Manoguerra, *Undersea Hyperb Med.,* 1999, **26**, 175-184.

[4]   L. Lehane, J. Olley, *Int J Food Microbiol.,* 2000, **58**, 1-37.

[5]   F. Horemans, J. Alenus, E. Bongaers, A. Weustenraed, R. Thoelen, J. Duchateau, L. Lutsen, D. Vanderzande, *Sens Actuators, B.,* 2010, **148**, 392-398.

[6]   J. Broeders, S. Duchateau, B. van Grinsven, W. Vanaken, M. Peeters, R. Thoelen, T. J. Cleij, P. Wagner and W. De Ceuninck. *Phys. Status Solidi A*, 2011, **208**, 1357–1363.

[7]   J. Broeders, D. Croux, M. Peeters, T. Beyens, S. Duchateau, T.J. Cleij, P. Wagner, R. Thoelen, W. De Ceuninck, accepted by IEEE Sensors Journal. DOI 10.1109/JSEN.2013.2256346

[8]   E. Lim Tan, W. Ni Ng, R. Shao, B.D. Pereles, K. Ghee Ong, *Sensors,* 2007, **7**, 1747-1756.

[9]   D. Croux, T. Vangerven, J. Broeders, J. Boutsen, M. Peeters, S. Duchateau, T.J. Cleij, W. Deferme, P. Wagner, R. Thoelen, W. De Ceuninck, *Phys. Status Solidi A,* 2012, DOI: 10.1002/pssa.201200743.

Chapter 6

General conclusion and outlook

This chapter provides a brief summary of the results which were obtained in this thesis. It discusses the MIP-based sensor platform with impedimetric read-out technique, which can be used for the fast and low-cost detection of histamine and serotonin in biological samples. We also presented a novel straightforward read-out technique, the heat-transfer method (HTM). Both methods are very promising, but not directly applicable in biosensors for point-of-care applications. Therefore, we have shown some alternative MIP sensor platforms for future use. Finally, a general outlook is provided to discuss some of remaining issues and suggestions are given to overcome these problems.

This project aimed at the development of a polymer-type sensor platform for the detection of histamine and serotonin for intestinal applications. The sensor platform should meet the following criteria:

i)   Specific detection of histamine and serotonin at physiologically relevant concentrations in biological samples.

ii)   The sensor setup should perform measurements at low-cost (~10 euro per material of chip) and with a fast response time (30 – 60 min).

iii)   The possibility of performing *in vivo* measurements for intestinal applications.

MIPs were used as polymer-type receptors since they are robust, can be produced at low-cost, and have a high affinity for their template molecules. While the direct packing of MIPs in separation columns is straightforward, the incorporation into sensing devices remains challenging. In the course of this PhD, MIPs with high affinity for serotonin and histamine were synthesized and a sensor platform was developed with two read-out strategies. The first method is based on electrochemical impedance spectroscopy, the second technique on heat-transfer resistance.

For serotonin, several MIP blends were synthesized which were characterized by optical batch rebinding experiments. The MIP with the highest affinity for serotonin was composed of the monomers methacrylic acid and acrylamide in a 1 : 3 ratio. This MIP was incorporated into an open addition setup and the impedance was measured in buffer solutions. With these measurements, a dose-response curve in the physiologically relevant regime was constructed. Next, biological samples were studied which required the design of a refined sensor-cell concept. The native serotonin plasma concentrations of three healthy volunteers were studied with impedance spectroscopy and the results were nicely in agreement with reference HPLC tests. Furthermore, we demonstrated that the impedance increase upon binding is due to the capacitive effect at the interface between MIP particles and the fluid.

Histamine is another target molecule of interest. In previous work was demonstrated that the histamine MIP with methacrylic acid as monomer exhibits pH dependent behavior. Therefore, no detection at acidic pH could be performed while the pH in the intestines can vary from pH 5 - 8. We proposed a statistical binding analysis model to explain this behavior. Based on these results, a novel MIP was synthesized with the monomer acrylic acid. Theoretically, this MIP should be able to bind more than 90%, compared to the 7% of the MIP with methacrylic acid. These results were experimentally verified by UV-vis spectroscopy, microgravimetry and impedance spectroscopy. To show the applicability in biological samples, the histamine concentration of mildly acidic bowel fluids samples of several test persons was analyzed. We demonstrated that the sensor with impedimetric read-out provides reliable data in the relevant physiologically concentration regime, which was validated independently by ELISA tests.

A second read-out technique is exploited based on differential heat-transfer resistance. This HTM approach is more straightforward than impedance spectroscopy, as it requires only two thermometers, one adjustable heat source and a PID controller. This effect in R_{th} is observed due to blocking of the heat transport by rebinding of the target molecules. For proof-of-principle measurements, L-nicotine concentrations in buffer solutions were studied. This was extended to the target molecules of interest for this thesis, respectively serotonin and histamine. The performance in biological samples has not been evaluated yet, but a first test with saliva samples spiked with L-nicotine showed that it was possible to construct a dose-response curve.

Next, both methods are evaluated to what degree they fulfill the criteria in terms of specificity, cost, and speed.

Table 1 (next page) shows the detection limits that are achieved for impedance spectroscopy and HTM in buffer solutions and biological samples.

Table 1: LOD in 1x PBS and biological samples with HTM and impedimetric read-out.

Target	HTM		Impedance spectroscopy		
	LOD Buffer	LOD Saliva	LOD Buffer	LOD Blood	LOD Bowel fluid
Serotonin	20 nM	-	3 nM	5 nM	-
Histamine	30 nM	-	15 nM	-	0.2 µM
L-nicotine	100 nM	~0.5 mM	100 nM	-	-

This shows that both methods are able to specifically detect the target molecules in buffer solutions. However, only the impedimetric read-out has been studied extensively with biological samples. Therefore, impedance spectroscopy seems to be the best method of choice. It has to be considered that HTM is not an established technology yet and there is still room for improvement. One aspect that should be studied is the noise ratio on the signal, which can be lowered by optimizing the PID parameters of the heat source. In a master project the noise was reduced nearly a factor threefold, thereby lowering the LOD for L-nicotine to 35 nM instead of 100 nM. The next step is to study biological samples with the optimized PID parameters.

The main advantage of MIPs is that they are low cost due to their straightforward synthesis. The cost of the chemicals is very low, but the equipment should also be considered. The impedance analyzer and sensor cell are all home made, with a total of around €1000 for the equipment. In this calculation man hours are not taken into account, but normally the setup can be mounted by one person in one work week. Other apparatuses that are required to produce and analyze the samples are a spincoater (€4500 – 5500), laptop (€1000) and hot plate (€200 – 400). For HTM only two thermometers (€10) and an adjustable heat source are required, ensuring this is even less expensive. The criterium of 10 euro per chip seems therefore reasonable, even if man hours would be taken into account. For the detection of serotonin and histamine HPLC is considered the 'gold standard'. To analyze a sample for diagnostic purposes with HPLC costs €25 – 30, the commercial rate can be even the double. This means that in terms of expenses, both methods have a big advantage over the traditional technique. One drawback of our setup is that we can measure only one sample at a time, while an ELISA test allows simultaneous dection of 96

samples. The transformation of our system to an array format is therefore a crucial point for reduction of both the costs and the measurement time.

The other criterium is the measurement time, which should be within 60 minutes. After adding a certain concentration to the MIP-functionalized electrode, the signal should be monitored for at least 18 minutes. Furthermore, the sample should be stabilized in 15 to 30 minutes, resulting in a total measurement time which is within the required time frame.

The impedimetric technique fulfills the criteria into a great extent since it is fast (<60 minutes), low-cost (~10 euro per chip) and has a high specificity even when measuring in biological fluids. The R_{th} approach has a high specificity in buffer solutions; however the performance in biological samples remains to be studied. An additional stroing point of the sensor platform is that the two techniques can be measured simultaneously, which enables direct validation of the results. The last requirement, measuring *in vivo* for intestinal applications, imposes some challenges.

The main disadvantage of the sensor platform is the sample preparation of the MIPs. Now, the MIP particles are prepared by bulk polymerization and then embedded into an adhesive MDMO-PPV layer by thermal treatment. While this method was proven very effective, it has several drawbacks. The surface coverage is not uniform, only between 20 – 30%, and varies slightly per sample. Furthermore, the adhesive MDMO-PPV layer is not commercially available and can degrade in several days, eliminating the possibility of repeating experiments with the same sample. If the MIPs are directly polymerized onto the surface, there is no more need for the adhesive layer and reproducibility should be improved. In the organic chemistry department first attempts were done with polymerizing MIPs directly onto titanium and silicon substrates. The first choice is titanium since it is biocompatible and already used *in vivo* with, for instance, cochlear implants. The maximum diameter of titanium electrodes inside the human body lies within the mm range, while the samples used now are 1 x 1 cm^2. This means the samples have to be further miniaturized, which can be done by developing new sensor cells. Another option is to polymerize on wire-like structures instead of using planar electrodes. Besides the biocompatibility of

the electrodes and platform, the biocompatibility of the MIP particles should also be considered. A first study on that aspect was done by Hoshino *et al.,* who injected MIP nanoparticles in the blood stream of mice. The particles were demonstrated to be nontoxic to cultured fibrosarcoma cells, showing a first promising result.

The final step is to enter into the commercial market of medical devices. We already presented some future MIP-sensor designs which can be further exploited. There are two more aspects we should consider, before thinking of commercialization of the product:

i) A clinical trial should be performed to study a larger amount of biological samples and, additional patient samples. The latter is indispensable to determine if the technique is sensitive enough to detect occurring aberrations.

ii) The sensor platform should be transformed to an array format which enables the simultaneous detection of a variety of targets.

Due to the speed, low-cost, and high specificity of the developed techniques, they can be considered as methods with a high clinical and commercial potential. These methods could also mean a first step into the direction of incorporating MIPs into sensing devices for *in vivo* purposes. Measurements performed directly in the gastro-intestinal tract would provide an important insight into the pathogenesis of several gastrointestinal system-related disorders. This may lead to the development of novel, effective treatments for these disorders.

Appendix 1

Nomenclature

5-HIAA	5- hydroxyindole Acetic Acid
5-HT	5-hydroxytryptamine (serotonin)
5-HTP	5-hydroxytryptophan (tryptophan)
AA	Acrylic Acid
ACG	American College of Gastoenterology
AIBN	Azobisisobutyronitrile
AM	Acrylamide
C	Capacitance
C_f	Free Concentration
CPE	Constant-phase Element
DMSO	Dimethylsulfoxide
EGDM	Ethylene Glycol Dimethacrylate
ELISA	Enzyme-Linked Immunosorbent Assay
FDA	Food and Drug Administration
GC	Gas Chromatography
GI	Gastrointestinal
HC	Healthy Controls
HPLC	High Performance Liquid Chromatography
HRQL	Health Related Quality of Life
HTM	Heat Transfer Method
IBS	Irritable Bowel Syndrome
IBS-C	Irritable Bowel Syndrome, predominant constipation
IBS-D	Irritable Bowel Syndrome, predominant diarrhea
IBS-M	Irritable Bowel Syndrome, mixed
IF	Imprint Factor
K_i	Binding Energy
L	Inductor
LOD	Limit of Detection
MAA	Methacrylic Acid
MIP	Molecularly Imprinted Polymer
NaOH	Sodium Hydroxide
NIP	Non-Imprinted Polymer

PDMS	Polydimethylsiloxane
PET	Poly(ethylene terephthalate)
PI	Post-Infectious
PID	Proportional-Integral-Derivative
PBS	Phosphate Buffered Saline
PPV	Poly(p-phenylene vinylene)
PVC	Polyvinylchloride
QCM	Quartz Crystal Microbalance
R_{th}	Heat-Transfer Resistance
S_b	Substrate Bound
SEM	Scanning Electron Microscope
SPE	Solid Phase Extraction
SSRI	Selective Serotonin Reuptake Inhibitor
TCA	Tricyclic Acid
T_g	Glass Transition Temperature
THF	Tetrahydrofuran
UV	Ultraviolet
Z	Impedance
ZnPP	Zinc Protoporphyrin

Appendix 2

Publications, Patents and Conference contributions

<u>Publications</u>

[1]   B. Geerets, <u>M. Peeters</u>, B. van Grinsven, K. Bers, W. De Ceuninck, P. Wagner, *submitted to Sensors (May 2013).*

[2]   <u>M. Peeters</u>, P. Csipai, B. Geerets, A. Weustenraed, B. van Grinsven, J. Gruber, W. De Ceuninck, T.J. Cleij, F.J. Troost, P. Wagner, *accepted by Analytical and Bioanalytical Chemistry,* DOI: 10.1007/s00216-013-7024-9.

[3]   J. Broeders, D. Croux, <u>M. Peeters</u>, T. Beyens, S. Duchateau, T.J. Cleij, P. Wagner, R. Thoelen, W. De Ceuninck, accepted by IEEE Sensors Journal. DOI 10.1109/JSEN.2013.2256346

[4]   J. Alenus, A. Ethirajan, F. Horemans, A. Weustenraed, P. Csipai, J. Gruber, <u>M. Peeters</u>, T.J. Cleij, P. Wagner, *accepted by Analytical and Bioanalytical Chemistry.*

[5]   D. Croux, T. Vangerven, J. Broeders, J. Boutsen, <u>M. Peeters</u>, S. Duchateau, T.J. Cleij, W. Deferme, P. Wagner, R. Thoelen, W. De Ceuninck, *Phys. Status Solidi A,* 2012, DOI 10.1002/pssa.201200743.

[6]   <u>M. Peeters,</u> F.J. Troost, R.H.G. Mingels, T. Welsch, B. van Grinsven, T. Vranken, S. Ingebrandt, R. Thoelen, T.J. Cleij, P. Wagner, *Anal Chem.,* 2013, **85**, 1475-83.

[7]   <u>M. Peeters</u>, F.J. Troost, B. van Grinsven, F. Horemans, J. Alenus, M.S. Murib, D. Keszthelyi, A. Ethirajan, R. Thoelen, T.J. Cleij, P. Wagner, *Sens. Actuators, B*, 2012, **171**, 602-610.

[8]   J. Broeders, S. Duchateau, B. van Grinsven, W. Vanaken, <u>M. Peeters</u>, R. Thoelen, T. J. Cleij, P. Wagner and W. De Ceuninck. *Phys. Status Solidi A*, 2011, **208**, 1357 – 1363.

[9]   G.J.M. Habraken, <u>M. Peeters</u>, P.D. Thornton, C.E. Koning, A. Heise, *Biomacromolecules,* 2011, **12**, 3761-3769.

[10]   Z. Deng, G.J.M Habraken, <u>M. Peeters</u>, A. Heise, G. de With, N.A.J.M. Sommerdijk, *Soft Matter,* 2011, **7**, 9685-9694.

[11]   G.J.M. Habraken, <u>M. Peeters</u>, C.H.J.T. Dietz, C.E. Koning, A. Heise, *Polymer Chemistry,* 2010, **1**, 514-524.

Patents

[1]   Heat-transfer resistance based analysis of bioparticles
        European patent application : **EP13157264.6**
        Inventors: Kasper Eersels, Marloes Peeters, Anitha Ethirajan, Bart van
        Grinsven, Ward De Ceuninck and Patrick Wagner.

Oral Presentations

[1]   Belgian Physical Society, Namur (25 – 05- 2011)
        Session: Biophysics and Medical Physics
        MIP-based biomimetic sensor for the detection of serotonin in plasma.
[2]   4th Graduate Student Symposium on Molecular Imprinting, London
        (28/30 – 09 – 2011)
        MIP-based biomimetic sensor for the detection of serotonin in human
        blood plasma.
[3]   Belgian Physical Society, Brussels (30 – 05 - 2012).
        Session: Biophysics and Medical Physics
        MIP-based biomimetic sensor for the electronic detection of serotonin in
        human blood plasma.
[4]   Invited lecture seminar: Diamond for biosensing and nanomedicine,
        Kladno, Czech Republic (15-04-2013)
        Molecularly Imprinted Polymers: synthetic receptors for medical devices

Posters

[1]   Gutday, Leuven (09-11-2012)
        Impedimetric detection of histamine in bowel fluids using synthetic
        receptors.
        M. Peeters, P. Csipai, F.J. Troost, R. Mingels, B. van Grinsven, T.
        Vranken, R. Thoelen, T.J. Cleij and P. Wagner.
[2]   EnFI 2012, Zweibrücken, Germany (16-/17 – 07- 12)
        MIP-based biomimetic sensor for the electronic detection of serotonin in
        human blood plasma.
        M. Peeters, F.J. Troost, B. van Grinsven, F. Horemans, J. Alenus, M.S.
        Murib, D. Keszthelyi, A. Ethirajan, R. Thoelen, T.J. Cleij, and P. Wagner.

[3]   Biosensors 2012, Cancún, Mexico (15/18 – 05 – 2012)

        MIP-based Biomimetic Sensor for the Detection of Serotonin in Plasma.
        M. Peeters, F.J. Troost, B. van Grinsven, F. Horemans, J. Alenus, M.S.
        Murib, D. Keszthelyi, A. Ethirajan, R. Thoelen, T.J. Cleij and P. Wagner.
        Increasing MIP sensor usability in field applications.
        J. Broeders, D. Croux, A. Weustenraed, M. Peeters (presenting), W.
        Vanaken, S. Duchateau, T.J. Cleij, P. Wagner, R. Thoelen and W. De
        Ceuninck
        Impedance spectroscopy for in situ cell growth monitoring.
        S. Duchateau, J. Broeders, D.Janssen, D.Croux, M. Peeters (presenting),
        M. Daenen, P. Wagner, W. de Ceuninck and R. Thoelen.

[4]   Nanosense Symposium, Hasselt (25-04-2012)
        MIP-based Biomimetic Sensor for the Detection of Serotonin in Plasma.
        M. Peeters, F.J. Troost, B. van Grinsven, F. Horemans, J. Alenus, M.S.
        Murib, D. Keszthelyi, A. Ethirajan, R. Thoelen, T.J. Cleij and P. Wagner.

[5]   Biomedica 2012, Liège (18-04-2012)
        MIP-based biomimetic sensor for the detection of serotonin in human
        blood plasma.
        M. Peeters, F.J. Troost, B. van Grinsven, F. Horemans, J. Alenus, M.S.
        Murib, D. Keszthelyi, A. Ethirajan, R. Thoelen, T.J. Cleij and P. Wagner.

[6]   EnFI 2011, Linz, Austria (18/19 – 06- 2011)
        MIP-based biomimetic sensor for the detection of serotonin in human
        blood plasma.
        M. Peeters, F.J. Troost, B. van Grinsven, F. Horemans, J. Alenus, D.
        Keszthelyi, A. Ethirajan, R. Thoelen, T.J. Cleij, and P. Wagner.

[7]   Biomedica 2011, Eindhoven, The Netherlands (07/08 – 04- 2011)
        In-vitro detection of serotonin based on molecularly imprinted polymers.
        M. Peeters, B. van Grinsven, F. Horemans, B. Billen, D. Keszthelyi, F.J.
        Troost, R. Thoelen, T.J. Cleij, and P. Wagner

[8]   IAP meeting, Hasselt (26-11-2010)
        Molecularly imprinted nanocavities: synthetic receptors for small
        molecules
        J. Alenus, M. Peeters, F. Horemans, E. Bongaers, A. Weustenraed, T.
        Welsch, D. Vanderzande, T.J. Cleij, and P. Wagner

<u>Awards</u>

Prize for Best Oral Presentation at Graduate Student Symposium on Molecular Imprinting, 28 – 30 September 2011, London

Prize for best Poster, EnFI 2012, 16/17-07-12, Zweibrücken.

Presenter: Dieter Croux.

D. Croux, J. Broeders, T. Vangerven, <u>M. Peeters</u>, J. Boutsen, W. Deferme, P. Wagner, R. Thoelen, W. De Ceuninck.

Appendix 3

List of Figures and Tables

Chapter 3: